PhD degree in Systems Medicine

Curriculum in Human Genetics

European School of Molecular Medicine (SEMM),

University of Milan and University of Naples "Federico II"

Telethon Institute of Genetics and Medicine

Disciplinary Sector: ING-IND/35 XXXV cycle

The CRISPRaTOR: A feedback controller in mammalian cells for Robust Perfect Adaptation

Supervisor:

Prof. Diego di Bernardo

Internal Advisor:

Prof. Maria Antonietta de Matteis

External Advisor:

Prof. Roman Jerala

Candidate:

Alessio Mallozzi

R12698

Academic Year 2022-2023

Contents

List of abbreviations

Abbreviation	Definition
Cas9	CRISPR-Associated protein 9
AIC	Antithetic Integral Controller
ARA	Arabinose
BHLH	Basic Helix-Loop-Helix
CRISPR	Clustered Regularly Interspaced Short Palindromic Repeats
CRISPRa	CRISPR activation
CRISPRi	CRISPR interference
dCas9	Dead Cas9
DNA	Deoxyribonucleic Acid
EMMA	Extensible Mammalian Modular Assembly
GFP	Green Fluorescent Protein
GOI	Gene of Interest
gRNA	Guide RNA
HDR	Homology Directed Repair
HSL	Homoserine Lactone
iPSC	Induced Pluripotent Stem Cells
IPTG	Isopropyl β-d-1-Thiogalactopyranoside
KRAB	Krüppel Associated Box
NHEJ	Non-Homologous End Joining
PCR	Polymerase Chain Reaction
PEI	Polyethylenimine
PFL	Positive Feedback Loop
PNFL	Positive Negative Feedback Loop
RBP	RNA-Binding Protein
RBS	Ribosome Binding Sequence
RNA	Ribonucleic Acid
RPA	Robust Perfect Adaptation
rtTA	Reverse Tet TransActivator
SAM	Synergistic Activation Mediator
sfgfp	Superfolder Green Fluorescent Protein
SV40	Simian Virus 40
TALEN	Transcription activator-like effector nuclease
TFEB	Transcription Factor EB
TMP	Trimethoprim
tTA	Tet TransActivator
UAS	Upstream Activation Sequence
VP16	Viral Protein 16
VP64	Viral Protein 64
WCB	Whole Cell Biosensor
WD	Wilson Disease
ZFN	Zinc Finger Nuclease

Abstract

Synthetic Biology, an interdisciplinary field merging genetic engineering with control theory, aims to achieve predictable behaviour in living systems. Its applications span diverse domains, from biotechnology to biomedicine, where engineered cells produce biofuels, recombinant proteins, and serve as precise biosensors and therapeutic agents. The toolbox to engineer living systems includes constitutive and inducible promoters, natural and engineered ribosome binding sites, and programmable endonucleases derived from the CRISPR/Cas9 system, just to name a few. However, achieving precise control in living cells necessitates a holistic perspective, recognizing that behaviour does not arise from single components but rather from their interactions. Viewing DNA, RNA, and proteins as electronic circuit components, Synthetic Biology seeks to emulate circuit topologies, such as Negative Feedback and Feedforward Loops, to attain predictable behaviour and desired functionalities. A crucial feature of natural endogenous gene regulatory networks is robustness, hence the capacity of the cell to maintain its state despite internal and external perturbations. More specifically, biological systems exhibit Robust Perfect Adaptation (RPA), i.e. the ability to maintain a constant output level despite changes in the input or the environment. RPA is essential for many cellular processes, such as chemotaxis, osmoregulation, and gene expression. In Control Engineering, RPA can be achieved by different mechanisms, such as integral feedback control, i.e. a specific implementation of Negative Feedback loops. However, the engineering of synthetic biomolecular circuits implementing an integral controller able to confer RPA in living cells is still an open problem, which if solved could a major impact in several applications. For example, in biofuels and recombinant protein production, RPA would ensure consistent production levels despite bioreactor conditions fluctuations; whole-cell biosensors would become more reliable, and cell therapies would gain safety within the complex human environment. Gene networks implementing an Antithetic Integral Controller in mammalian cells were still unavailable when the work described in this thesis started, and some attempts have only been presented very recently using mRNA pairs and inteins. In this thesis, I used a different approach, and I implemented the CRISPRaTOR, an Integral Controller based on the interaction between a CRISPR/Cas9-derived transcription factor and the recently discovered anti-CRISPR proteins, demonstrating its capability to achieve robust perfect adaptation in cell lines to various disturbances. I showcase precise, tunable, and robust control of a synthetic gene of interest and harness the programmable nature of the CRISPR/Cas9-derived transcription factor to apply this controller to an endogenous gene of interest. Additionally, I showcased an application of the CRISPRaTOR to enhance the linearity and robustness of a whole-cell biosensor of intracellular copper.

Introduction

1. Synthetic Biology: achieving control

1.1. From the discovery to the manipulation of the DNA

In the past few decades, the convergence of biology with engineering principles has given rise to the field of Synthetic Biology, an interdisciplinary discipline that aims to design and construct novel biological systems with desired functionalities. At the core of synthetic biology lies the manipulation and engineering of genetic circuits, enabling the reprogramming of living organisms for various applications, ranging from biofuel production to medical therapies. This is only made possible by the manipulation of the DNA, and, while our knowledge of inheritance began with the pioneering work of Mendel, it was after the discovery of DNA structure by Watson, Crick and Franklin in 1953[1] that we began to understand how to manipulate and engineer DNA for various purposes, revolutionizing fields such as genetics, molecular biology, biotechnology, and medicine. The insights gained from comprehending the double-helix structure of DNA laid the groundwork for several advancements that contributed to our current knowledge and technologies. In 1955, Arthur Kornberg discovered DNA polymerase, an enzyme responsible for catalysing the synthesis of DNA strands[2]. In the following years, the discovery of restriction enzymes by Arber, Smith and Nathans, paved the way to the first examples of DNA manipulation[3]. Restriction enzymes are indeed capable of cutting the DNA in specific sites and they subsequently made possible the creation of recombinant DNA molecules by Paul Berg in 1972[4]. He was the first one to combine DNA molecules in a controlled manner to create a novel genetic sequence. He used DNA coming from two different species, taking a fragment of DNA from the lambda bacteriophage, and joining it together with a DNA fragment coming from the simian virus SV40, linearizing DNA coming from both organisms with the restriction enzyme EcoRI. Other important advancements are the invention of DNA sequencing by Frederick Sanger in 1977[5], which allowed researchers to determine the order of nucleotides in a DNA sequence, and the invention of the gel electrophoresis in the mid-1970s by Edwin Southern, that enabled to analyze and purify DNA fragments based on their size[6]. All these discoveries, taken together with other important advancements in the field, allowed the creation of molecular cloning techniques for inserting DNA fragments into vectors, such as plasmids, enabling the replication and the engineering of specific DNA sequences. From the creation of recombinant DNA made by Berg, researcher started to assemble pieces of DNA in a rational way, creating tools that would have revolutionized the field, as for examples the pBR322 plasmid[7], a circular DNA fragment containing origin of replication for E. Coli, together with antibiotic resistance and multiple restriction sites that can be easily manipulated. This invention paved the expression of exogenous protein in a foreign organism, as it was used to express the human protein somatostatin in E. Coli in 1977[8], demonstrating the potential of recombinant DNA

technology for producing biologically active and relevant proteins. Some years later, in 1979, researchers managed to express the human protein insulin into E. Coli, by taking the human gene and placing it into a plasmid[9]. The resulting recombinant insulin was then used to treat diabetes, substituting the old method, when insulin was primarily sourced from animal pancreases, which posed challenges in terms of supply, purity, and potential allergic reactions in patients. Sourcing insulin from engineered bacteria could be considered the first application of Synthetic Biology, as rational DNA engineering was used to reprogram a living organism to have the desired output, hence the production of recombinant insulin. This was made possible by the complex and challenging process of cutting the insulin gene from the human DNA and placing it in the expression plasmid, requiring careful manipulation of DNA fragments, plasmids, and bacterial hosts, with the techniques available at the time. Things got easier some years later, with one of the most groundbreaking inventions of the last century, the Polymerase Chain Reaction by Kary Mullis in 1985[10], which led him the Nobel Prize for Chemistry in 1993. This technique allows the amplification of specific DNA sequences and revolutionized DNA manipulation by making it possible to generate millions of copies of a DNA fragments and it is indeed one of the most used techniques even today, almost 40 years after its first introduction. The amplification of specific DNA fragments allowed researchers to develop more complex and efficient DNA cloning techniques, that are still used today. At the beginning, plasmids were built by taking advantage of restriction enzymes, using the so called "cut and paste" method, that allow the exertion of one DNA sequence from a larger DNA fragment and the subsequent insertion in another DNA sequence, that needed to be compatible with the insert to clone. One of the main limitations of such technique is that restriction enzymes cut only at some specific sites in the DNA, hence it is not always possible to cut the DNA fragment of interest. PCR helped in overcoming this bottleneck, as this technique makes not only possible to amplify the fragment of interest, but also to add ad-hoc nucleotides, allowing the introduction of specific restriction sites at the end of the amplified DNA fragments, easing the process of "cut and paste". This resulted in the first standardized cloning method, the BioBrick[11], in which DNA parts are cloned in standardized cloning vector, rationally enclosed between specific restriction sites. The BioBrick became soon popular among Synthetic Biologist, establishing a growing database of standardized parts that allowed researchers to isolate the DNA fragment of interest and to ligate with other useful parts in a predictable manner, by exploiting compatible ends created by the restriction enzymes and the presence of different antibiotic resistance in the destination vector. Nowadays, cloning vector became even more versatile with the creation of techniques such as Golden Gate cloning[12] and Gibson assembly[13]. Golden Gate still relies on restriction enzymes, but it harnesses a specific class known as Restriction Enzyme Type IIs. These enzymes cleave DNA sequences outside of their recognition sites, resulting in 5' or 3' overhangs that can be composed of any nucleotide sequence. This feature greatly enhances the potential for standardization and allows for precise programming of the order in which DNA fragments are to be ligated together. Examples of kit developed using the Golden Gate standard are MoClo[14] and

EMMA assembly[15], with the latter containing standardized parts specific for their use in mammalian cells. The other mentioned method, the Gibson Assembly, is not as standardized as the Golden Gate, but it is more versatile, as it allows to ligate together whatever DNA fragments of interest, without relying on any restriction enzyme. It indeed relies on custom – created overhangs, added to the DNA fragments of interest by mean of the PCR technique, and to other enzymes that make the overhangs single – stranded (exonuclease) and that ligate the fragments together (ligase). The overhang introduced in one DNA fragment will be complementary to the overhang created in the DNA fragment that must be ligated afterwards, allowing the ligation of many DNA fragments together with high specificity. Furthermore, this method leaves the resulting DNA fragments *scarless*, simplifying the assembly of DNA coding sequences and facilitating the creation of DNA fragments that will encode novel fusion proteins. Modern cloning methods are now often integrated with chemical DNA synthesis techniques. The cost of DNA synthesis has significantly decreased in recent years, enabling the construction of custom DNA parts and their assembly into more complex configurations. This synergy between cloning and DNA synthesis technologies has opened new possibilities for manipulating biological systems, fostering ongoing exploration and innovation in the field[16].

1.2. Gene expression control

Achieving standardization and synthesis of DNA parts to encode novel function does not solely rely on technical advancements, but it also hinges on our understanding of DNA components and their precise functions within biological systems, as well as the discovery and the engineering of molecular tools that allow the precise control of gene expression. While the concept of coding sequences and the mapping of specific codons to amino acids[17], together with the discovery of promoters[18] had already emerged during the 1960s, the discovery of other DNA sequences that regulate gene expression was fundamental to advance the field of genetic engineering. For example, the concept of enhancers arose later, with the discovery that the presence of the SV40 DNA was able to increase the expression of the recombinant β-globin gene transfected in HeLa cells[19]. The availability of whole – genome sequencing data made possible to find these *enhancer* sequences also in animals such as worms, human and mice, underlying their constancy in genetic content[20]. Furthermore, new insights into the process of translation began to emerge with the identification of Ribosome Binding Sites (RBS). These are specific DNA sequences that enable transcribed mRNA to bind to ribosomes, a concept first discovered in bacteria by the identification of the Shine-Dalgarno sequence[21]. Notably, differences in translational initiation mechanisms between eukaryotes and prokaryotes were also elucidated[22] and this understanding played a crucial role in predicting and engineering different RBS to tune the translation process[23]. Another insight in advancing our understanding of gene expression was the concept of *promoter strength*. One of the first

findings emerged in 1986, when researchers found that the bacteriophage T7 polymerase – dependent promoter allowed high yield gene expression in E. Coli, producing high amount of mRNA that was saturating the bacterial translational machinery[24]. Similar approaches have been employed for expressing recombinant genes in mammalian cells using the CMV promoter, which is derived from the human Cytomegalovirus (CMV). This promoter has demonstrated its ability to achieve high yields in recombinant protein production[25]. The identification and isolation of other promoters, such as EF1α and PGK, along with the development of synthetic promoters like the CAG promoter, have played crucial roles in fine-tuning gene expression to achieve desired levels, as they demonstrated different strength across a variety of cell lines[26]. Although these promoters can transcribe various amount of mRNA, they all remain *constitutive*, meaning that they drive gene expression continuously, regardless of external signals or inducers. They're widely used when researchers need a stable and constant supply of a specific protein or when they want to study the effects of a gene's continuous expression. Inducible promoters are instead able to regulate gene expression in response of specific signal or inducer molecule, turning a gene of interest "on" or "off". They are indeed useful when there is the need to tune the timing and level of gene expression. One of the earliest examples is the lac promoter, derived from the lac operon of E. coli[18]. In the absence of lactose, the repressor protein, LacI, binds to the promoter, blocking RNA polymerase binding and transcription. In the presence of lactose, LacI binds to this molecule and undergoes a conformational change, freeing the DNA substrate for RNA polymerase access and turning the promoter on. Since lactose is part of the bacterial own metabolism, researchers have been using IPTG (Isopropyl β-D-1-thiogalactopyranoside), a molecule structurally similar to lactose but that cannot be metabolized by E. coli. By means of IPTG as an inducer, researchers have established a reliable way to express recombinant protein *on demand*. Efforts have been made to adapt bacterial IPTG-inducible promoters for use in mammalian cells, with successful expression of a functional LacI protein that was indeed able to bind to LacO sequences and block the expression of a gene. However, IPTG, despite being rapidly taken up by mammalian cells, exhibits slow induction kinetics and achieves only a moderate level of induction[27]. The first successful inducible system established in mammalian cells is the Tet-Off system, which was developed in 1992[28]. It is derived from the Tet Operon of E. Coli, in which the repressor TetR does not bind to the TetO sequence in its cognate promoter in presence of the antibiotic tetracycline, preventing transcription of the Tetracycline – resistance gene. The Tet-Off system has been engineered by fusing the Tet repressor protein (TetR) with the transcriptional activator Virion Protein 16 (VP16) derived from the Herpes Simplex Virus, resulting in the creation of the tetracycline-controlled TransActivator (tTA). Additionally, a custom promoter has been synthesized by combining the Tet operator (TetO) sequences with a minimal promoter derived from the CMV promoter. Consequently, in the presence of tetracycline, tTA cannot bind to the TetO-hybrid promoter, preventing transcription while in its absence the transactivator can bind to the promoter and initiate gene expression. Unlike the Lac Operon-derived

system, the Tet-Off system is constitutively active but can be turned off in the presence of tetracycline. Studies have demonstrated that TetR exhibits high specificity for the TetO sequence and has a strong binding affinity for tetracycline, whose chemical and physiological properties make the Tet-Off system a preferable alternative to the IPTG-inducible system. Using a luciferase gene as a reporter, it has indeed been demonstrated that it is not only possible to switch gene expression on or off but also to regulate it over up to five orders of magnitude by adjusting the concentration of Tetracycline. To address certain limitations of the Tet-Off system, such as the constant requirement for Tetracycline to maintain gene suppression, researchers devised a modified version of the Tet Transactivator (tTA) known as the Reverse TransActivator (rtTA)[29]. This innovative transcriptional activator was created by introducing specific mutations into the Tet Repressor (TetR) protein, rendering it incapable of binding to the TetO-hybrid promoter in the absence of the inducer. Importantly, a derivative of Tetracycline known as Doxycycline was introduced as the inducer molecule. The resulting Tet-On system operates in a manner opposite to the Tet-Off system, allowing for gene suppression under normal conditions and activation in the presence of Doxycycline. This system exhibits improved dose-response correlation compared to the Tet-Off system, making it a superior choice for engineering animal models, and achieving precise control over gene expression. Over the years, researchers have conducted mutations on rtTA to increase its affinity for Doxycycline and reduce leakiness, thereby achieving lower expression levels in the absence of the inducer molecule[30]. These advancements culminated in the development of the Tet-On TRE3G system owned today by Takara Bio, which now represents the state-of-the-art inducible gene expression system in mammalian cells. To expand the toolkit for controlling the expression of recombinant genes in mammalian cells, researchers have developed various methods over the years, often adapting bacterial regulatory elements for use in mammalian cells. Examples include the cumate-inducible promoter, derived from an operon and functioning similarly to the Tet-On and Tet-Off systems[31], promoters inducible by glucocorticoids and hormones[32], metals such as Zinc and Copper[33], as well as light-inducible promoters[34].

1.3. CRISPRi and CRISPRa

While control systems for recombinant genes have been widely available, regulating endogenous genes has proven more challenging. Traditionally, overexpressing a gene of interest often involved synthetizing and transfecting a plasmid encoding a copy of the endogenous gene under the control of a strong promoter, such as T7 in bacteria or CMV in mammalian cells. However, the landscape changed with the discovery of the CRISPR/Cas9 system, a breakthrough technology that revolutionized genetic engineering in various ways. It was already known that repeated sequences are present in the genome of bacteria and archea[35,36], defined as Clustered regularly interspaced

short palindromic repeats (CRISPR)[37], together with proteins defined as Cas (CRISPR Associated)[38,39]. The subsequent discovery that these sequences worked together with the Cas proteins, helped understanding that the CRISPR/Cas system confers adaptive immunity to bacteria and archea against the invasion of viruses[40]. The revolutionary discovery that fundamentally transformed our understanding of the CRISPR-Cas9 system occurred in 2012[41], leading to the Nobel Prize in Chemistry awarded to Emmanuelle Charpentier and Jennifer Doudna in 2020. They elucidated that a family of Cas proteins functions as RNA-guided endonucleases. In their pioneering work, particularly focusing on the Cas9 protein, they unveiled that it is guided by two distinct RNA molecules: CRISPR RNA (crRNA) and trans-activating CRISPR RNA (tracrRNA). These two RNA molecules hybridize to form a guide RNA complex that directs the Cas9 protein to precisely target and create a double-strand break in DNA sequences complementary to the crRNA. Additionally, Charpentier and Doudna identified specific domains within Cas9 responsible for cleaving the complementary and noncomplementary DNA strands, showcasing the system's versatility even when using a chimeric RNA composed of crRNA and tracrRNA. The advent of RNA-programmable DNA endonucleases marked a transformative leap in genome editing, enabling precise DNA manipulation by leveraging the cell's own repair mechanisms, such as Homologous Directed Repair (HDR) and Non-Homologous End Joining (NHEJ), to insert exogenous fragments into endogenous coding sequences. Prior to the emergence of RNA-programmable systems like CRISPR-Cas9, other molecular tools for targeted DNA cleavage existed, such as Zinc Finger Nucleases (ZFNs) and transcription-activator-like effector nucleases (TALEN)[42–44]. However, these tools posed challenges in programming the target DNA sequences and were often cost-prohibitive. The CRISPR-Cas9 system emerged as a significantly more versatile alternative. Its ease of programming, achieved by designing RNA sequences complementary to the target DNA, coupled with its cost-effectiveness, due to the unnecessary manipulation of the protein, garnered widespread attention within the scientific community. Researchers began to engineer and refine the system, making it simpler and expanding its applications beyond genome editing. Its efficacy was demonstrated in both in procaryotic and eukaryotic cells, together with the possibility to engineer the chimeric RNA composed of crRNA and tracrRNA as a single guide RNA (gRNA)[45]. Its use to edit the DNA of human cells was immediately explored, as well as the possibility to perform *in vivo* genome editing, paving the way for a revolution in the field of gene and cell therapy[46,47]. Moreover, by combining various gRNAs with the Cas9 protein it has been possible to target multiple DNA loci at the same time[48]. Protein engineering of the Cas9 protein have led to modify the wild-type Cas9 endonuclease, that cut both the DNA strands, into a nickase, just cutting one strand of the DNA[49]. This kind of approaches have also led to the development of the so called *dead Cas9* (dCas9), a Cas9 in which the nuclease domain has been mutated, but it has retained its DNA binding activity in the presence of a guide RNA (gRNA). The dCas9 can be utilized as a fusion protein with transcriptional activators, repressors, or epigenomic modifiers to achieve precise control over these

enzymes at targeted genomic locations. This versatility has paved the way for several key techniques widely used today. The fusion of dCas9 with epigenomic modifiers has proved invaluable for gaining insights into the role of epigenetic modifications in chromosomal structure, while the fusion of dCas9 with transcriptional repressors and activators has given rise to two prominent techniques: CRISPR interference (CRISPRi) and CRISPR activation (CRISPRa) (**Figure 1**). CRISPRi is employed for gene silencing, while CRISPRa is used for gene overexpression. This remarkable capability allows for the direct control of endogenous genes in both bacterial and mammalian cells using a sequence-specific platform and, since the dCas9 can be targeted to any DNA sequence of interest, it can also be employed to exert control over genes driven by synthetic promoters. For CRISPRi in bacterial cells, simply redirecting dCas9 to a promoter of interest is sufficient to prevent RNA polymerase binding, thereby inhibiting gene expression by preventing transcription and subsequent translation[50]. In contrast, mammalian cells present a more complex scenario where dCas9 alone is often insufficient to efficiently suppress gene expression. However, researchers have achieved high repression levels, up to 15-fold, by fusing dCas9 with transcriptional repressors such as the Krüppel-associated box (KRAB) domain derived from Kox1[51]. Furthermore, additional studies have enhanced the efficacy of CRISPRi by combining the KRAB domain with epigenetic factors like MeCP2, resulting in repression levels reaching up to 250-fold for endogenous genes and up to 400-fold when applied to genes controlled by synthetic promoters[52]. The same principles used for CRISPRi in mammalian cells have been used when engineering the CRISPRa system to overexpress a gene of interest. Initially, the dCas9 has been fused to 4 copies of the transcriptional activator VP16 or to the well-characterized p65 activation domain. The resulting dCas9-VP64 and dCas-p65AD, transfected in Hek293T cells together with the proper gRNA, were able to drive overexpression of a GFP under the control of the yeast – derived UAS promoter up to 12- and 25-fold, respectively, scoring the importance of the transcriptional activator used to achieve efficient gene overexpression[51]. The programmable dCas9-VP64 transcription factor has been later used to overexpress endogenous genes, by designing gRNA complementary to the endogenous gene promoter, achieving fold activation from tens to thousands of times, depending on the gene to overexpress. Moreover, combining more gRNAs that target the same promoter in different regions, it is possible to increase the fold activation[53]. Efforts have been made also to understand the parameters for gRNA design and to target it to precise loci of the promoters. Furthermore, genome – scale gene overexpression has been achieved, together with multiplexed gene overexpression, when transfecting more gRNA towards different promoters, together with the dCas9 – bases transcription factors[54,55]. The understanding that transcriptional activators could significantly impact the level of gene overexpression pushed researchers to engineer novel transcriptional domains. One notable advancement involved the fusion of the VP64 activator, composed of four copies of the VP16 domain, with the activation domains p65 and Rta, creating the potent VPR activator. Subsequently, this hybrid transcriptional activator was fused to the dCas9 protein[56]. The

outcome was the dCas9-VPR transcription factor, which exhibited a remarkable 22- to 320-fold increase in activation compared to dCas9-VP64 in Hek293T cells. Furthermore, its effectiveness was tested in multiplexed gene overexpression experiments, including overexpressing endogenous genes in *Saccharomyces cerevisiae*, *Drosophila melanogaster* S2R+ cells, and *Mus musculus* Neuro-2A cells. Researchers also explored the contributions of the VP16, p65 and Rta activation domains, emphasizing the essential role of all three for achieving such high levels of activation and determining the optimal order for fusing them together. Additionally, other potent transcriptional activators have emerged, such as the Synergistic Activation Mediator (SAM), where transactivation domains are recruited to the target site through the engineered sgRNA scaffold[54], and the SunTag system [57], which employs a peptide array to recruit effector proteins fused with antibodies. Comparisons among these three transcriptional activators fused to dCas9 revealed their capability to achieve gene overexpression within a similar order of magnitude in Hek293T cells. Multiplexed gene overexpression was achieved with all three activators tested. Furthermore, it was confirmed that a negative correlation exists between the basal expression of a target gene and the extent of achievable overexpression. Experiments conducted in various cell lines indicated some variations in performance, with HeLa cells demonstrating higher overexpression with the SAM system, whereas in U-2OS and MC7 cells, VPR and SunTag showed better performance. In cells derived from *Drosophila melanogaster* and *Mus musculus*, all three activators exhibited similar performance levels, contingent on the specific target gene under consideration[58]. The potential for achieving substantial fold activation and repression with CRISPRa and CRISPRi, coupled with the ability to regulate multiple genes simultaneously, has paved the way to comprehensive screens to investigate the combined effects of multiple genes. This approach has been important in unravelling the functions of specific genes and gaining insights into the mechanisms of various biological pathways[59–61]. Both CRISPRi and CRISPRa are being investigated for various applications, including therapeutic ones. CRISPRi offers enhanced specificity compared to RNAi, as it has been demonstrated to be more efficient in silencing miRNA clusters when compared to short hairpin RNAs and short interfering RNAs[62]. Multiplexed silencing of genes related to neurodegeneration, such as SNCA, MAPT, HTT, and APP, has been achieved in cancer cell lines by leveraging dCas9 without the need for additional repressor domains[63]. Furthermore, preclinical studies have explored the potential of CRISPRi in mice. For example, dCas9-KRAB has been utilized to repress ΔNp63, a potent oncogenic variant of the tumor suppressor TAp63[64]. Mouse models of Retinitis Pigmentosa have also been employed to assess the ability of CRISPRi to inhibit the expression of the Nrl gene, which, when silenced, can reprogram rod cells into cone-like cells[65]. Also CRISPRa enables cell reprogramming, including the conversion of somatic cells into induced Pluripotent Stem Cells (iPSCs) and iPSC differentiation[66–68]. For example, dCas9-VPR-mediated upregulation of NEUROD1 has been used to convert iPSCs into neurons[69], and the overexpression of Ngn2 and Isl1 has been employed to transform mouse astrocytes or embryonic fibroblasts into motor neurons[70]. These results represent the possibility of

using gene therapy to restore neural cells following brain or spinal damage. CRISPRa has also been applied to overexpress genes like Sim1 and Mc4r in mice to rescue obesity-related phenotypes[71], highlighting its potential as a valuable alternative for treating diseases where gene silencing has led to disease phenotypes. However, there are some limitations to CRISPRa. It requires constant expression of the dCas9-based transcription factor to sustain overexpression of the gene of interest. Additionally, concerns include the potential immunogenicity of dCas9, the transcriptional domain, and the challenges associated with delivering this complex system into the human body. Another important consideration is the need for fine-tuning gene expression levels to avoid potential toxicity in certain cells[72].

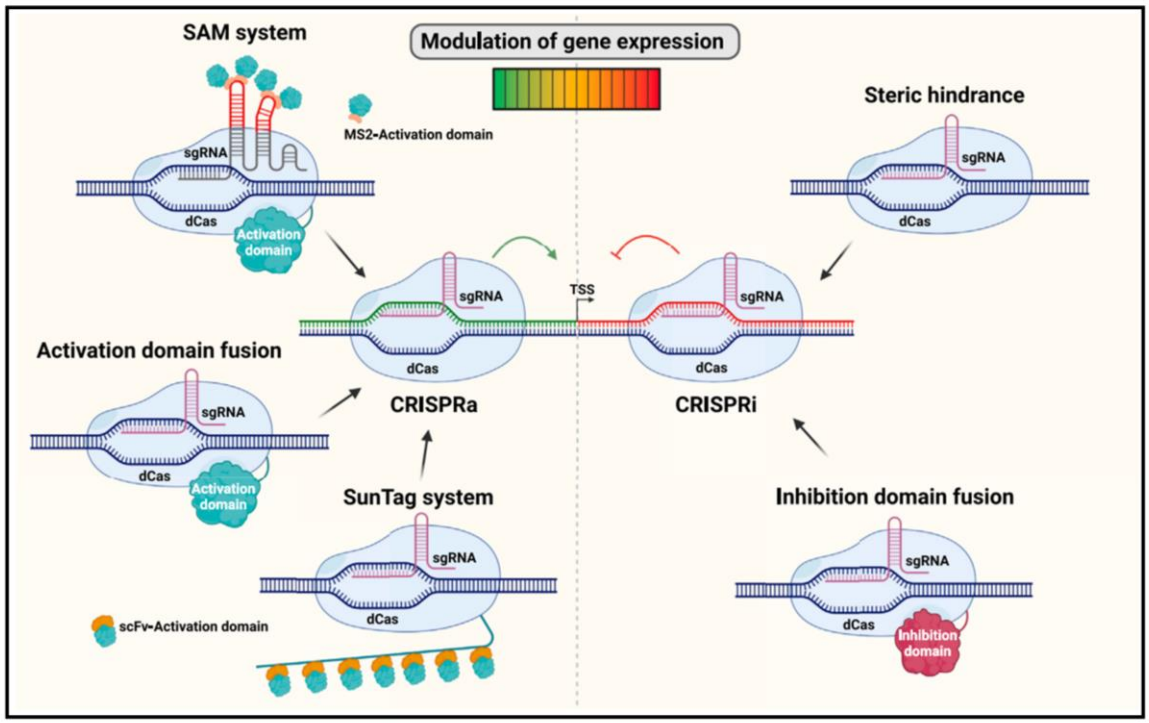

Figure 1 – CRISPRa and CRISPRi. Schematic representation of the CRISPRa and CRISPRi systems. In CRISPRa, the dCas9 protein is fused to transcriptional activators, such as SAM system, VPR or the SunTag system, to start transcription when directed towards a promoter. In CRISPRi, the dCas9 is used alone, mostly in bacteria, or fused to transcriptional inhibitors such as KRAB. When directed to a promoter of interest, the dCas9 stop transcription avoiding the recruitment of transcription factor, by steric hindrance or compacting the chromatin through transcriptional repressors, rendering it inaccessible. Figure from [73]

2. Synthetic Biology: engineering living systems

2.1. Gene circuits

The progress made in DNA manipulation, together with the precise identification of the necessary parts to rationally retrieve and engineer gene expression, led to new, fundamental questions, hence how the different components interact with each other and if they could somehow be programmed to behave in a predictable manner. While the toolbox of genetic tools has expanded, it has become apparent that these tools alone are insufficient for precise control and tuning of gene expression. Living organisms rely on intricate pathways involving various molecules that interact in complex ways. It is here that, in the realm of modern biology, the fusion of engineering principles with biological system has given rise to a transformative field known as Synthetic Biology, with genetic circuits serving as its architectural blueprint. In essence, they function as biological counterparts to electronic circuits, albeit composed of biological components. While electronic circuits are built on silicon chips or other semiconductors materials and are made of components such as resistors, capacitors and transistors, biological circuits are implemented in living cells, and are composed of DNA sequences, RNA molecules and proteins, that interact together with similar dynamics. Electronic circuits process information in the form of electrical signals, voltages, and currents, utilizing Boolean gates and binary code for data processing. In contrast, biological circuits process information encoded within DNA sequences through the actions of RNA and proteins[74]. The translation into synthetic biology allows a gene to be turned on or off when determined conditions are satisfied and leverages on promoter that control the desired output that is activated or repressed when other regulatory molecules such as effector proteins or RNAs are present or not in the cells, or when chemical inputs are provided. This concept allows to program decision – making gene network that can be implemented in living system and to make cells perform the necessary tasks. Several predictable biological circuits have been successfully implemented in both bacterial and mammalian cells, for example oscillators, toggle switches and logic gates. Oscillators are genetic circuits that generate repetitive, oscillatory patterns of gene expression over time. These oscillations are achieved through specific molecular interactions within a feedback loop, often involving components like activators and repressors[75,76]. After the initial development of oscillators in both bacterial and mammalian cells, researchers have optimized these systems to achieve highly regular and robust oscillations[77]. Additionally, these oscillators have found application in studying complex bacterial population dynamics during gut colonization in mice[78]. Potential application of these circuits involves controlled drug delivery in mammalian cells. By linking drug release to oscillatory behaviour, researchers can develop drug delivery systems that release medications in a pulsatile manner, mimicking natural hormone secretion. Another noteworthy genetic circuit is the toggle switch, which represents one of the earliest synthetic gene networks created without the need for specific parts[79,80]. This genetic device consists of two stable states that can be switched between each other under chemical induction. Typically, a toggle switch involves two mutually inhibitory

components, and its arrangement allows it to exist in one of two states: either the first component is active while the second is repressed, or vice versa. Once set to one of these two states, the toggle switch remains in that state until another signal triggers it to switch to the other state, a property known as genetic memory. This feature has been exploited to engineer bacteria able to sense tetrathionate, a marker of inflammation in the mouse gut, and to retain memory of exposure[81]. Logic gates emulate the logical operations found in electronic circuits but are implemented using genetic elements within living cells. These gates process biological signals, typically encoded in the form of gene expression levels or molecular interactions, to produce specific output responses based on predefined logical rules. Genetic logic gates can perform logical operations such as AND, OR, NOT, NAND, and more, allowing the construction of complex genetic circuits that respond to various inputs in a programmable and predictable manner. Logic gates have been successfully established in both bacterial and mammalian cells[82,83]. They are currently under exploration for the development of intelligent cell therapies, which release their output only when exposed to multiple inputs. An example of this application is smart CAR-T cells, engineered to initiate the immune response exclusively in the presence of multiple antigens. This approach enhances specificity while diminishing off-target[84–86]. The implementation of the gene circuits involves complex regulatory networks that exhibit logic reminiscent of their electronic counterparts. These regulatory networks, controlling gene expression, have been identified in organisms ranging from bacteria to mammals and have been subsequently engineered in living organisms. Furthermore, it has been observed how these networks contain a series of recurring regulation and connectivity patterns, called network motifs. Examples of network motifs with their own characteristics are Negative Feedback Loop and Feedforward Loop[74], able to increase feature in gene expression such as robustness, linearity, noise – filtering and fold change[87–91]. By combining different parts interacting together, resembling known and new network motifs, researchers implemented genetic circuits in living cells to make gene expression predictable and controllable.

2.2. Robustness and Negative feedback loop

Robustness is a fundamental property that enables biological systems to maintain their stability and functionality despite ongoing fluctuations in biochemical parameters. These parameters govern the behaviour of biological systems and encompass genetic factors, including mutations that may affect the interactions among DNA, RNA, and proteins, all collaborating to define the system's state. Moreover, non-genetic factors involve variations in the internal and external microenvironment, such as metabolic changes, nutrient availability, and shifts in parameters like temperature. While genetic mutations are inherently infrequent, alterations in internal and external parameters are pervasive and continuous. Consequently, biological systems must possess the capacity to operate effectively across a broad spectrum of parameter values, rather than being limited to a narrow range

of conditions. This adaptability is essential for their survival and functionality. These observations hold true across a wide range of biological systems, spanning from the initial stages of gene transcription and subsequent protein translation to the intricate mechanisms that maintain homeostasis within complex organisms. Therefore, explaining robustness goes beyond examining individual components within a system, requiring analysis of their complex architecture and of the interactions between them[92–94]. A good example is the decision-making of λ phage in entering the lysis or lysogeny pathways. It was once believed to be influenced by the affinity of different transcription factors to promoters. However, it has been demonstrated that this mechanism instead relies on a combination of positive and negative feedback loops and it indeed exhibits resistance to point mutations in the promoter[95–97]. Another significant example can be seen in the chemotaxis of E. coli, which has been found to operate independently of ligand concentration. It occurs across a range of different concentrations due to integral internal feedback mechanisms that lead to perfect adaptation[98]. Similar phenomena have also been observed in higher organisms, such as Drosophila Melanogaster, where polarity segmentation remains resistant to changes in its initial stages. These same principles extend to morphogen-pattern formation[99,100]. In humans, diseases such as diabetes and cancer can hijack the internal systems responsible for ensuring adaptation, thereby promoting the disease state[101,102]. This highlights the critical role of circuit robustness in both normal biological processes and pathological conditions. It has been observed that robustness can be conferred by different network motifs, such as feedback loops and feedforward loops. Robustness to initial changes observed in Drosophila Melanogaster is attributed to positive feedback loops, while the resistance of E. coli chemotaxis is due to negative feedback loops. In a feedback loop, the output can influence the input. If species X serves as the input and species Y as the output, in a positive feedback loop, Y positively regulates X, for example, acting as a transcriptional activator. In contrast, in a negative feedback loop, species Y represses X, such as in the case of a transcriptional repressor. A feedback loop confers robustness by sensing the output and adjusting it to the desired state. A feedforward loop comprises three species: X, Y, and Z. Species X controls both Z and Y, and Y, in turn, controls Z. The type of regulation, whether negative or positive, that X exerts on Z and Y, and the regulation of Y on Z, define the specific type of feedforward loop[74]. While feedback loops confer robustness by monitoring the output and making corresponding adjustments to the input, feedforward loops operate by sensing disturbances and executing countermeasures on the output to counteract them[94]. However, it is worth noting that negative feedback loops are more commonly found as sources of robustness. Moreover, negative feedback loops are known to impart additional properties to gene networks, such as linearity and predictability, both of which arise as consequences of robustness. The countermeasures enacted by negative feedback loops in rejecting disturbances contribute to a linear relationship between input and output, enabling the prediction of the final output when the input is known.

2.3. Implementation of robustness

The understanding of how robustness is achieved in living systems posed the next fundamental question in synthetic biology: how can we engineer a gene network to confer robustness to changes? Natural robust systems consist of specialized components, and reproducing such properties in engineered systems presents unique challenges. However, achieving this robustness is fundamental for the successful application of engineered systems in real–life situations. As applications of synthetic biology devices continue to expand, it becomes increasingly vital to enable these devices to withstand changes in both internal and external microenvironments. This ensures their reliable performance across a wide range of parameters, enhancing their versatility and adaptability for diverse applications. While engineered microorganisms and mammalian cells hold great potential, the expression of synthetic cassettes can often lead to metabolic stress and burden, potentially impairing cell growth and payload expression[103]. Constructing robust gene networks that decouple the expression of synthetic cassettes from the host cells' own metabolism can significantly enhance performance and predictability under varying conditions. Furthermore, this approach can confer resistance to external perturbations. In biotechnology, engineered cells play a crucial role in producing biofuels, pharmaceuticals, and industrial chemicals. These applications require engineered organisms to maintain consistent performance, even in the face of changing environmental conditions, substrate availability, or metabolic stress. For example, in antibody production, cells are often genetically engineered to efficiently produce the desired protein[104]. However, bioreactor conditions can fluctuate, making it essential to ensure that engineered cells consistently yield the intended products for cost-effective and scalable production. Robustness is equally important in the development of whole-cell biosensors, where cells are engineered to sense and report analyte concentrations in the environment. It enhances the reliability of biosensors and contributes to a correct input-output relationship[105]. In the medical field, synthetic biology holds great promise in the development of cell therapies, where engineered cells are designed to deliver therapeutic genes to patients. These therapies must function reliably within the complex and dynamic environment of the human body, underscoring the necessity for robust genetic circuits capable of withstanding biological variability and immune responses[106]. For these reasons, numerous efforts have been dedicated to engineering robust gene networks, with a recurrent focus on harnessing the well-established negative feedback loop. A pioneering study validated the efficacy of the negative feedback loop by implementing a genetic circuit in Escherichia coli (E. coli)[88]. In this research, the scientists employed the TetR repressor protein in conjunction with a lambda promoter containing TetO sites to drive its transcription. Consequently, in the presence of Tetracycline, TetR could hinder its own transcription, performing negative feedback control. To evaluate the system's performance, TetR was fused with a Green Fluorescent Protein, and open-loop configurations were constructed through TetR mutations or alterations in the promoter's binding regions, thus impeding TetR binding and disrupting the feedback loop. Experimental findings, supported by quantitative

analyses, illustrated the enhanced robustness conferred by the negative feedback loop. Specifically, it demonstrated increased resistance to perturbations and a narrower, more uniform distribution of fluorescence. However, it is noteworthy that under specific conditions, autoregulatory systems of this nature may not consistently offer robustness. A similar study, which resembled a Toggle Switch and featured a negative feedback loop, was conducted in mammalian cells[107]. Here, the transcription factor tTA, regulated by its cognate promoter CMVTet, drives its own transcription along with a fluorescent reporter in the same cistron. Additionally, it governs the expression of a human miRNA, also controlled by the CMVTet promoter within a separate cassette. The miRNA can inhibit the tTA-reporter mRNA by binding to four complementary sites added to the mRNA's end. This setup establishes a dual feedback mechanism: the miRNA performs negative feedback, inhibiting translation, while tTA performs positive feedback, promoting its own transcription. Consequently, the authors termed this circuit a "Positive Negative Feedback Loop" (PNFL). For comparison, a control circuit was constructed without the presence of the miRNA, resembling a "Positive Feedback Loop" (PFL). Through quantitative analysis of fluorescent reporter levels and their distribution, the authors demonstrated reduced protein noise and lower fluctuation levels in the PNFL compared to the PFL. These findings underscore the significant role of miRNA-mediated negative feedback in achieving these outcomes. Subsequently, similar strategies have been employed, utilizing miRNAs and RNA Binding Proteins (RBPs) to implement negative feedback mechanisms for controlling protein translation, demonstrating reduced metabolic burden, enhanced robustness, and linear expression profiles for exogenous genes[108,109]. Another strategy involved the engineering of the bacterial histidine kinase EnvZ and its phosphatase OmpR for their use in mammalian cells, creating a synthetic covalent modification cycle through a negative feedback loop between the two proteins[110]. Efforts have also been directed towards enhancing robustness through the engineering of feedforward loops. In one approach, a promoter drives the expression of both a fluorescent output and the endoRNase CasE, capable of cleaving the mRNA at a specific target site. By strategically placing this target site within the mRNA of the output protein, the researchers devised an incoherent feedforward loop that demonstrated resilience to resource competition when co-expressed with another fluorescent protein. Furthermore, this circuit exhibited robustness to variations in DNA copy number when different amounts of the circuit were transfected[111]. Similar results have been obtained through the implementation of a feedforward loop leveraging on miRNA, demonstrating how feedforward loops are indeed suitable to achieve robustness[112]. However, this topology achieves robustness by sensing and responding to disturbances, thus requiring a sufficiently descriptive model of how these disturbances affect the output. In contrast, negative feedback loops don't impose such a requirement and possess the potential to confer robustness against uncertainties inherent to the controlled system itself[94](**Figure 2**). When thoughtfully designed and integrated, feedback controllers can even achieve robust perfect adaptation (RPA).

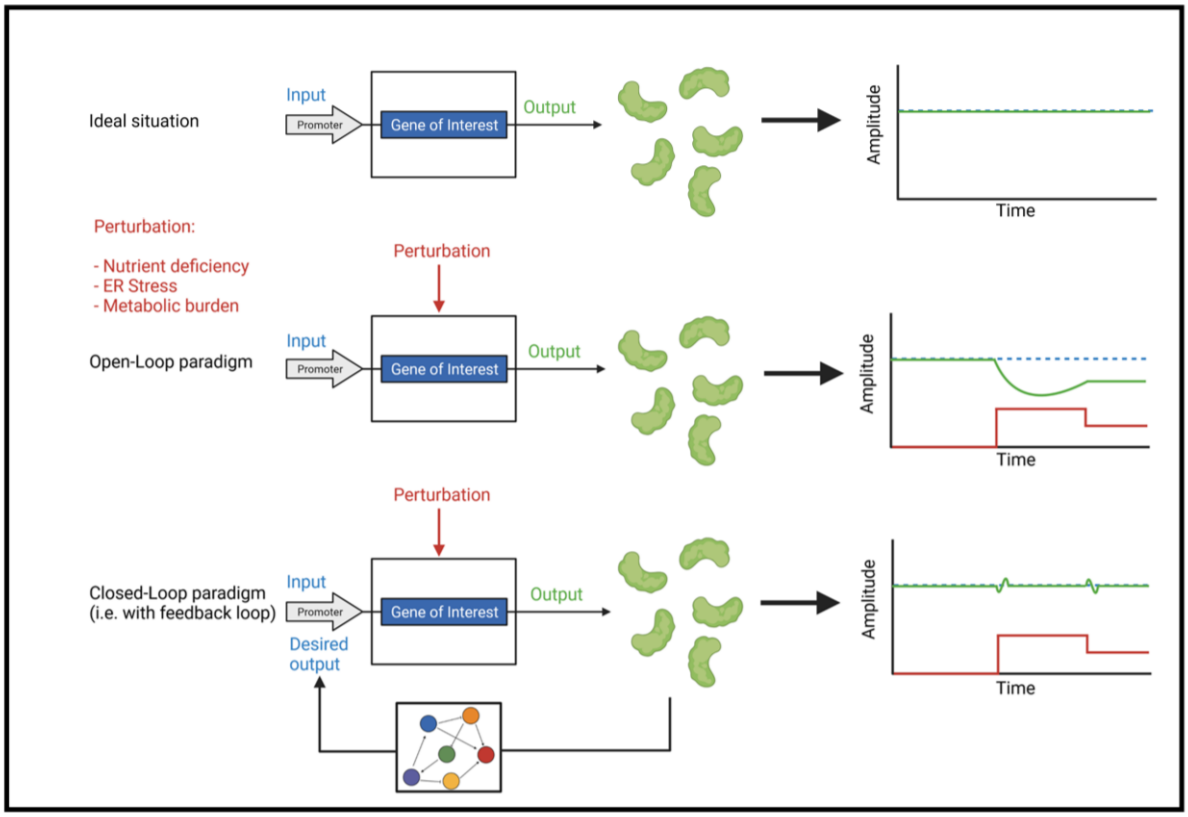

Figure 2 – Robustness conferred by negative feedback loop. Schematic representation of robustness and feedback. In an ideal scenario, where a gene promoter serves as the input and the resulting protein is the output, it would be expected to have constant expression of the gene over time. However, in an uncontrolled, open-loop system, perturbations such as nutrient deficiencies, ER stress, metabolic burdens, as well as interactions with the internal and external microenvironment, can reduce the protein output. In a closed-loop system, which operates as a feedback mechanism, the output is adjusted based on the input. When protein production decreases due to perturbations, the input is modified to counteract this decrease. A negative feedback loop can be properly designed and engineered to achieve Robust Perfect Adaptation (RPA).

2.4. Robust perfect adaptation and the Antithetic Integral Controller

While robustness is the property that allows a system to maintain its functionality despite changes in the internal or external environment, Robust Perfect Adaptation (RPA) is a specific form of robustness in which a biological system not only maintains its functionality but also generates an output that returns to its fixed, unperturbed level, defined as the *set point*, without the needing to tune the system's parameters. Indeed, RPA is a network property independent of rate constant values, while non-robust perfect adaptation requires a fine-tuning of rate constant values[113,114]. Examples of RPA in nature are evident in both calcium homeostasis within mammalian cells[115] and the previously mentioned chemotaxis in E. Coli[98,116]. In the case of chemotaxis, when an attractant is initially introduced uniformly, there is a sharp reduction in the frequency of tumbles in bacterial movement. However, over time, the system adapts to the attractant's concentration prior to its introduction. This adaptation is achieved through the coordinated action of the enzymes CheR and CheB. CheR plays a pivotal role by methylating and activating surface receptors. These activated

receptors, in their active states, subsequently phosphorylate flagella motors, leading to tumbling. Notably, receptors are most active when unbound to an attractant ligand, correlating tumbling activity with external ligand concentration. Conversely, when receptors bind to a ligand, their phosphorylation activity diminishes. The key to adaptation lies in the actions of CheB, which serves as a demethylase, inactivating the receptors. This inactivation enables CheR to methylate the receptors once more, allowing the system to respond to the new ligand concentration. Significantly, CheB exhibits higher activity when receptors are heavily methylated, creating a correlation with receptor activity[114,117]. Studies have demonstrated that this adaptation is robust even when there are changes in the concentration of the network's proteins. Later it has been demonstrated how this robustness can be attributed to the presence of integral feedback loops within the system[118]. Similar integral feedback mechanisms have been identified in other biological processes, such as the nuclear enrichment of the MAP kinase Hog1 in *Saccharomyces cerevisiae*[119]. In control engineering, an integral controller is employed to achieve homeostasis. This controller works by continuously integrating the error signal over time, which represents the difference between the desired set point and actual value of the output. It then utilizes this accumulated error to adjust the control input to change the system behaviour. In contrast to proportional controller, which focuses on the real-time correlation between input and output and adjusts output based on the current error, integral feedback addresses cumulative errors over time. It does so by adjusting the control signal based on the total accumulated error, rather than just the current error[120]. This means that a system driven by a proportional controller will show a certain degree of adaptation to disturbances, but this adaptation will not be perfect. Motifs ensuring robust perfect adaptation have been reported in a negative feedback loop with a buffering node and an incoherent feedforward loop with a proportioner node[91]. However, the presence of integral feedback in nature, together with their wide implementation in engineering application, pushed researchers to find a solution towards this direction. A potential implementation of an integral controller was proposed in 2016, leveraging two controller molecular species identified as Z_1 and Z_2[121] **(Fig. 3a)**. In this kind of system, called the Antithetic Integral Controller, Z_1 produces another species X_1, proportional to its amount, that, when active as X_I, promotes the production of Z_2. The two controller species Z_1 and Z_2 must annihilate each other in a way that this annihilation doesn't result in a physical destruction of the two species, rather than in their deactivation, for example with a formation of an inactive dimer. This reaction calculates the integral of the error between the desired output, recorded by Z_1, and the actual output, represented by Z_2 that is proportional to X_I, hence the controlled species. Briat et al., the authors of this study, mathematically demonstrated that the amount of the controlled species X_I will only depend on the ratio between the production rates of two controller species Z_1 and Z_2, independently from the other network's parameters, therefore a system equipped with this controller will exhibit set – point tracking and Robust Perfect Adaptation. The authors hypothesized that such controller species could be a component of the RNA polymerase from E. Coli, called sigma factor 70, σ^{70}, and its regulator anti-sigma factor, σ^{-70}, which binds σ^{70} very tightly, preventing its participation in the core

of the RNA polymerase enzyme and preventing transcription. Moreover, σ^{-70} expression is driven by a σ^{70} promoter, suggesting the possible implementation of the system. Subsequently, the *in vitro* realization of the Antithetic Integral Controller was developed, exploiting the interaction between σ^{70} and σ^{-70} in E.Coli[122]**(Fig. 3b)**. In this setup, σ^{70} is regulated by the HSL (Homoserine Lactone) inducible promoter pLux and it drives the transcription factor AraC, together with the fluorescent reporter SGFP (superfolder green fluorescent protein) under the control of the promoter SigW, dependent from σ^{70} itself. Both AraC and GFP are fused with the Pdt degradation tag, rendering them susceptible to degradation when exposed to the *Mesoplasma florum* protease Lon (MfLon). MfLon expression is controlled by another cassette, utilizing the anhydrotetracycline (aTc)-inducible promoter pTet, offering precise control over the disturbance to the system. The transcription factor AraC, in the presence of ARA (arabinose), induces transcription of the promoter pBAD, that drives the expression of σ^{-70}, which closes the loop sequestering σ^{70}. The amount of AraC, responsible to regulate the transcription of σ^{-70}, is determined by the amount of σ^{70}. A reduction in the level of AraC leads to a corresponding decrease in σ^{-70}, resulting in reduced sequestration of σ^{70} and consequently increased transcription of AraC. This rebalancing mechanism restores equilibrium and returns the system to the unperturbed state. The authors demonstrated the system's robustness to varying levels of perturbation, in terms of degradation of AraC and its reporter SGFP. Furthermore, they proved this feature tuning the system at different set points, adjusted with HSL and ARA. This work was the demonstration that the Antithetic Integral Controller can confer Robust Perfect Adaptation, opening new avenues for its application. Notably, the same research group has recently extended this concept to mammalian cells, employing two distinct strategies. In one of the two, the molecular species Z_1 and Z_2 are represented by a pair of sense and antisense mRNA[123], encoding the transcription factor tTA. In this design, a constitutive promoter drives the transcription of the tTA mRNA, that is subsequently translated into the tTA protein. The tTA protein binds to its cognate promoter CMVTet, that drives the transcription of the antisense mRNA of the tTA itself. The researchers monitored tTA by fusing it with a GFP marker and introduced perturbations into the system using the Asunaprevir-sensitive degradation tag, Smash, demonstrating Robust Perfect Adaptation. Another approach leveraged split inteins to perform the sequestration reaction[124]. Split inteins are proteins domain that can heterodimerize and perform protein splicing, forming a new peptide bond. The authors engineered various transcription factors suitable for mammalian cells with the split inteins to perform the sequestration reaction, once again showcasing Robust Perfect Adaptation in mammalian cells. However, it's worth noting that both approaches have their limitations. The use of RNA pairs could potentially trigger the cells' immune response, as double-stranded RNAs are generated during viral replication. Meanwhile, the split inteins approach necessitates the engineering of transcription factors, suggesting that the strategy might not be straightforward. These limitations suggest the need for further exploration and development of alternative Antithetic Integral Controllers in mammalian cells.

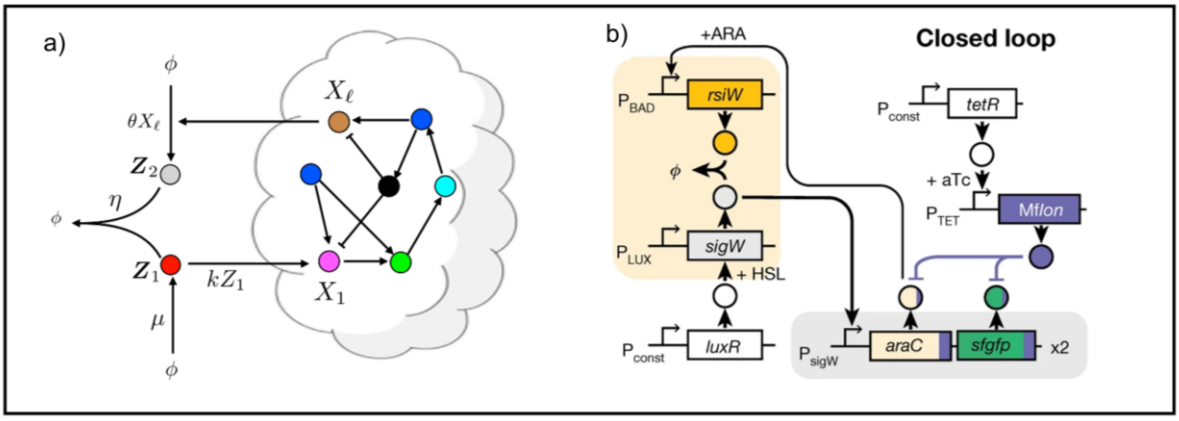

Figure 3 – The Antithetic Integral Controller (AIC): **a)** Schematic representation of the Antithetic Integral Controller. The species Z_1 acts as an activator of the species X_1, which, when active as X_a, drives the expression of the species Z_2, that, in turns, annihilates with Z_1, inhibiting it. The annihilation reaction between Z_1 and Z_2 calculates the integral of the error between the desired and the actual output[125] **b)** Implementation of the AIC in bacteria. The RNA polymerase component σ^{70}, that represent Z_1, is inducible with HSL, and drives the transcription of AraC, that represent the species X_1. When translated into a protein, AraC is active under the induction of arabinose, becoming the species X_1, and can express $\bar{\sigma}^{70}$, which represents the species Z_2. The latter binds and inhibits σ^{70}, thus closing the feedback loop. The amount of AraC and of its reporter *sgfp* can be reduced when expressing Mflon in a dose-dependent matter with Tetracycline. When the amount of AraC decreases, so will do the amount of $\bar{\sigma}^{70}$, freeing part of σ^{70}, that will express AraC again, allowing the system to come back to the setpoint[126]. Figures adapted from [125,126]

Results

3. Building the CRISPRaTOR

One of the main challenges for the implementation of an Antithetic Integral Controller (**AIC**) in mammalian cells is the choice of the two molecular species participating in the sequestration reaction (**Fig. 4a**), one acting as the *Activator* (Z_1) and the other one being the *Inhibitor* (Z_2). In particular, the activator needs to drive the expression of a gene of interest (**GOI**, X1, active as X_1), which, in turns, activates the Inhibitor, that quenches the activity of the Activator. The AIC is a negative feedback loop that regulates the expression of the Gene of Interest (GOI). The GOI also controls the expression of an Inhibitor, which quenches the activity of an Activator. The Activator, in turn, drives the expression of the GOI. Therefore, when the expression of the GOI decreases due to changes in the intra- or extracellular environment, the Inhibitor expression also decreases, allowing more Activator to be active. The active Activator then increases the expression of the GOI, restoring it to its original level. It can be mathematically demonstrated that the two molecular species of interest should be stable and ideally get inactivated only when they are bound together[121,127]. Moreover, taking in consideration proteins as the molecular species, the Activator needs to be a Transcription Factor, while the Inhibitor needs to be a protein that binds to the Activator, preventing it from binding its cognate DNA sequence. Additionally, as the GOI needs to activate the Inhibitor, it must also function as a Transcription Factor to facilitate a straightforward strategy. Here, I designed the **CRISPRaTOR**, a protein – protein based AIC and I experimentally built it in mammalian cells. The CRISPRaTOR implements a negative feedback loop by means of a programmable transcriptional regulator based on the (CRISPR)/Cas9 system, acting as the Activator, and the recently characterized anti-CRISPR proteins (Acrs), acting as the Inhibitor. Specifically, the nuclease-deficient Cas9 (dCas9) is fused to the transactivation domains VP64, p65, and Rta (VPR) linked in tandem, and it encodes the *activator*, while the Anti-CRISPR protein AcrIIA4, which has been shown to efficiently inhibit VPR-dCas9 driven transcriptional activation in mammalian cells[128], encodes the *inhibitor*. By fusing the Transactivation domains to the dCas9 protein, the latter becomes a Transcription Factor that can bind any DNA sequence of interest by designing a fragment of RNA, called Guide RNA (**gRNA**), complementary to the DNA sequence where the Cas9 protein needs to bind. Nevertheless, the same principle is appliable to engineered variants of the Cas9 protein, as its nuclease deficient variant dCas9, making the fusion protein VPR-dCas9 a versatile transcription factor that can activate any promoter of interest[56]. To express the Gene of Interest (GOI), I exploited a set of three synthetic promoters that had previously been demonstrated to be activated by synthetic transcription factors[129,130], harbouring different numbers of repeats of an artificial sequence of 22 bps that can be bound by VPR-dCas9 in the presence of the cognate gRNA sequence. These three promoters harbour 1 binding site for the gRNA_AB (*1AB_pMin*), 10 binding sites for the same gRNA_AB (*10AB_pMin*) and 7 binding sites for another cognate gRNA called gRNA_B (*7B_pMin*), before a minimal promoter. They were cloned upstream

a fluorescent mCherry protein and the resulting plasmids (1AB_pMin_mCherry, 7B_pMin_mCherry and 10 AB_pMin_mCherry) were transfected in Hek293T with or without the Activator VPR-dCas9 with the appropriate gRNA (**Fig. 4b**), to evaluate fluorescence, thus gene activation, by flow cytometry. For this experiment, the threshold to quantify the fluorescent signal was established using wild type, untransfected Hek293T cells, which only exhibit autofluorescence (data not shown). As shown in **Fig. 4c, 4d** and **4e**, while all the three promoters are inducible in the presence of the VPR-dCas9 protein and the cognate gRNA, they have different fold activations. Indeed, the 1AB_pMin promoter results in almost absence of fluorescence when transfected alone, but shows low mCherry activation, with a small percentage of activated cells. The 10AB_pMin promoter, shows higher mCherry activation when bound by the gRNA-VPR-dCas9 complex, with more that 50% of the cells that exhibit fluorescence, but suffers from leakiness in its absence, with 13% of the cells that show fluorescence in the uninduced condition. In contrast, the promoter with 7 binding sites for the gRNA (*7B_pMin*) demonstrates an optimal balance between VPR-dCas9-driven induction, comparable to the results measured with the 10AB_pMin promoter, and minimal leakiness in the absence of the protein and gRNA, exhibiting similar measurements to those observed with the 1AB_pMin promoter. For these reasons, I selected the 7B_pMin promoter for my further experiments to characterize the Inhibitor and build the whole circuit.

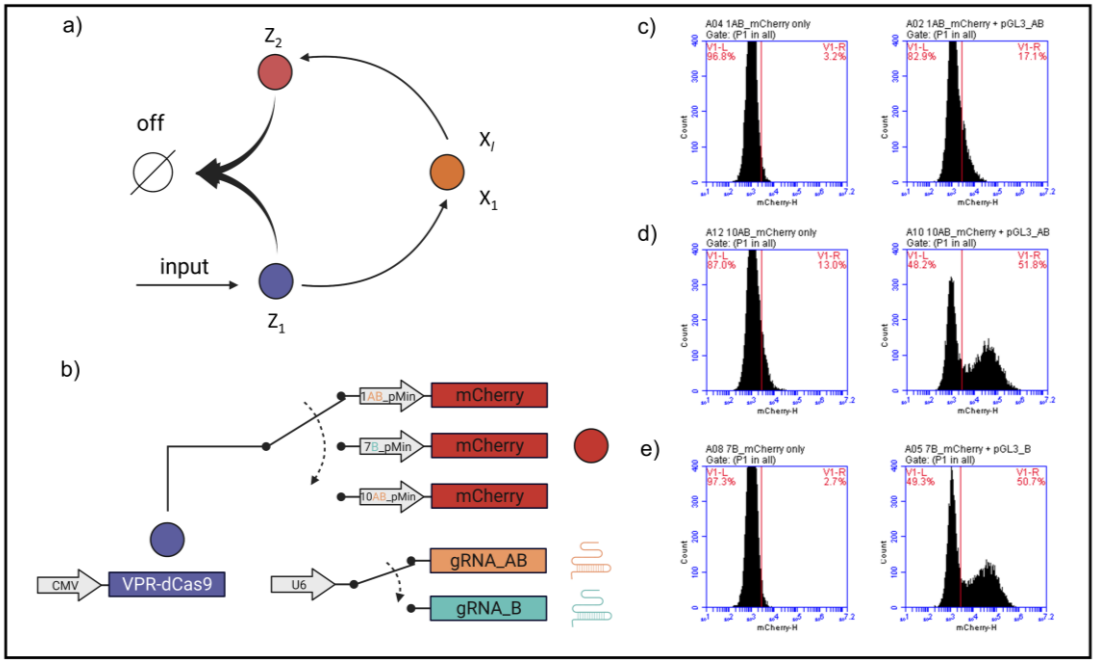

Figure 4 – VPR-dCas9 inducible promoter: **a)** Schematic representation of the Antithetic Integral Controller. The *activator* Z_1 expresses the species to control, X_1, that in-turns, as X_I, binds to the promoter of the *inhibitor* Z_2, that binds to Z_1 quenching its activity and closing the loop. **b)** Schematic representation of the experiment to measure VPR-dCas9 driven mCherry fluorescence. The fluorescent protein has been cloned downstream of three different synthetic promoters with 1 or 10 binding sites for the gRNA_AB or 7 binding sites for the gRNA_B, constitutively expressed from the U6 promoter. **c,d,e)** Flow cytometry measurements showing mCherry fluorescence expressed by the three synthetic promoters, respectively 1AB_pMin, 10AB_pMin and 7B_pMin,

when transfected with VPR-dCas9 and the proper gRNA. As a negative control, cells have been transfected with pMin_mCherry protein only.

3.1. Enhancing CRISPR – anti-CRISPR Interaction by means of synthetic coiled-coils.

The inhibitor, the anti-CRISPR protein AcrIIA4, is a bacteriophage – derived protein[131]. The CRISPR-Cas system is an immune defence of bacteria that recognizes and cut the viral DNA and the presence of anti-CRISPR protein as AcrIIA4 in the viral genomes is currently understood as a countermove from the bacteriophages to avoid Cas9-induced DNA breaks. Because of the recent discovery of anti-CRISPRs (Acrs), their mechanism of action is not completely known, even though structural studies have demonstrated that AcrIIA4 binds to Cas9 in the same pocket where the DNA should bind, thus preventing nucleic acid recognition, binding, and subsequent cutting[132]. To be an AIC biomolecular circuit, the sequestration reaction should happen in a 1:1 molar ratio, meaning that every molecule of the inhibitor should inactive one molecule of the activator[121]. However, even if it was demonstrated that AcrIIA4 is able to inhibit a dCas9-based transcription factor from driving transcription, the experiments were performed with a molar excess of transfected anti-CRISPR[128]. Therefore, to improve the repression activity of AcrIIA4, I decided to increase its affinity towards the VPR-dCas9. To this end, I exploited the recently developed synthetic Coiled-Coils (CCs) protein domains[129]. CCs consist of two 33 amino acid synthetic protein domains that act as "molecular magnets" and can reciprocally bind to each other, and, when fused to two proteins of interest, can cause their dimerization. These CC domains have demonstrated high efficacy in Hek293T cells, as the authors have shown that, fusing one of the coiled coil domains to the dCas9 protein, and another one to the VPR transcriptional domain, it is possible to recruit the two proteins together and get transcriptional activation[129]. I thought that, by fusing one coiled coil domain to the AcrIIA4 protein and its orthogonal partner to the VPR-dCas9 protein, I could enhance their binding affinity. Moreover, the two proteins should remain bound and get degraded thus together, respecting another parameter to realize the Antithetic Integral Controller. I decided to use the strongest CC domains published, called N7 and N8[133]. I fused the N7 CC domain to the AcrIIA4 protein (AcrIIA4-N7) and the N8 CC domain to the VPR-dCas9 protein. I then verified that the engineered VPR-dCas9-N8 protein was still able to act as a transcription factor and that AcrIIA4-N7 was able to inhibit VPR-dCas9-N8 more strongly than its wild-type counterpart, as shown in **Fig. 5a**. To this end, I cloned the luminescent reporter Firefly Luciferase (**fLuc**) downstream of the synthetic 7B_pMin promoter and I then transfected it in Hela and Hek293T cells, together with: (i) either the VPR-dCas9, or its engineered variant VPR-dCas9-N8, under the control of the constitutive promoter CMV; (ii) the cognate gRNA_B under the control of the constitutive promoter U6; (iii) either with the AcrIIA4 driven by the promoter CMV, or its engineered variant AcrIIA4-N7, or without either of the two, as negative control. I performed

luciferase assays by measuring the emitted luminescence in for each condition. Results in **Fig. 5b** and **5c** show that VPR-dCas9-N8 is still able to drive gene expression, although slightly less efficiently than the original VPR-dCas9. I also confirmed that AcrIIA4 can indeed inhibit VPR-dCas9 – driven gene expression, and so does the engineered variant AcrIIA4-N7, even though less effectively when paired with VPR-dCas9. Interestingly, as reported in **Fig. 5d** and **5e** in terms of fold repression, the AcrIIA4-N7 is able to repress VPR-dCas9-N8 activity with more than 3-fold higher repression, for Hek293T cells, and more than 6-fold higher repression, for HeLa cells, when compared to the original proteins without CCs.

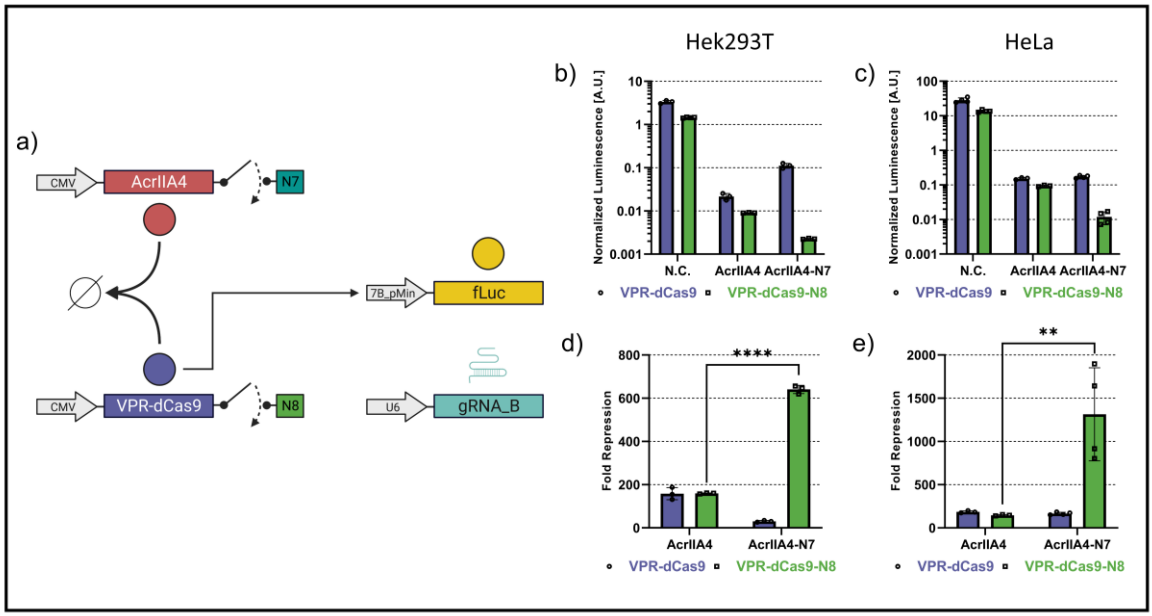

Figure 5 – CRISPR – AntiCRISPR Interaction a) Schematic representation of the constructs transfected in cells to perform luciferase-based assays to assess the transcriptional activity of VPR- dCas9 and AcrIIA4, with or without the cognate coiled-coiled domains N7 and N8. The promoter 7B_pMin, which consists of repeats of the 22 bps sequence cognate to the co-transfected guide RNA (gRNA_B), drives expression of the firefly luciferase (fLuc). **b,c)** Firefly Luciferase (fLuc) normalized luminescence in the presence of either VPR-dCas9 (violet bars) or of the coiled-coiled fusion variant VPR-dCas9-N8 (green bars) without anti-CRISPR protein (Negative Control – N.C.), or in presence of AcrIIA4, or of the coiled-coiled fusion variant AcrIIA4-N7. Data are shown in Hek293T (b) and HeLa cells (c). Firefly Luciferase luminescence values are normalized against the constitutively expressed Renilla Luficerase. **d,e)** Fold change of Firefly Luciferase (fLuc) repression, obtained by dividing normalized luminescence values by the values in the presence of either VPR-dCas9 (violet bars) or of the coiled-coiled fusion variant VPR-dCas9-N8 (green bars), in presence of AcrIIA4 or of the coiled-coiled fusion variant AcrIIA4-N7. Data are shown in HEK293T (d) and Hela cells (e). *The values represent measurements of n=4 biological replicates. A minimum of n=3 when one of the measurements was identified as an outlier (Grubbs' test, alpha=0.2). Statistics analysis has been conducted through two-way ANOVA test.*

3.2. Experimental implementation of the CRISPRaTOR

After characterizing the inhibitor and the activator, I aimed at selecting the GOI, that as I stated above, needs to be a transcription factor whose expression can be driven by the VPR-dCas9-N8 protein and that can in turn activate the expression of the AcrIIA4-N7 gene. It is theoretically possible to have the activator drive a species X_1 that, through a signaling process like a phosphorylation cascade, could activate a subsequent species X_i to induce the expression of the

inhibitor. However, opting for a more straightforward approach, I decided to take advantage of the Tet-On 3G by Takara Bio, a state-of-the-art inducible gene expression system, consisting of the bacterial derived transcription factor reverse-tet-TransActivator (rtTA)[29], that, in presence of Doxycycline, binds a synthetic prompter TRE3G promoter. Therefore, as shown in **Fig. 6a**, I cloned rtTA under the control of the 7B_pMin promoter and, to close the feedback loop, I cloned AcrIIA4-N7 under the control of the rtTA-cognate promoter TRE3G.

The CRISPRaTOR consists of a constitutive promoter CMV driving the expression of the engineered transcriptional activator VPR-dCas9-N8 that, in the presence of the constitutively expressed gRNA binds the 7B_pMin promoter upstream of the reverse-tet-TransActivator (rtTA) gene. The rtTA protein, in the presence of Doxycycline, binds the TRE3G promoter and drives expression of the modified anti-CRISPR protein AcrIIA4-N7 in a Doxycycline – dependent matter. This in turn binds and inhibits the VPR-dCas9-N8 protein, thus closing the negative feedback loop. The firefly luciferase reporter (fLuc) protein is also expressed by the gRNA inducible 7B_pMin promoter and I used to indirectly track rtTA expression.

As a negative control, as shown in **Fig. 6a**, I built an *open loop* circuit where the rtTA is under the control of the constitutive promoter EF1a, thus disabling the feedback loop. I measured the fLuc luminescence at different concentrations of Doxycycline, as reported in **Fig. 6b**. The CRISPRaTOR works as expected as increasing doxycycline concentration cause a decrease in the rtTA level, as evidenced by the fit between experimental data and simulated data from a mathematical model of the CRISPRaTOR, developed in our lab by Mrs Virginia Fusco (model not shown). Moreover, the dynamic range (i.e. the difference between the maximal and minimal luminescence) of the CRISPRaTOR is much higher than that of the open loop. To demonstrate that the synthetic CCs do impact the circuit's performance, I built an additional version of the CRISPRaTOR but this time using the original variants of VPR-dCas9 and AcrIIA4, i.e. those without CCs, and I then performed the same doxycycline dose-response experiment (**Fig. 6c**). As shown in **Fig. 6d**, this circuit exhibits higher luminescence than the CRISPRaTOR with CCs for all doxycycline concentrations, suggesting a weaker inhibitory action of the AcrIIA4 on the VPR-dCas9, as expected. While both systems exhibit AIC behaviour, in the case of the system with CCs, fitting the experimental and simulated data reveals that it more closely approaches an ideal behaviour. The stronger interaction between the inhibitor and activator better approximates the characteristics of a mathematical model that doesn't take in account the degradation ratio of the two molecules, as the one used for fitting the data.

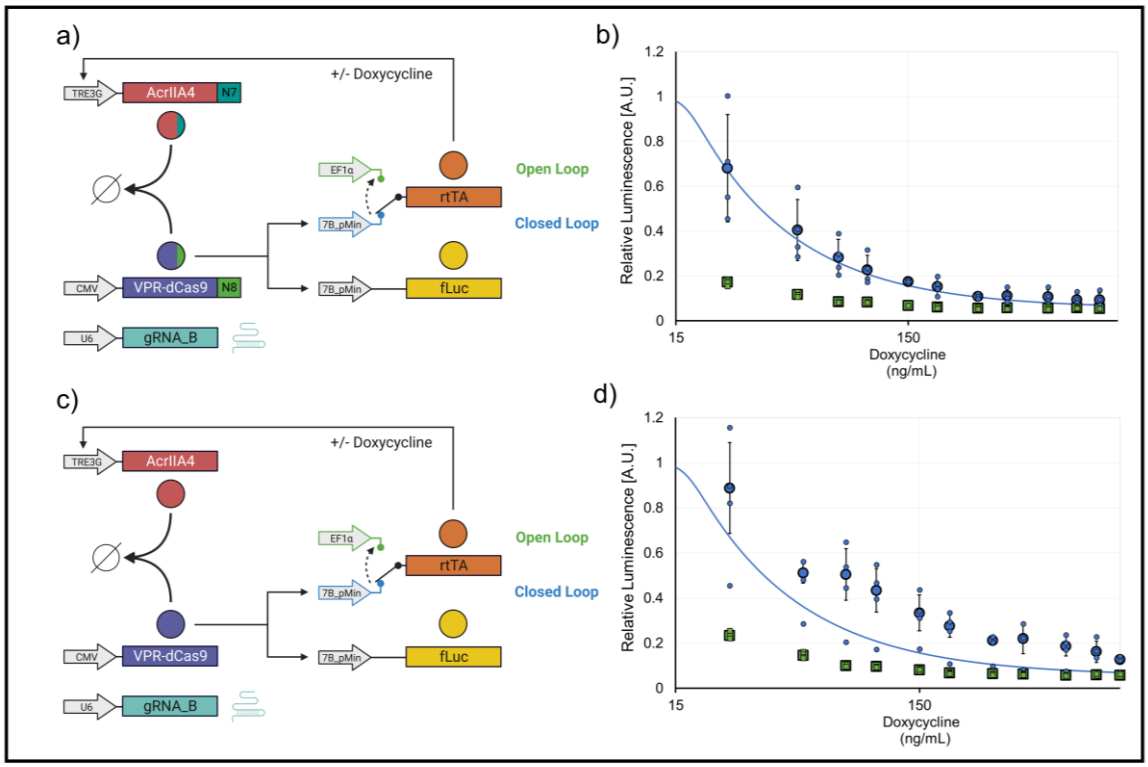

Figure 6 – Characterizing the CRISPRaTOR: a) Schematic representation of the system. The constitutive promoter CMV drives the expression of VPR-dCas9-N8 protein, which, in the presence of the gRNA_B, binds the 7B_pMin promoter, allowing the expression of the synthetic doxycycline-inducible transcription factor rtTA. In the presence of doxycycline, rtTA binds the TRE3G promoter driving expression of the AcrIIA4-N7 protein that binds and inactivates the VPR-dCas9-N8, thus closing the negative feedback loop. The firefly luciferase (fLuc) under the control of the 7B_pMin promoter is used as a reporter to track VPR-dCas9 activity. In the open loop configuration, the rtTA is under the control of the constitutive non-cognate promoter EF1α. **b)** Relative luminescence of the CRISPRaTOR, with the coiled-coils system, in response to doxycycline in Hek293T cells. Luminescence of the fLuc was first normalized against Renilla luminescence, to obtain normalized luminescence values. Normalized luminescence was divided by its value without Doxycycline induction to obtain the Relative luminescence. **c)** Schematic representation of the system represented and described in Figure 3a, using the original variants of VPR-dCas9 and AcrIIA4, without the addition of the cognate coiled-coils. **d)** Relative luminescence of the CRISPRaTOR, without the coiled-coils system, in response to doxycycline in HEK293T cells. *The values represent measurements of n=4 biological replicates. A minimum of n=3 when one of the measurements was identified as an outlier (Grubbs' test, alpha=0.2).*

3.3. Robust Perfect Adaptation

To experimentally test the ability of the CRISPRaTOR in maintaining homeostasis in the face of perturbations, i.e. Robust Perfect Adaptation, I had to find a way to perturb the controlled species, hence the transcription factor rtTA. To this purpose, I exploited a bacterial derived Destabilization Domain (DD)[134], a 12-kDa (107-amino-acid) tag based on a mutated FKBP protein. When a protein of interest is expressed as a fusion with the DD tag, it is destabilized and rapidly degraded in the cell by proteasomes, unless the membrane – permeant small molecule Shield1 is added in the culture medium. Shield1 binds the DD and protect the fusion protein from degradation allowing it to accumulate in the cell. It is important to notice that the amount of Shield1 added to the medium is

proportional to the amount of protein that is stabilized. I fused Destabilization Domain (DD) to the transcription factor rtTA to obtain DD-rtTA, which is therefore controlled by Shield1, as shown in **Fig. 7a**. Hence, by administering various amount of Shield1, it is possible to explore different intensities of perturbation. To test the degradation of DD-rtTA protein and its rescue by Shield1 and to assess that the tagged rtTA still maintains its function as a transcription factor, I cloned it downstream the strong constitutive promoter EF1α. Moreover, I cloned the fluorescent protein mCherry under the control of the rtTA – cognate Doxycycline – responsive TRE3G promoter. I transfected the plasmids in both Hek293T and HeLa cells and I performed flow cytometry experiment when adding no drug, saturating conditions of Doxycycline (1000 ng/ml) alone, saturating conditions of Shield1 (1000 nM) alone and both the drugs together, as shown in **Fig. 7**. As already done before, the threshold to quantify the fluorescent signal was established using wild type, untransfected Hek293T cells (data not shown). Since Shield1 stabilized DD-rtTA and Doxycycline facilitates its binding to the TRE3G promoter, full expression of mCherry is achievable only in the presence of both drugs. I confirmed the correct functioning of the DD-tagged protein in both cell lines, as I show in **Fig. 7b** and **7c**, thus obtaining a tool to perturb the system on demand.

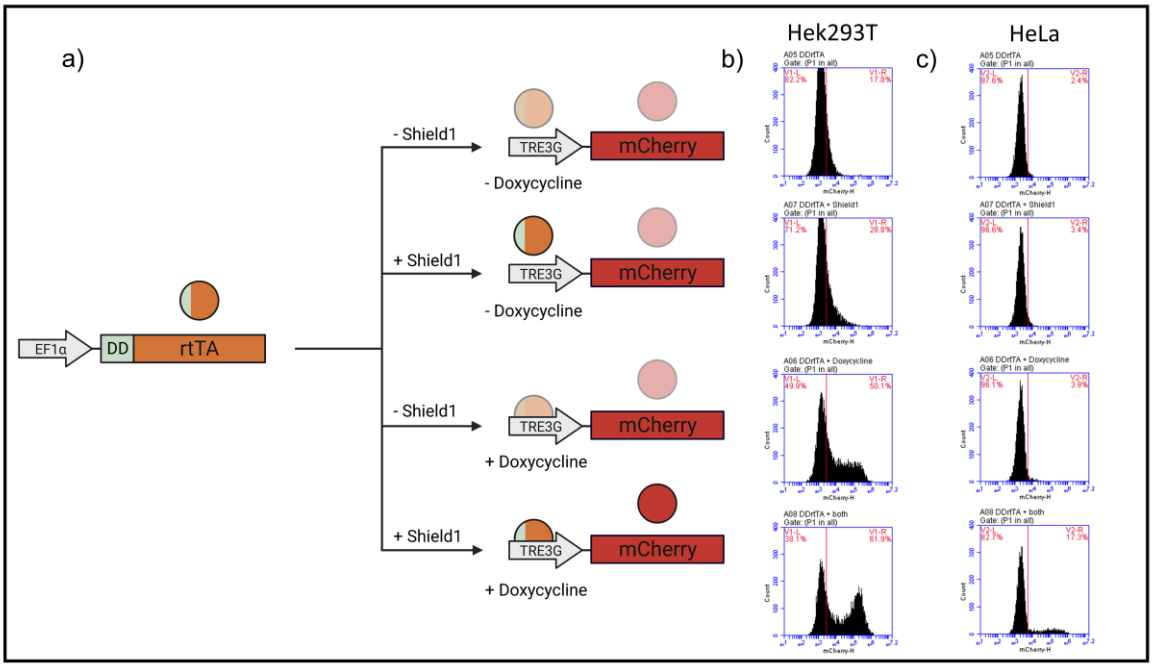

Figure 7 – Destabilization Domain: a) Schematic representations of the experiment to test DD-rtTA, constitutively expressed by the EF1α promoter, while TRE3G promoter drives mCherry expression. In the absence of Doxycycline, DD-rtTA cannot bind TRE3G promoter thus initiating mCherry transcription, while in the absence of Shield1 DD-rtTA is unstable and quickly degraded. **b,c)** mCherry fluorescence measured through flow cytometry in Hek293T and HeLa cells, respectively, upon transfection and drug treatment. Cells have been transfected with EF1α-DD-rtTA and TRE3G mCherry and they've been treated with no drugs, Doxycycline only (1000ng/ml), Shield1 only (1000nM) and both the drugs together.

I thus substituted the original rtTA with its destabilised version (DD-rtTA) in the CRISParator, as shown in **Fig. 8a.** To track rtTA levels, I placed the luciferase reporter protein under the control of

the TRE3G promoter. Since the Luciferase protein is expressed by the TRE3G promoter, its level is directly correlated with the amount of rtTA present in the cell. As a negative control, I implemented an *open loop* circuit where AcrIIA4-N7 is absent and substituted by an empty plasmid. Since in the *closed loop* system both the Anti-CRISPR protein AcrIIA4-N7 and the reporter fLuc are under the control of the same Doxycycline – responsive promoter TRE3G, I first performed a dose-response curve in terms of luminescence for increasing concentrations of doxycycycline, while keeping a constant Shield1 concentration of 1000 ng/ml to stabilize the rtTA protein. Results are reported in **Fig 8b** and show a linear proportionality between doxycycline concentration and luciferase expression. Doxycycline allows us to set its level of expression, thus exploring different conditions in which the system is robust. To test the ability of the CRISPRaTOR in maintaining the luminescence level in the face of perturbations, I fixed Doxycycline concentration and varied Shield1 concentrations to change the DD-rtTA stability, starting from 1000 nM, a dose that stabilizes the DD-tagged protein. As reported in **Fig. 8c**, for a fixed concentration of Doxycycline of 25 ng/ml, the fLuc luminescence in the Open Loop circuit decreases proportionally with the Shield1 concentration. This is expected, as the DD-rtTA protein stability decreases while its mRNA level is unchanged, thus causing an overall decrease in DD-rtTA protein level, and hence of the expression of fLuc downstream of the DD-rtTA regulated TRE3G promoter. On the contrary, in the case of the CRISPRaTOR (**Fig. 8c**), the luminescence level remains constant, thus demonstrating Robust Perfect Adaptation; this can be explained by the fact that as DD-rtTA protein degradation increases, this transiently decreases the DD-rtTA protein level, which in turn decreases the anti-CRISPR amount, thus more VPR-dCas9-N8 will be available to increase DD-rtTA mRNA expression, thus re-establishing the correct level of DD-rtTA protein and hence of the downstream Luc. The same results hold true when fixing Doxycycline at 50 ng/ml, as shown in **Fig. 8d**. For the sake of completeness, I have included in **Fig. 9a** and **9b**, the normalized, rather than relative, luminescence from the experiments in **Fig. 8c, d** to show that the CRISPRaTOR reduces the overall emitted luminescence, thereby decreasing the final output. This outcome aligns with expectations, as the presence of the anti-CRISPR interferes with a portion of the VPR-dCas9-N8 molecules, limiting their ability to promote transcription and performing the negative feedback loop activity necessary for maintaining homeostasis. This reduction in output is a characteristic feature of negative feedback loops, as they inherently yield lower outputs compared to unregulated systems. To further explore the experimental conditions in which Robust Perfect Adaptation is maintained, I repeated this experiment with Doxycycline concentrations fixed at 75 and 100 ng/ml and Shield 1 concentrations from 300nM to 1000nM. **Figure 9c** and **9d** show the results for all the concentrations tested. To make the comparison easier, I built two heatmaps containing the results of the open loop and closed loop systems for all the tested concentrations, as shown in **Fig. 9e** and **9f**. The overall results demonstrate that the closed loop CRISPRaTOR guarantees RPA in a wide range of experimental conditions, and RPA is lost only for very strong perturbations (i.e. Shield1 less or equal to 400 nM), whereas the open loop control fails to maintain RPA as expected.

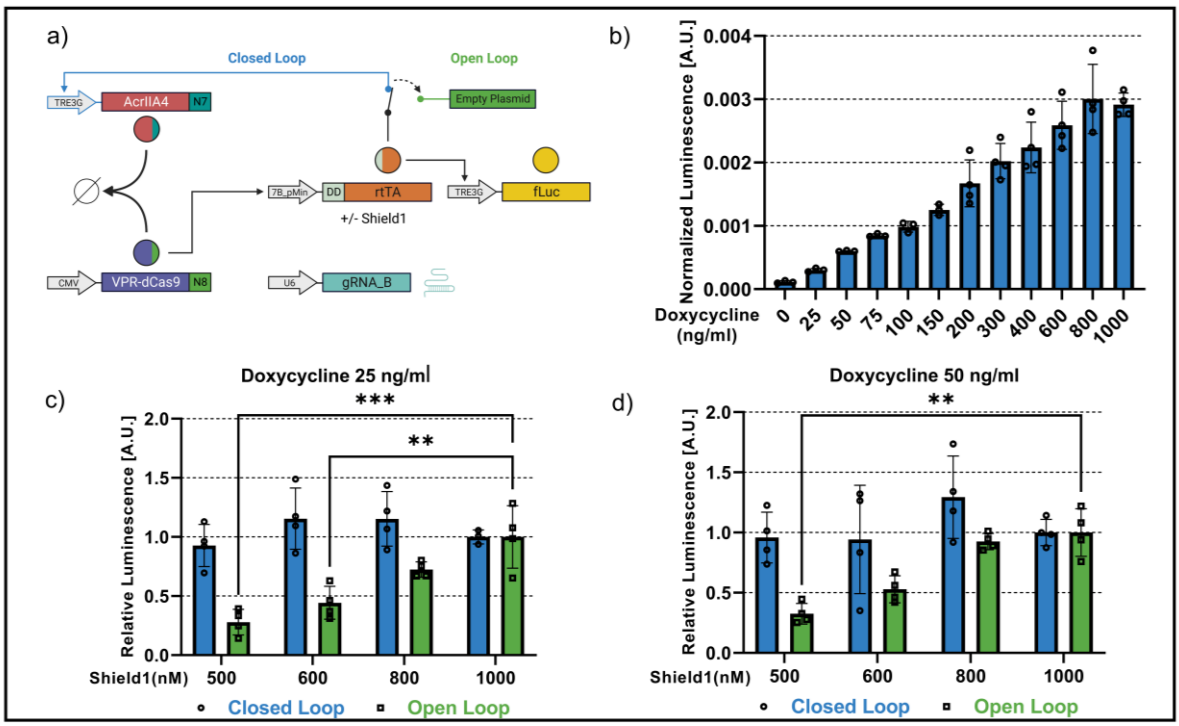

Figure 8 – Robust Perfect Adaptation: a) Schematic representation of the construct transfected to test Robust Perfect Adaptation in Hek293T cells. The rtTA is fused to the FKBP derived Destabilization Domain (DD) enabling the protein to be degraded by reducing the concentration of the small molecule Shield1 and thus the system to be perturbed. The DD-rtTA transcription factor drives the expression of the firefly Lucifarease (fLuc) from the TREG promoter, and only in the Closed Loop configuration, also of the AcrIIA4-N7 protein. In the Open Loop configuration, the plasmid encoding for the anti-CRISPR protein AcrIIA4-N7 has been substituted by an empty plasmid **b)** Dose-response curve of the Closed Loop system when increasing Doxycycline amount. Normalized luminescence has been obtained by dividing the absolute Firefly Luciferase luminescence by the luminescence derived from the constitutively expressed Renilla Luciferase. Shield1 has been kept constant at 1000 ng/ml to stabilize DD-rtTA. **c,d)** Demonstration of robust perfect adaptation (RPA) in Hek293T cells. Relative luminescence of the fLuc reporter at the indicated concentration of the Shiled1 molecule,that stabilizes the DD-rtTA transcription factor in a dose dependent manner. The concentration of doxycycline is kept constant at 25 (c) and 50 (d) ng/ml. Luminescence of the fLuc was first normalised against Renilla luminescence, to obtain normalised luminescence values. Normalised luminescence was divided by its value in the presence of Shield1 at a 1000 nM concentration to obtain the Relative luminescence. *The values represent measurements of n=4 biological replicates. A minimum of n=3 when one of the measurements was identified as an outlier (Grubbs' test, alpha=0.2). Statistics analysis has been conducted through two-way ANOVA test.*

To further investigate the robustness of the CRISPRaTOR, I also changed the amount of the plasmid encoding DD-rtTA relative two the other two plasmids encoding VPR-dCas9-N8 and AcrIIA4-N7, to assess the ability of the CRISPRaTOR to counteract these perturbations.

As shown in **Fig. 9g**, increasing or decreasing the relative amount of the DD-rtTA up to 50% had a strong effect on the open loop control, whereas the closed loop CRISPRaTOR was able to maintain the relative luminescence constant for most of the plasmid concentrations. Taken together these results demonstrate that the CRISParator implements an effective AIC motif conferring linearity and Robust Perfect Adaptation.

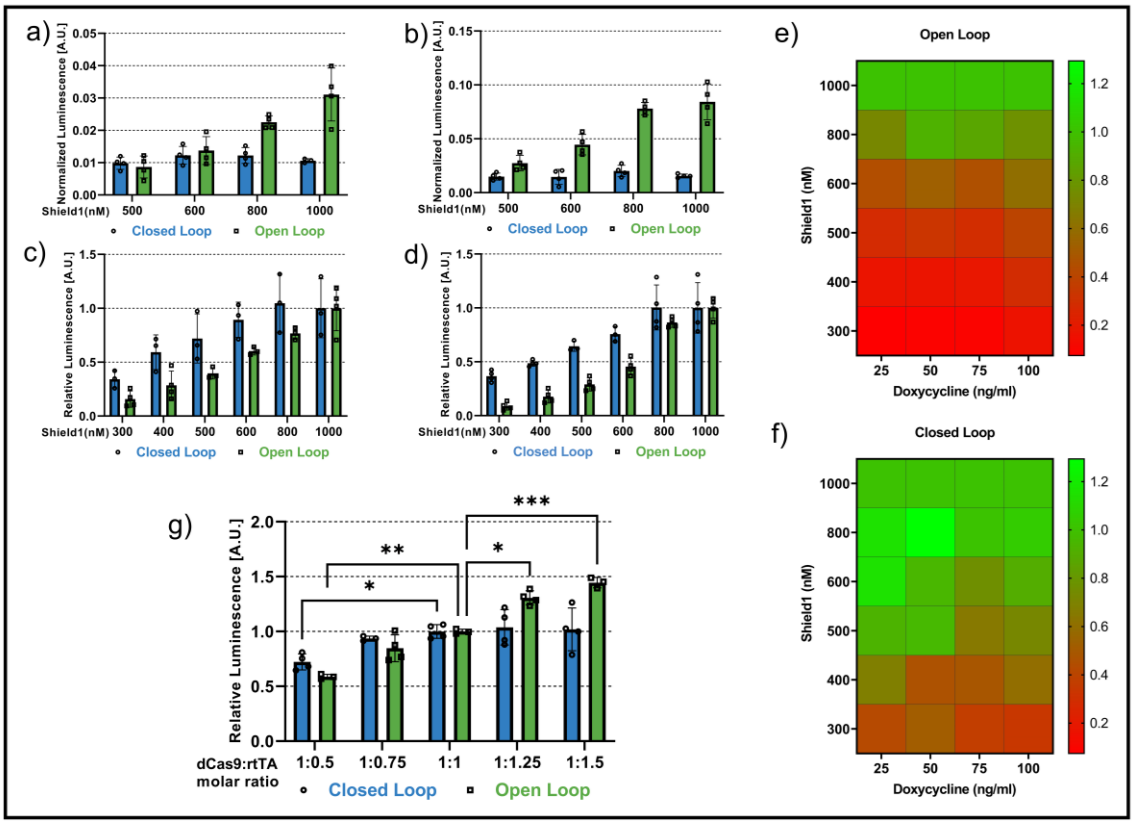

Figure 9 – Exploring robustness parameters: a, b) Normalized luminescence of the fLuc reporter at the indicated concentration of the Shield1 molecule that stabilizes the DD-rtTA transcription factor in a dose dependent manner. The concentration of doxycycline is kept constant at 25 (a) and 50 (b) ng/ml. Luminescence of the fLuc was normalised against Renilla luminescence. **c, d)** Relative luminescence of the fLuc reporter at the indicated concentration of the Shield1 molecule that stabilizes the DD-rtTA transcription factor in a dose dependent manner. The concentration of doxycycline is kept constant at 75 (c) and 100 (d) ng/ml. Luminescence of the fLuc was first normalised against Renilla luminescence, to obtain normalised luminescence values. Normalised luminescence was divided by its value in the presence of Shield1 at a 1000 nM concentration to obtain the Relative luminescence. **e, f)** Experimental exploration of the parameter space in which RPA is achieved. By changing the levels of doxycycline, it is possible to modulate the strength of rtTA transcriptional activity and thus explore the robustness of the CRISPRaTOR against changes in the characteristics of its composing elements. The heatmaps report the relative luminescence at the indicated concentration of Shield1 and Doxycycline for the closed loop (e) and the open loop (f) configurations. The relative luminescence in each column was obtained by dividing the normalized luminescence by its value at a Shield1 concentration of 1000 nM. **g)** Robust Perfect Adaptation experimentally tested increasing or decreasing the amount of transfected rtTA in respect to the dCas9 amount. The concentration of doxycycline is kept constant at 25ng/ml. Luminescence of the fLuc was first normalized against Renilla luminescence, to obtain normalized luminescence values. To obtain the Relative luminescence, normalized luminescence was divided by its value in the condition in which DD-rtTA and VPR-dCas9-VPR are transfected in 1.1 molar ratio. Shield1 has been kept constant at 1000nM in order to stabilize DD-rtTA. *The values represent measurements of n=4 biological replicates. A minimum of n=3 when one of the measurements was identified as an outlier (Grubbs' test, alpha=0.2). Statistics analysis has been conducted through two-way ANOVA test.*

4. The CRISPRaTOR as an evolution of CRISPRa

4.1. A self – regulating CRISPRa system

After implementing and testing the properties of our Negative Feedback Loop system, the CRISPRaTOR, I aimed at controlling endogenous genes instead of synthetic ones. While control of synthetic genes has been achieved in different models, exploiting a variety of topologies, the landscape of endogenous gene regulation presents unique challenges. Synthetic parts are typically designed to be orthogonal to the host cell's regulatory machinery, simplifying their implementation in genetic circuits. For instance, the Tet-On 3G system, derived from the bacterial TeT Operator[29], limits the transcription factor rtTA to bind only the TRE3G promoter in the mammalian genome, reducing potential off-target effects. In contrast, endogenous genes are subject to intricate regulation within the native cellular environment, featuring complex interactions with other genomic elements and cellular pathways. Their regulation often involves a delicate balance of multiple transcription factors and regulatory elements that respond to various internal and external stimuli. Consequently, precise control of endogenous gene expression is more challenging, and suitable tools for this purpose are often lacking.

Among endogenous genes whose regulation may have relevant implications for biotechnology and biomedicine are transcription factors, as they are key regulators of biological processes inside the cells and precisely controlling them would impact both biotechnologies, for example by making producer cells more resilient to apoptosis, and in biomedicine as therapeutic target. For instance, Xbp1s can regulate the expression of genes that are capable of ameliorating proteins' folding in a cell[135], ultimately controlling the ER Stress; GADD34 is involved in Integrated Stress Response (ISR) processes and in EF2α dephosphorylation[136], maintaining it in an active state thus increasing the amounts of proteins produced by the cell. Other genes, such as Transcription Factor EB (TFEB), could be potential therapeutic target for neurological diseases caused by protein accumulation, but their level of expression must be tightly controlled to avoid side effects[137].

The state-of-the-art method for endogenous gene overexpression is represented by CRISPRa, a technology that harnesses the programmable capabilities of the CRISPR-Cas9 system. In CRISPRa, a deactivated Cas9 (dCas9) protein is fused with various transcriptional activator domains, such as the VPR (VP64-p65-Rta)[56]. The CRISPRa system can activate target gene expression when guided by a guide RNA (gRNA) designed to target the endogenous promoter region of interest. Upon binding to the promoter, the dCas9-based transcription factor recruits transcriptional machinery, resulting in the overexpression of the gene. Despite the potential of CRISPRa for endogenous gene control, it lacks robustness and fine-tunability, like many traditional gene expression systems. Here, I propose to combine the power of CRISPRa with the advantages of negative feedback control, by employing the CRISPRaTOR to fine tune the expression levels of endogenous transcription factor with accuracy and stability. As illustrated in

Fig. 10a, I introduce a modification of the CRISPRaTOR circuit wherein: (i) the activator VPR-dCas9-N8 is controlled by the TRE3G promoter; (ii) the rtTA gene is constitutively expressed by the EF1α promoter; (iii) the GOI is an endogenous transcription factor whose expression is regulated by the VPR-dCas9-N8 by designing an appropriate gRNA; (iv) the promoter upstream of the AcrIIA4 is designed to be responsive to the GOI . This scheme can be applied to control the expression of any endogenous transcription factor.

As a proof of concept, I decided to control the neuronal-differentiation transcription factor NEUROD1, a crucial transcription factor that plays a fundamental role in cellular differentiation, specifically in the context of neurogenesis, the process by which neural stem or progenitor cells differentiate into mature neurons, forming the intricate neural circuits that underlie brain function[138]. NEUROD1 is a key player in this process, acting as a master regulator that drives neural progenitors toward a neuronal fate. It belongs to the family of bHLH (basic helix-loop-helix) transcription factors, which are known for their involvement in cell fate determination and differentiation. Upon activation, NEUROD1 binds to the E-Box sequence (CANNTG) within the target gene promoters. Through this binding, NEUROD1 acts as a transcriptional activator, promoting the expression of genes that drive neuronal differentiation and maturation[139]. While differentiating somatic cells into neurons in vitro, it has been demonstrated a critical role in NEUROD1's level of expression, a key to achieve efficient neuronal reprogramming from different cell types[140]. Moreover, NEUROD1 has been already overexpressed by CRISPRa in Hek293T cells, reaching high level of expression[56,58]. These features make NEUROD1 an ideal candidate for our CRISPRaTOR-based control system.

4.2. Controlling NEUROD1

To overexpress NEUROD1 in Hek293T cells, I took advantage of 3 already published gRNA directed towards NEUROD1's endogenous promoters[56] and I cloned in the pGL3 backbone already used for the synthetic gRNA_B and gRNA_AB. To test the overexpression of NEUROD1, I performed transfection of the three gRNAs together with the dCas9-VPR-N8 controlled by the CMV promoter, followed by RNA extraction and retrotranscription to cDNA after 48 hours. As a scramble guide that must not go on NEUROD1's endogenous promoter, I choose to use the synthetic gRNA_B that I used in previous experiments (**Fig. 10b**). NEUROD1 expression level was quantified through RT-qPCR, designing primers directed to its coding sequence. In **Fig. 10c**, I confirmed that mixing all the gRNAs leads to high level of overexpression, as already reported in literature[58]. As described earlier, to modify the CRISPRaTOR to regulate NEUROD1 expression, there is the need of a NEUROD1 – responsive promoter upstream of the AcrIIA4-N7 gene. To this end, I employed a synthetic promoter containing 7 repetitions of the E-Box motif upstream of a minimal promoter, that is named NiClear[141] (**Fig. 10d**). To assess correct binding of NEUROD1 to this promoter, I cloned it

upstream to the fLuc protein and I transfected it alone or together with a plasmid expressing the NEUROD1 transcription factor under the control of the constitutive promoter EF1α. Luciferase assay performed 48 after transfection shows a weak but significant induction of the luciferase gene when NEUROD1 is overexpressed, as reported in **Fig. 10e**. Nevertheless, a stronger promoter could risk to totally abolish the overexpression of the gene of interest as the repression of the dCas9-VPR-N8 protein inhibited by AcrIIA4-N7 would be too strong.

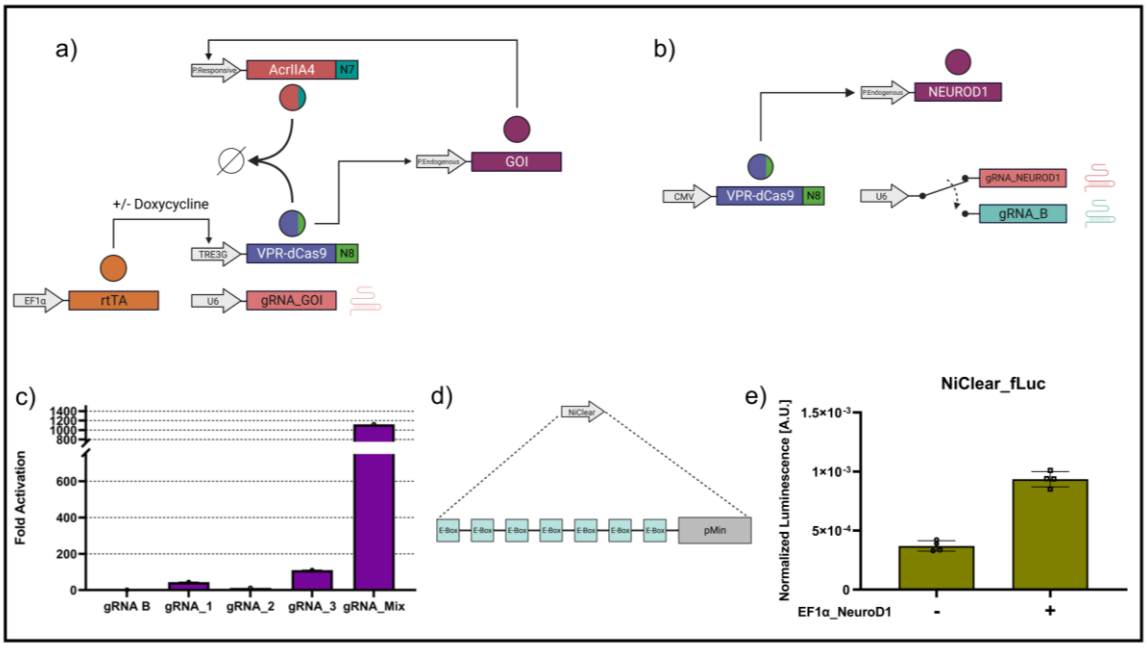

Figure 10 – Characterizing the circuit's components: a) Scheme of the circuit for controlling an endogenous gene of interest (GOI). The VPR-dCas9-N8 in presence of gRNA complementary to the endogenous promoter of the GOI, binds the promoter itself, promoting transcription and GOI expression. The GOI, a transcription factor, binds to a responsive promoter, driving the expression of the AcrIIA4-N7 protein, that inhibits VPR-dCas9-N8, thus closing the loop. **b**) Scheme of the classic CRISPRa system used to overexpress NEUROD1. The constitutively expressed VPR-dCas9-N8, in presence of the gRNA (1, 2, 3 or a mix of them) binds to the endogenous promoter of NEUROD1, thus promoting transcription. In the presence of the gRNA _B, used as a scramble guide, hence not having any binding sites in the genome, the VPR-dCas9-N8 doesn't promote transcription. **c**) Quantification of NEUROD1 RNA detected by Real Time PCR. The 3 gRNAs complementary to NEUROD1 promoter have been transfected together with the constitutively expressed VPR-dCas9-N8. A mix of all the 3 gRNAs together has been transfected as well. The gRNA_B has been used as a scramble guide to normalize the values. **d)** Scheme of the NiClear promoter, in which 7 repetitions of the E-Box (CANNTG, where N stands for one of the 4 bases, in this case CACGTG) have been cloned upstream a minimal promoter **e**) NiClear promoter activation detected with Luciferase assay. NiClear_fLuc has been transfected in Hek293T cells with or without EF1α_NEUROD1 expressing plasmid. Firefly Luciferase luminescence has been normalized on the constitutively expressed Renilla Luciferase.

I thus performed an experiment to compare the performance of the classic CRISPRa system (**Fig. 11a**), the CRISPRaTOR (**Fig. 11b**), and a negative control in which the AcrIIA4-N7 protein expression is constitutive (**Fig. 11c**). As shown in **Fig. 11d**, NEUROD1 is overexpressed in the CRISPRa system, and in the CRISPRaTOR, but not in the negative control with constitutive expression of the AcrIIA4-N7. Finally, to fine-tune expression of endogenous genes, I used the

modified version of the CRISPRaTOR in **Fig. 11e,** where the VPR-dCas9-N8 is under the control of the doxycycline inducible pTRE3G promoter. As a control, I used the open loop CRISPRa version where the plasmid encoding AcrIIA4-N7 is substituted with an empty plasmid, shown in **Fig. 11e**. Following transfection of both the closed loop modified CRISPRaTOR and of the open loop CRISPRa control in Hek293T cells, I measured NEUROD1 mRNA expression 48 hours after transfection, at different dosages of doxycycline. As shown in **Fig. 11f**, despite both the closed loop and open loop being able to increase the expression of NEUROD1, proportional to the Doxycycline concentrations, only the modified CRISPRaTOR does it so more efficiently. This is evident in **Fig. 11g** where I reported the fold-activation computed as the luminescence value at each doxycycline concentration divided by its value at 0 ng/ml of Doxycycline. In this uninduced condition, NEUROD1 should not be expressed at all in this cell line (Hek293). Indeed, while this is the case for the CRISPRaTOR, it's not the same for the CRISPRa system. This might be due to the basal "leaky" expression of VPR-dCas9-N8 in the CRISPRa system even in the absence of the inducer molecule Doxycycline. This leaky expression is abolished in the modified CRISPRaTOR system thanks to the anti-CRISPR protein. Finally, it is also apparent in Fig.8f that the maximal achievable expression of of NEUROD1 in the modified CRISPRaTOR is lower than the one of the open loops CRISPRa. This is to be expected because of the presence of the AcrIIA4-N7. Indeed, to demonstrate the dependency of the effect on AcrIIA4-N7 activation resulting from NEUROD1 overexpression, I conducted measurements of AcrIIA4-N7 levels upon induction of NEUROD1 using 200 ng/ml of Doxycycline (**Fig. 11h**). This revealed an elevated mRNA level compared to when I transfected the scramble guide gRNA_B.

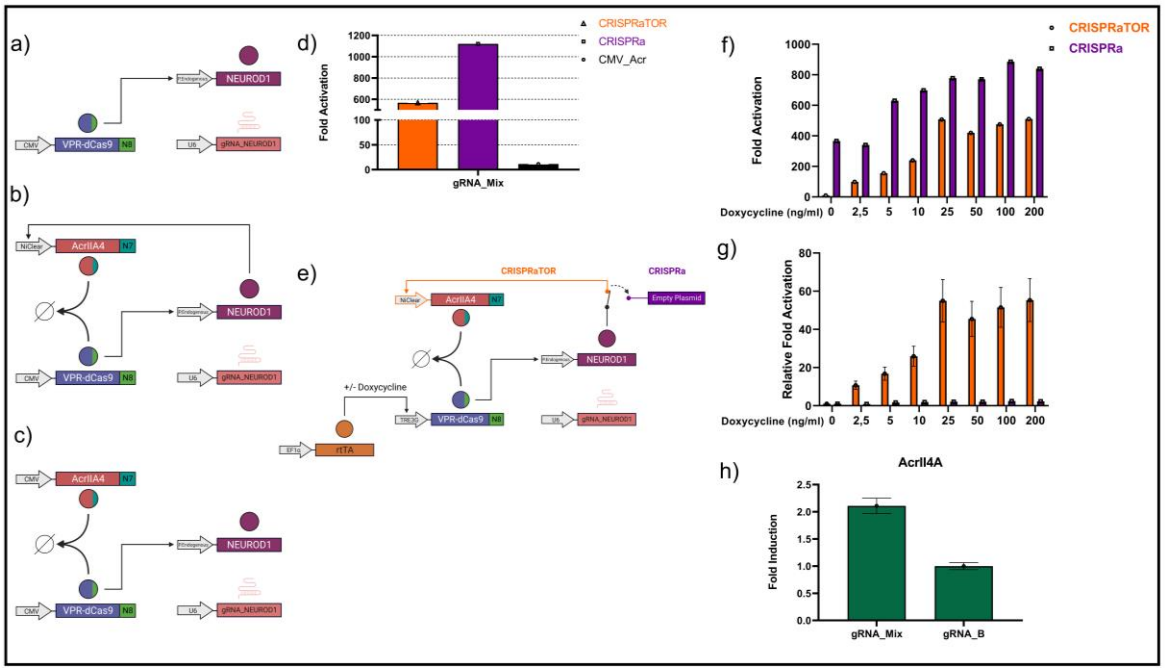

Figure 11 – The CRISPRaTOR controls NEUROD1 overexpression: a, b, c) Scheme of the circuits u sed to overexpress NEUROD1 through VPR-dCas9-N8 and the gRNA mix. In the three circuits, the anti-CRISPR protein AcrIIA4-N7 is absent (a, CRISPRa), controlled by NEUROD1 – inducible NiClear promoter (b, CRISPRaTOR) and controlled by the strong – constitutive CMV promoter (c, CMV_Acr). **d)** Quantification of NEUROD1 RNA performed by Real Time – PCR. NEUROD1 has been overexpressed with a constitutively expressed VPR-dCas9-N8, together with the mix of all the three tested gRNAs, in absence of AcrIIA4-N7 protein (CRISPRa), in the presence of AcrIIA4-N7 protein controlled by the NEUROD1-respondive NiClear promoter (CRISPRaTOR) and in the presence of the AcrIIA4-N7 protein controlled by the strong constitutive CMV promoter (CMV_Acr). The values have been normalized on the overexpression obtained by using the scramble guide gRNA_B. **e)** Quantification of AcrIIA4-N7 RNA level of AcrIIA4 when NEUROD1 is overexpressed (gRNA_Mix) and when it is not overexpressed (gRNA_B), obtained through Real Time – PCR. **f)** Scheme of a tunable circuit for NEUROD1 overexpression, with (CRISPRaTOR) or without (CRISPRa) the anti-CRISPR protein. The VPR-dCas9-N8 is driven by TRE3G promoter. In the presence of Doxycycline, the constitutively expressed rtTA transcription factor binds to the TRE3G promoter, hence expressing VPR-dCas9-N8. In the CRISPRaTOR configuration, the overexpressed NEUROD1 protein binds to the NiClear promoter, hence driving the transcription and expression of AcrIIA4-N7 protein, that binds to VPR-dCas9-N8, thus closing the loop. **g)** NEUROD1 RNA levels detected by Real Time – PCR. Cells have been transfected with the tunable CRISPRa or the tunable CRISPRaTOR and have been administered with increasing doses of Doxycycline to tune VPR-dCas9-N8 overepxression. gRNA_B has been used for both circuits as a scramble guide to normalize the values. **h)** Relative RNA level of NEUROD1. All the values for both circuits have been normalized on the RNA amount when Doxycycline is not administered (0 ng/ml), hence the uninduced condition. The graph shows then the fold change of expression when increasing Doxycycline doses.

5. The CRISPRaTOR as a Biosensor

5.1. Biosensors and Whole – Cells Biosensors (WCBs)

A biosensor is a device composed of both biological and electronic parts, capable of identifying and quantifying biological or chemical reactions by transforming them into discernible signals directly correlated with the concentration of the analyte, a particular substance within the reaction that needs to be detected. One of the principal components of a typical biosensor is a bioreceptor, often a biomolecule like an enzyme, aptamer, DNA, or antibody, that serves as the molecular recognition element, directly interacting with the analyte to be measured and starting the reaction. The transducer is needed to convert one form of energy to another, for example the biochemical interaction between the analyte and the bioreceptor in a measurable optical or electric signal, proportional to the amount of the analyte. Accompanying the transducer is the electronics component, which processes and refines the signal. It performs tasks such as signal amplification and conversion from analog to digital form, ensuring the output is suitable for interpretation. Finally, the display unit provides a visual or numerical representation of the biosensor's output, making the information accessible and meaningful to the user. This interplay of components in a biosensor harmonizes biology, chemistry, and electronics to deliver precise and actionable information across various applications, spanning environmental monitoring, disease identification, food safety, defense, drug discovery, and more[142]. A significant application lies in detecting biomolecules indicative of diseases or targets for drug development. For instance, electrochemical biosensors serve as clinical tools for detecting cancer protein biomarkers. Another example of commonly used biosensors is the blood glucometer, used for monitoring the blood glucose level. Although molecular – based biosensors are highly selective, the challenge of identifying suitable bioreceptors, coupled to the considerations of stability, cost, and the manufacturing complexity of all biosensor components, poses significant hurdles in the development of new biosensors[143]. An answer to these challenges might be represented by Mammalian whole-cell biosensors (**WCBs**), cells equipped with the necessary parts to detect and quantify an analyte[105]. This approach would result in a significant improvement in manufacturing, as all the necessary components to detect, quantify and display the analyte would already be genetically encoded into the cells. Therefore, while whole cell-based biosensors may exhibit less sensitivity to environmental fluctuations compared to their molecular-based counterparts, these biosensors can be easily modified using straightforward genetic engineering techniques. This adaptation enables them to detect a range of intricate responses within living cells. Furthermore, these biosensors offer insights beyond the capabilities of molecule-based counterparts, including information concerning sample pharmacology, cell physiology, and sample toxicity[143]. Synthetic biology allows the development of genetic circuits with specific characteristics and predictable behaviour, and this may be key to developing a new generation of WCBs, addressing some of their

current limitations[105]. One of the most common implementations of WCBs relies on specific transcription factors that are active only in the presence of the analyte. Following the interaction between the analyte and the transcription factor, the latter becomes active and binds to cognate DNA promoter sequence, to start transcription of a reporter gene whose expression will be proportional to the amount of the analyte[144]. The integration of synthetic gene networks, linking natural transcriptional responses with the expression of colorimetric, fluorescent, or bioluminescent reporter genes, empowers WCBs to engage in continuous surveillance of biomolecules and furnish meticulous real-time data[145]. In comparison to conventional techniques such as spectroscopy and chromatography, WCBs stand out as a beacon of innovation, offering an array of advantages including rapid response, specificity, on-site capabilities, and cost-effective real-time monitoring[145]. Despite their great potential, developing WCBs has met various challenges that impeded their wide adoption. One of the main features of a biosensor is linearity, hence the proportional relationship between the concentration of an analyte and the response of the biosensor. When this relationship is linear, it means that as the concentration of the analyte increases or decreases, the biosensor's response also changes in a proportional and consistent manner, allowing accurate and reliable quantification across a range of concentrations. When a biosensor has a linear response, it becomes easier to interpret the sensor's output and make quantitative measurements. However, it is worth noting that biosensors exhibit linearity over a limited range of detection, and usually exhibit deviations from linearity at extreme concentrations[146–149]. Since it is well known that negative feedback loops confer linearity to gene expression systems[150], here I decided to test the CRISPRaTOR as an innovative platform to develop a biosensor able to detect the analyte in a consistent and proportional way. This can be achieved by simply swapping the constitutive promoter CMV upstream of the VPR-dCas9-N8 in the CRISPRaTOR in **Fig. 11b** with an analyte – responding promoter. In what follows I will describe the implementation of the CRISPRaTOR as a biosensor of intracellular copper concentrations, which could find applications in research on rare genetic disorders such as Wilson's Disease.

5.2. The CRISPRaTOR as Copper – Biosensor in Wilson's disease

Wilson's disease (WD), that takes its name from Samuel Wilson, who first characterized it in 1912, is autosomal recessive metabolic disorder linked to mutations in the ATP7B gene, which encodes a copper-transporting ATPase involved in copper excretion and ceruloplasmin synthesis in hepatocytes[151,152]. These pathological states lead to the accumulation of copper within the liver, resulting in the subsequent release of copper into the bloodstream, potentially allowing it to enter the brain, which can lead to neurological and psychiatric symptoms. WD displays a wide range of symptoms and typically emerges between ages 5 and 35. Although WD is rare, with symptomatic cases estimated at 1 in approximately 30,000 individuals, recent molecular studies suggest a higher

prevalence of genetic WD based on pathogenic mutations in two alleles[152]. Currently, there is no definitive diagnostic test for WD, with liver copper content measurements being used to enhance accuracy. Due to the vague clinical manifestations of WD, diagnostic procedures involving laboratory and clinical assessments often experience delays. Such delays can potentially influence clinical outcomes and impact family members when considering late or missed diagnoses during the disease's progression[151]. Clinical evaluation considers patient history, physical examination, laboratory tests, and imaging. While genetic analysis can be insufficient due to variable impacts on protein function, diagnostic methods include assessing ophthalmic signs like Kayser–Fleischer rings and checking ceruloplasmin levels in the blood (below 10 mg/dL within a normal range of 20–50 mg/dL). For symptomatic patients, liver biopsy confirms diagnosis if liver tissue copper content surpasses 250 mg/g of dry weight. However, this method has limitations due to potential errors caused by uneven copper distribution and low tissue levels in advanced disease. The modified Leipzig scoring system omits hepatic copper quantification. Diagnosis often relies on blood ceruloplasmin levels, urinary copper excretion, and molecular analysis, which are now more accessible for genetic verification. The absence of a gold standard diagnostic test for Wilson's disease (WD) highlights the need for the development of whole-cell biosensors (WCBs) to accurately quantify copper levels. I leveraged a Copper Responsive promoter[153], containing four metal – responsive elements from the mouse metallothionein 1A promoter (MRE) cloned upstream a minimal Eb1 promoter, in order to induce transcription in the presence of copper (**Fig. 12a**). These MREs serve as binding sites for the metal-responsive transcription factor 1 (MTF-1), which binds to its cognate DNA sequence in the presence of metals such as copper[153]. Since the promoter has already been shown to respond to increasing concentration of Copper Dichloride (CuCl2), I first sought to enhance copper – induced transcription. For this reason, to recruit more MTF-1, I used a synthetic promoter with eight MRE elements upstream of a minimal CMV promoter (named 8xMRE_pMin), which was synthetized in the lab by Mr Francesco Ragazzini, as reported in (**Fig. 12b**). I cloned the Firefly Luciferase gene (fLuc) downstream to both promoters and I transfected both constructs in Hek293T cells, administering increasing concentrations of CuCl2, from 0 to 150 nM. After 48 hours, I lysed the cells and performed Luc assay and as shown in **Figure 12c**, the 8xMRE_pMin is indeed more effective in inducing transcription, as it is evident from the higher luminescence levels than the 4xMRE-pMin counterpart. Notably, both promoters exhibited a strongly non-linear copper detection responses, especially the high – expressing 8xMRE_pMin, saturated at concentrations above 50nM. To address this issue, I developed a CRISPRaTOR based copper biosensor by cloning the 8xMRE_pMin promoter upstream of the VPR-dCas9-N8 gene as shown in **Fig. 12d**. I then performed a dose-response curve experiment as before to characterize the CRISPRaTOR biosensor at a fixed concentration of Doxycycline (1000 ng/ml). To test the features of the copper – responsive CRISPRaTOR, I transfected the circuit in Hek293T cells, using the same concentrations of copper used in previous experiments. As a control, I transfected the

8xMRE_pMin controlling the reporter fLuc. As reported in **Figure 12e, f**, the CRISPRaTOR expresses higher luminescence and more importantly it confers a linear dose-response curve eliminating the saturation present in the original promoter. The developed CRISPRaTOR system offers a significant advantage in enhancing the utility of biosensors for diagnosing analyte-related diseases like Wilson's disease (WD). By imparting a linear response to copper concentrations, the CRISPRaTOR addresses a critical limitation observed in the traditional promoter-driven biosensors, where non-linearity complicates the accurate determination of analyte concentrations. The linearity achieved by the CRISPRaTOR simplifies the interpretation of biosensor outputs, allowing for a straightforward conversion of signal intensity into actual copper concentration values.

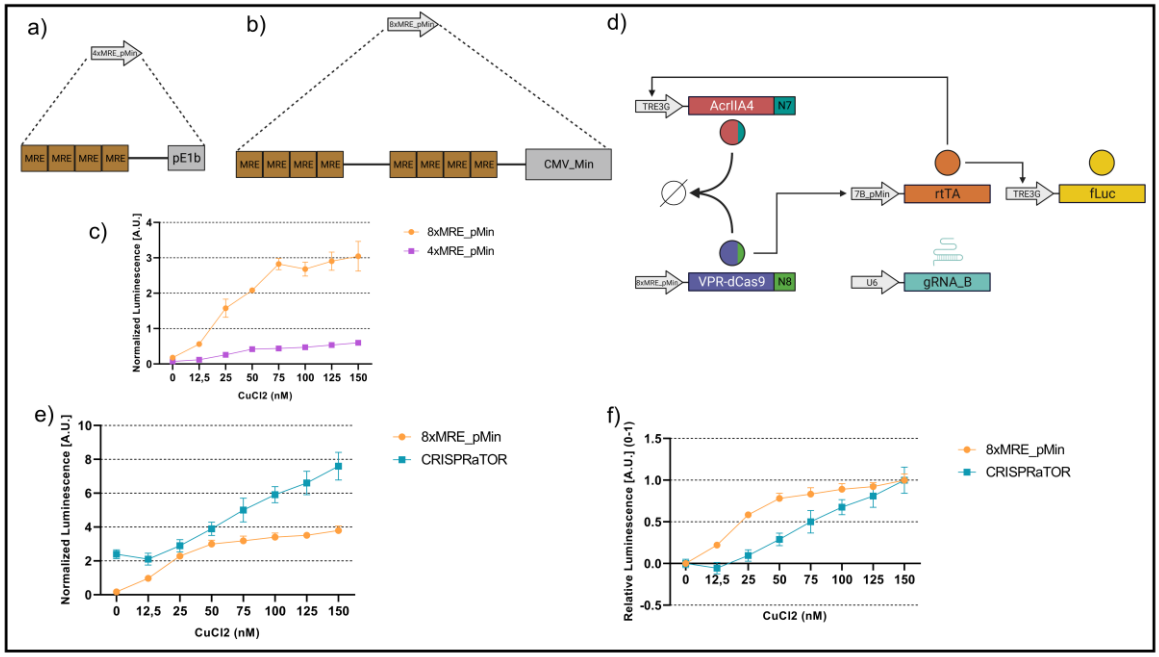

Figure 12 – The CRISPRaTOR as a Copper Biosensor: a) Schematic representation of 4xMRE_pMin promoter, with 4 binding sites for MTF1 upstream the E1B minimal promoter. **b)** Schematic representation of 8xMRE_pMin promoter, with 8 binding sites for MTF1 upstream the CMV minimal promoter. **c)** Luciferase assay showing the performance of both promoters. Firefly luciferase has been cloned downstream both the promoters and has been transfected in Hek293T cells, treated with increasing concentrations of CuCl2. Cells have been lysed and measured after 48 hours. Firefly Luciferase luminescence has been normalized on constitutively expressed Renilla Luciferase. **d)** Schematic representation of the CRISPRaTOR as a Copper Biosensor, in which the activator VPR-dCas9-N8 is expressed by the copper – responsive 8xMRE_pMin promoter. **e)** Luciferase assays of the performances of the copper – controlled CRISPRaTOR vs the 8xMRE_pMin promoter controlling firefly luciferase only. Cells have been transfected and treated with increasing concentrations of CuCl2. Cells have been lysed and measured after 48 hours. Firefly Luciferase luminescence has been normalized on constitutively expressed Renilla Luciferase. **f**) Luciferase assays of the performances of the copper – controlled CRISPRaTOR vs the 8xMRE_pMin promoter controlling firefly luciferase only, with values normalized between 0 and 1.

Discussion

Synthetic Biology has the potential to make a real – world impact in a variety of fields, from biotechnology to biomedicine. In recent years, the implementation of known gene network motifs allowed to predict and control the behaviour of engineered cells. However, problems to be solved to make Synthetic Biology applications more reliable and safer still remain. Here, we discuss one of the features that still needs proper implementation: robustness, specifically Robust Perfect Adaptation (RPA). RPA enables a system to maintain its output stability despite internal or external perturbations. In this thesis, I demonstrated the implementation of a protein-protein-based Antithetic Integral Controller (AIC) in mammalian cells, leveraging the interaction between VPR-dCas9, a CRISPR/Cas9 system derived transcription factor, and the anti-CRISPR protein AcrIIA4. Initially, I aimed at engineering the pair of proteins to experimentally implement the annihilation reaction at the core of the AIC. Indeed, as described in Chapter 2.4, the AIC relies on the interaction of the two molecular species – one acting as the activator and one acting as the inhibitor. In an ideal scenario, every inhibitor molecule should bind and inhibit only one activator molecule, with a 1:1 molar ratio. In the ideal AIC, this stochiometric reaction will result in an expression level of the controlled molecule (the transcription factor rtTA) at steady-state equal to the ratio of the production rate between the two molecular species This balance is maintained because the concentration of the inhibitor is determined by the controlled molecule's concentration, which is, in turn, regulated by the activator. As the controlled molecule's level decreases, so does the inhibitor concentration, releasing some of the activator. Their strong interaction ensures that the free activator molecules are just sufficient to readjust the controlled molecule's level. A weak interaction between them would lead to an excessive number of activator molecules when the inhibitor decreases due to a reduction in the controlled molecule's concentration. This excessive activation of the activator would result in an incorrect level of the controlled molecule. This is why the primary objective of our research was to engineer the interaction between VPR-dCas9 and AcrIIA4 using the synthetic coiled-coil domains. While I did not directly measure the strength of this protein interaction, I successfully demonstrated the enhanced performance of the engineered AcrIIA4-N7 in inhibiting the engineered VPR-dCas9-N8. My hypothesis that a stronger interaction between these two molecular species is essential aligns with literature evidence[121] and is supported by the mathematical model to predict our circuit's behaviour developed by Mrs Virginia Fusco in the lab. In this thesis, I demonstrate that the AIC can achieve Robust Perfect Adaptation and I show how this property is maintained both when perturbing the system by degrading the controlled species rtTA, reducing Shield1 amount, and when changing the amount of transfected rtTA encoding plasmid. The resistance of the implemented AIC to both types of disturbances underscores its ability to not only withstand perturbations that decrease the output but also those that could potentially increase it. Furthermore, it is worth highlighting that the CRISPRaTOR, i.e. my implementation of the AIC, is tunable with Doxycycline. This tunability feature is essential for practical applications,

as it allows for the precise control of rtTA expression levels and, consequently, downstream gene expression. This flexibility also enabled me to determine the specific parameter ranges within which the conditions for achieving RPA are met. In an ideal scenario, an Antithetic Integral Controller should consistently achieve RPA regardless of the type of perturbation or setpoint. However, other factors, such as promoter strength and protein turnover rates, can influence this property. Therefore, in the practical application of our circuit, it is crucial to carefully adjust the system to ensure that these parameters align with the conditions required for RPA achievement. Another important consideration regards the output of our system. In demonstrating Robust Perfect Adaptation (RPA), I consistently normalized each data point against the unperturbed state to establish an expression level ranging from 0 to 1. Comparatively, the absolute values of the output of the closed-loop system, incorporating the anti-CRISPR protein, tend to be lower than that of the open-loop system, which lacks the anti-CRISPR component. The AcrIIA4-N7 protein's role is to inhibit the VPR-dCas9-protein, thereby reducing the quantity of the transcription factor responsible for driving rtTA expression. Hence, a lower output is indeed an expected outcome. A potential user of the CRISPRaTOR should keep in mind that its purpose is not primarily to maximize output; instead, its focus is on maintaining a stable and constant level of output. Another noteworthy property of the CRISPRaTOR, which is a Negative Feedback Loop, is its ability to confer linearity between input and output. I demonstrated this property while regulating an endogenous transcription factor, NEUROD1, revealing a linear dose-response between the input (i.e., the doxycycline concentration) and the output (the mRNA level of NEUROD1). In this context, I envision the CRISPRaTOR as an advancement beyond the traditional CRISPRa system, which I used as a control in my experiments. While it is possible to introduce tunability into CRISPRa, as I demonstrated by incorporating the rtTA to regulate the expression of VPR-dCas-N8, the classical CRISPRa system lacks the essential components required to achieve precise and robust control. I believe that the possibility of controlling endogenous genes is a key factor of the CRISPRaTOR, that is made only possible by using VPR-dCas9-N8 as a transcription factor. Unlike conventional transcription factors that typically require a consensus binding sequence for promoting transcription, CRISPR/Cas9-based transcription factors possess a unique feature—they can be programmed with custom guide RNAs (gRNAs). My demonstration of finely tuning an endogenous transcription factor holds significant potential applications, such as directing the differentiation of stem cells into specific cell types. Differentiation is a process involving the simultaneous and precise action of several transcription factors to promote the transcription of downstream genes. By regulating these transcription factors, programmed differentiation could be achieved. Moreover, it is important to underline how the VPR-dCas9 offers the chance to perform multiplexed gene expression. This involves designing distinct guide RNAs targeting various promoters, thereby enabling the simultaneous control of multiple genes. However, it's important to note that to complete the feedback loop, the transcription factors must bind to the promoter governing the expression of AcrIIA4. This necessitates the design of cognate promoters for each transcription

factor or a promoter capable of being bound by multiple transcription factors concurrently. Promoters responsive to multiple transcription factors have also emerged, such as those induced by transcription factors involved in the ER stress and Unfolded Protein Response (UPR)[154]. This presents an opportunity to concurrently regulate these genes, thereby modulating both the ER Stress and UPR pathways to enhance protein production. While these pathways can inhibit protein production to prevent apoptosis, they also stimulate the production of enzymes that aid in protein folding[155,156]. Thus, maintaining an optimal level of ER Stress and UPR could prove advantageous for increasing protein yield in engineered cells within a bioreactor[157].

On the biomedical front, the CRISPRaTOR system holds promise for finely regulating disease-related genes. For instance, TFEB serves as a master regulator of autophagy and lysosomal biogenesis and is under investigation as a potential therapeutic target for neurological diseases and kidney cancer[137,158]. However, precise control over its expression is essential to avoid toxicity and unwanted effects, and the CRISPRaTOR system offers the means to achieve such precise regulation. It's also important to notice that our system is not immediately ready for translation into clinical applications for several reasons. Firstly, the plasmids we used to encode the components of the CRISPRaTOR are approximately 15 kilobases in size, posing a delivery bottleneck for use in humans. An initial step would involve optimizing the vectors to reduce their size. Furthermore, our circuit incorporates components of viral origin, such as the transcriptional activator VPR, which could potentially trigger immunogenic reactions in humans. One potential solution could involve substituting VPR with transcriptional activators of human origin, such as those derived from human mechanoreceptors[159,160]. It's worth noting that dCas9 itself is a relatively large protein and may also have immunogenic properties. In recent developments, the introduction of mini Cas9 enzymes has been explored to reduce size[161]. Additionally, there has been the recent discovery of Fanzor, a eukaryotic endonuclease with characteristics similar to Cas9[162]. While the applications of Fanzor are still lacking, this protein has the potential to follow a trajectory similar to Cas9, with potential modifications to its nuclease domain that could render it a programmable transcription factor compatible with the human system. While the hypothetical need for an anti-Fanzor exists, we speculate that the discovery of this new eukaryotic protein will motivate researchers to develop the necessary tools to regulate it, given its significant potential. These considerations underscore that the CRISPRaTOR is not designed as a ready-to-use therapeutic device but rather as a proof of principle to demonstrate that a protein-protein-based Antithetic Integral Controller (AIC) can indeed confer robustness and linearity to a connected gene network. To illustrate a more immediate practical application, I demonstrated how the CRISPRaTOR could be employed to engineer whole-cell-based biosensors with enhanced metrological features. By utilizing a copper-responsive promoter, I established a direct and linear correlation between the copper dosage and the system's output. This paves the way for a potential diagnostic tool based on this kind of biosensor. While applying the CRISPRaTOR directly for the regulation of human genes would necessitate the delivery of these circuits into patients, an application of a diagnostic tool could rely on encapsulation of

engineered cells into biocompatible devices. Furthermore, it is feasible to create whole-cell-based biosensors within microfluidic devices designed to detect environmental contaminants, including heavy metals[163]. The demonstrated linearity and robustness of the system can be harnessed to construct reporter systems for drug screening purposes. For instance, one approach could involve placing a disease-related promoter upstream of the dCas9-VPR-N8 construct to investigate the impact of a drug on a specific pathway. This relies on the strong correlation established between the input (drug concentration) and the system's output, making it a valuable tool for drug screening and pathway analysis. When this work began, there were no other implementations of the AIC motif in mammalian cells. In the last year, however, two examples of Antithetic Integral Controllers (AICs) in mammalian cells have emerged, one based on mRNA pairs[123] and the other on split-inteins[124]. While both controllers demonstrated Robust Perfect Adaptation (RPA), they each had their limitations. The mRNA-based AIC has the potential to trigger an immune response, and the split-inteins-based AIC requires careful engineering of the transcription factor. With my system, I believe I have addressed some of these limitations by developing a versatile platform that not only regulates synthetic genes of interest but also endogenous ones. The versatility of VPR-dCas9 opens a multitude of possibilities for applications. However, I also acknowledged the drawbacks of the CRISPRaTOR and proposed potential improvements to expand its range of applications. Through this work, I aimed to demonstrate the potential of gene circuits in precisely controlling gene expression, surpassing the benefits of engineering individual components. I emphasized how a Synthetic Biology approach can greatly benefit the field of genetic engineering. My goal was to provide the scientific community with a new tool for achieving robustness in gene networks, and I hope to inspire researchers to further modify and apply this system in the realms of biotechnology and biomedicine.

Materials and Methods

Plasmid construction: Most of the plasmids were constructed using the Golden-Gate based EMMA assembly kit[15], following authors' protocol[164], while in other cases the plasmids have been constructed using the Gibson assembly method[13]. During the initial phases of the project, Golden Gate cloning was preferred because it allows for the assembly of plasmids from standardized parts. This means that the part of interest can be cloned into a vector that will be stored in a library and used for subsequent cloning, making it a time-effective method for creating new plasmids from scratch. Later on, Gibson assembly was preferred due to its versatility, even though it does not provide the option to store the part in a library, as each part is specific to the cloning being carried out at that moment. After building a considerable number of plasmids, Gibson assembly offers the opportunity to modify them and change some of the parts in a rapid and scarless manner. All the

sequences regarding N7 and N8 coiled coils[133], used to modify the CRISPR-antiCRISPR system, AcrII4A and FKBP-derived DD[128], gRNA inducible constructs with 7 binding sites for gRNA B[130] and 1 or 10 binding sites for gRNA AB[129], gRNAs sequences[129],dCas9-VPR[165] and the MRE promoter[153] have all been taken from published papers. The Tet-On® 3G system, consisting of the TRE3G promoter and the rtTA protein, was acquired from Takara Bio. I chose to utilize this system as it represents the state-of-the-art inducible system in mammalian cells. Indeed, being one of the first inducible systems developed, researchers have invested considerable efforts over the years to optimize its components, such as achieving maximum system activation. While other inducible systems are available for mammalian cells, such as the cumate-inducible system, the Doxycycline-inducible system is by far the most widely used. Maps of the resulting plasmids obtained from these parts are available in the appendix.

Cell culture and transfection: The HEK293T cell line (ATCC) was cultured in DMEM Glutamax (Gibco) supplemented with 10% Tet-Free Fetal Bovine Serum (Euroclone) and 1% Penicillin-Streptomycin (Euroclone), while the HeLa cell line (ATCC) was cultured in DMEM (Gibco) supplemented with 10% Tet-Free Fetal Bovine Serum (Euroclone), 1% L-Glutamine (Euroclone) and 1% Penicillin-Streptomycin (Euroclone). Both the cell lines have been kept at 37°C in a 5% CO2 environment. For luciferase experiment, 1,5x10^4 (HeLa) and 2x10^4 (HEK293T) cells per well were seeded in CoStar White 96-well plates (Corning), while for Flow Cytometry assay the same numbers of cells have been seeded in 96-well cell culture plates (Corning). When doing the same experiments in reverse, 3x10^4 (HeLa) and 4x10^4 (HEK293T) cells per well were seeded. After 18 hours of seedling, or immediately after seedling for reverse transfection, cells have been transfected using a home-made solution of PEI (MW 25000, Polysciences, stock concentration 0,324 mg/ml, pH 7.5) using 250ng of DNA per well. For HEK293T cells, 5 µl of PEI solution for each µg of DNA were used, while for HeLa 4 µl of PEI solution for each µg of DNA were used. The choice between conducting a traditional transfection, where cells are seeded and transfected the day after, and a reverse transfection, where cells are transfected immediately after seeding, was primarily based on time constraints. I found that both methods yielded similar transfection efficiency. The cell quantity before transfection was intentionally optimized to achieve 70-80% confluence at the time of transfection. It was observed that lower confluence levels resulted in inhibited cell growth in the subsequent days, likely due to the cytostatic effect of the transfection reagents. The amount of PEI used was optimized through experiments performed on a flow cytometer, where a plasmid encoding a fluorescent reporter was transfected. For both cell lines, I tested 150, 200, and 250 ng of DNA, using 2, 3, 4, 5, 6, and 7 µl of PEI for each µg of DNA. I selected the PEI/DNA ratio that provided an ideal balance between transfection efficiency, the percentage of transfected cells, signal intensity, and minimal cytotoxicity. To normalize reporter values for transfection efficiency, I used 10 ng of phRL-TK (encoding for Renilla Luciferase) in the luciferase experiments. A transfection reporter was employed to enable comparisons across

different experiments. Although we assessed transfection efficiencies of approximately 90% for HEK293T cells and 80% for HeLa cells, it's important to note that transfection is a complex process influenced by various factors, such as cell passage and inherent biological variability. As a result, all values obtained from the Firefly Luciferase, which was consistently used as a readout for the tested systems, were divided by the Renilla Luciferase value. Renilla Luciferase was consistently expressed under the control of a constitutive promoter.

Luciferase assay: The cells were collected 48 hours after transfection and lysed with 50 µl of 5X Passive Lysis Buffer (Biotin) diluted in water. Firefly Luciferase and Renilla Luciferase expression were measured using the Dual Luciferase Assay (Promega) on a Glomax Explorer plate reader (Promega). Firefly Luciferase Arbitrary Units (fLuc [A.U.]) were calculated by normalizing each sample's Firefly Luciferase activity to the constitutive Renilla activity detected in the same sample. Relative fLuc [A.U.] values have been calculated by dividing each sample's Firefly Luciferase Arbitrary Units by the Firefly Luciferase Arbitrary Units of the sample with no Doxycycline induction, in the case of Doxycycline dose-response curves. In the case of Shield1 treatment, Relative fLuc [A.U.] values have been obtained by dividing each sample's Firefly Luciferase Arbitrary Units by the Firefly Luciferase Arbitrary Units of the sample treated with the maximum dose of Shield1 used, 1000 nM. I chose to conduct experiments using the Luc Assay method due to its cost-effectiveness and efficiency in measuring the readout of our experiments. I developed a 'Do-It-Yourself' recipe that eliminated the need for relying on commercial buffers and substrates for detecting Renilla and Firefly Luciferases. This approach allowed me to prepare my own solutions from powders and chemicals, enabling me to conduct a greater number of experiments. Additionally, I optimized a protocol that facilitated the simultaneous screening of multiple conditions, with four replicates for each condition. Furthermore, the Glomax Explorer provided the capability to dispense the solutions required for detecting Firefly and Renilla Luciferase directly into each well of a 96-well plate, thanks to a set of injectors. This feature allowed me to measure several plates sequentially, streamlining the data collection process.

Flow Cytometry: Cells were collected 48 hours after transfection, washed and resuspended with PBS (Euroclone). Flow Cytometry analysis were carried out using an Accuri C6 (BD Biosciences), analyzing 10000 cells for each sample. A 488-nm laser with a 670 nm LP filter were used to excite and detect mCherry fluorescence. I chose to conduct flow cytometry experiments when I required data regarding the cell population rather than a system readout. The Luc assay is a quantitative method of detection and provides an average of the cell population, while flow cytometry, although semi-quantitative, also provides information about the behaviour of individual cells. Flow cytometry was employed to assess the transfection conditions, allowing me to obtain information about cell viability 48 hours after transfection, the percentage of transfected cells, and the intensity of the fluorescent signal, indicating the amount of DNA successfully delivered into the cells. Additionally,

flow cytometry was used to evaluate the functionality of the gRNA-inducible promoter. This enabled me to determine how many cells exhibited fluorescence in the absence of the gRNA-dCas9-VPR complex and how many of them activated the signal in its presence.

Real Time – PCR: For Real Time – PCR experiments, 1.25x10^5 HEK293T cells have been seeded in a 24-well cell culture plates (Corning) and, after 18 hours, transfected using a home-made solution of PEI (MW 25000, Polysciences, stock concentration 0,324 mg/ml, pH 7.5) using 700ng of DNA per well. After 48 hours, mRNA has been extracted with RNeasy Mini Kit (Quiagen) and retrotranscribed to cDNA with QuantiTec Reverse Transcription Kit (Quiagen). Real – Time PCR reaction has been performed with 25 ng of template DNA, using the LightCycler® 480 SYBR Green I Master (Roche) and quantified through LightCycler® 96 System (Roche). Primers to detect NEUROD1 RNA were already designed and published[58] while primers to detect AcrII4A has been designed.
AcrII4A_Fw: CAACGATCTGATCCGGGAGA
AcrII4A_Rv: TACTCGTTGCCGTCGTTGTT

Drug treatments: When treated with Doxycycline (Clontech), Shield1 (MedChemExpress) and/or copper dichloride (Sigma-Aldrich), cells were treated immediately before transfection. Drugs' concentrations are referred to the medium volume before adding the transfection mix, while copper concentrations are referred to the medium after adding the transfection mix. Doxycycline was dissolved in H2O while Shield1 was dissolved in DMSO. I utilized Shield1 to stabilize the DD-tagged protein. There are other ligand-dependent destabilization systems available, such as the DHFR-derived destabilization system, which is stabilized by the small molecule TMP. However, I conducted tests with this destabilization domain, and despite being able to restore mCherry fluorescence, I was unable to obtain a functional rtTA when it was fused with the Destabilization Domain.

Appendix

Figure A1: Plasmid expressing the fluorescent reporter mCherry under the control of the gRNA-inducible 1AB_pMin promoter

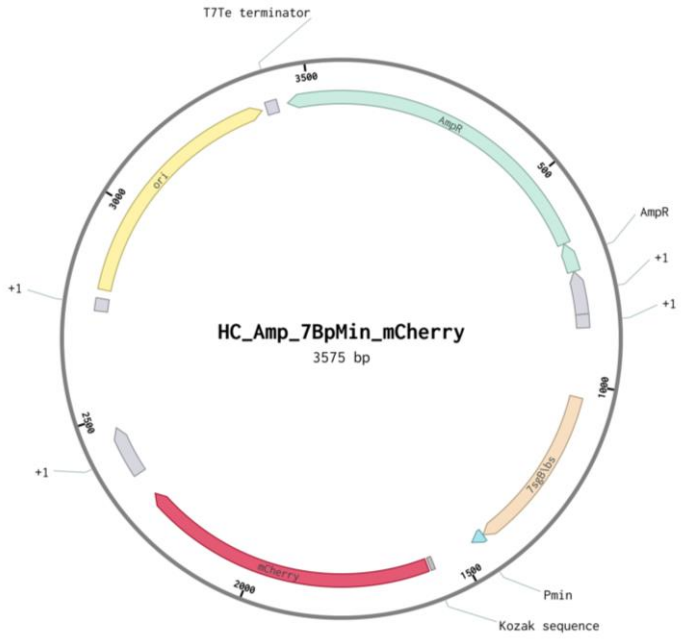

Figure A2: Plasmid expressing the fluorescent reporter mCherry under the control of the gRNA-inducible 7B_pMin promoter

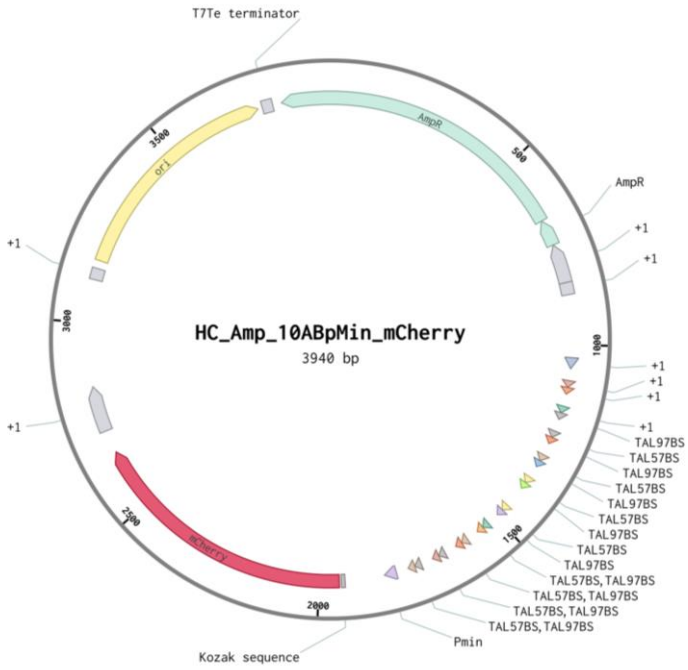

Figure A3: Plasmid expressing the fluorescent reporter mCherry under the control of the gRNA-inducible 10AB_pMin promoter

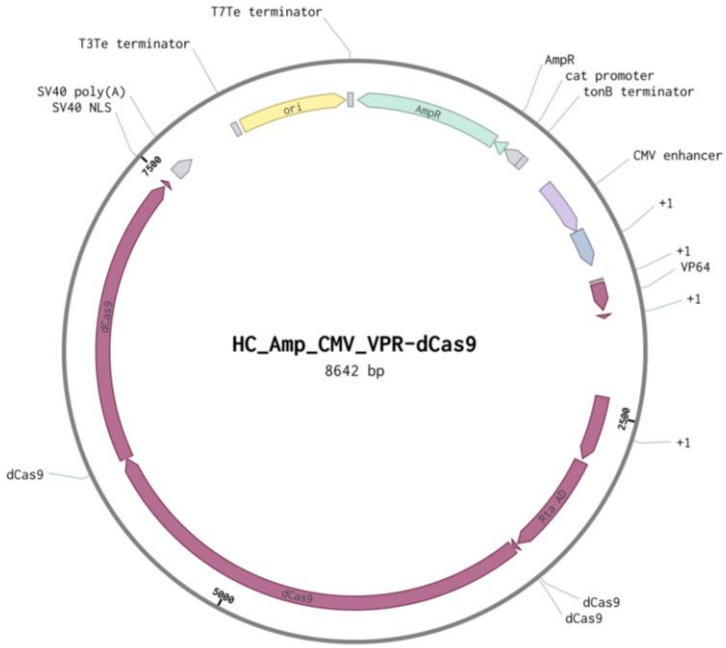

Figure A4: Plasmid expressing the transcription factor VPR-dCas9 under the control of the constitutive promoter CMV

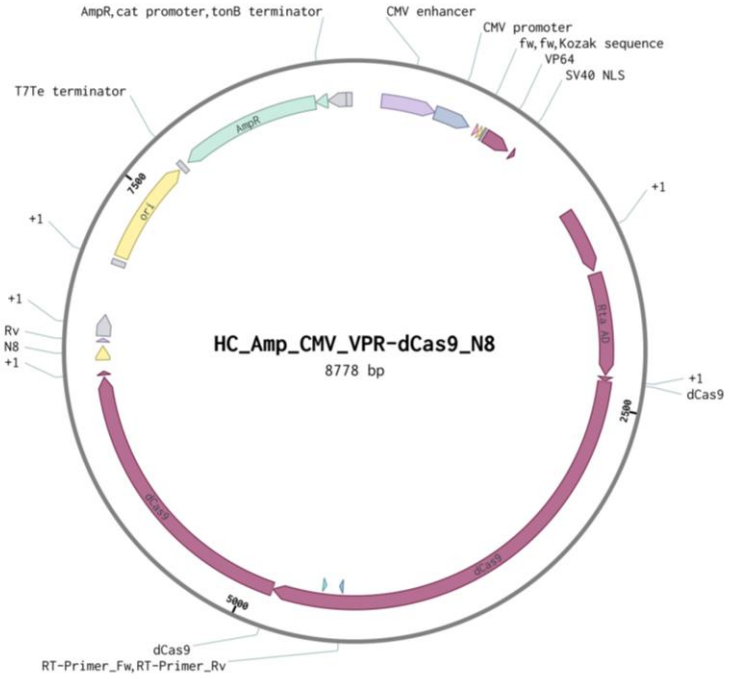

Figure A5: Plasmid expressing the transcription factor VPR-dCas9, fused with the Coiled Coil N8, under the control of the constitutive promoter CMV

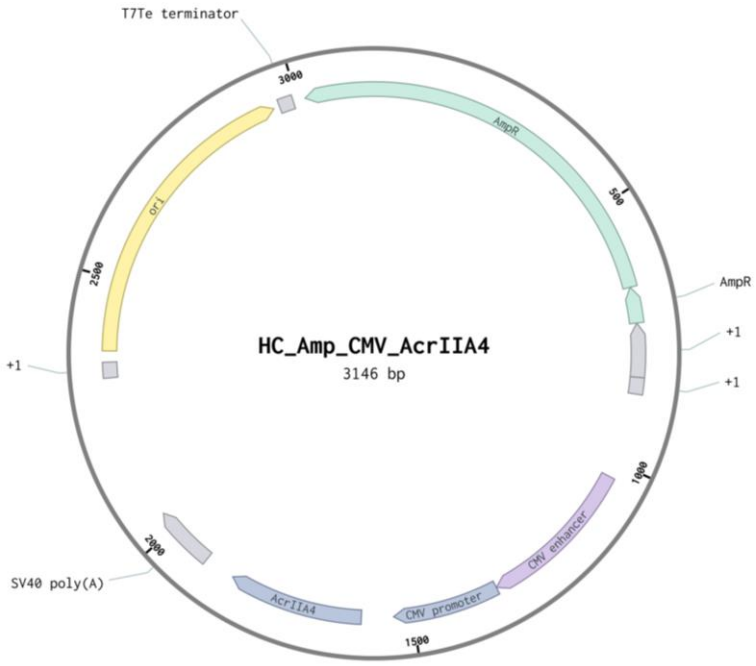

Figure A6: Plasmid expressing the anti-CRISPR protein AcrIIA4 under the control of the constitutive promoter CMV

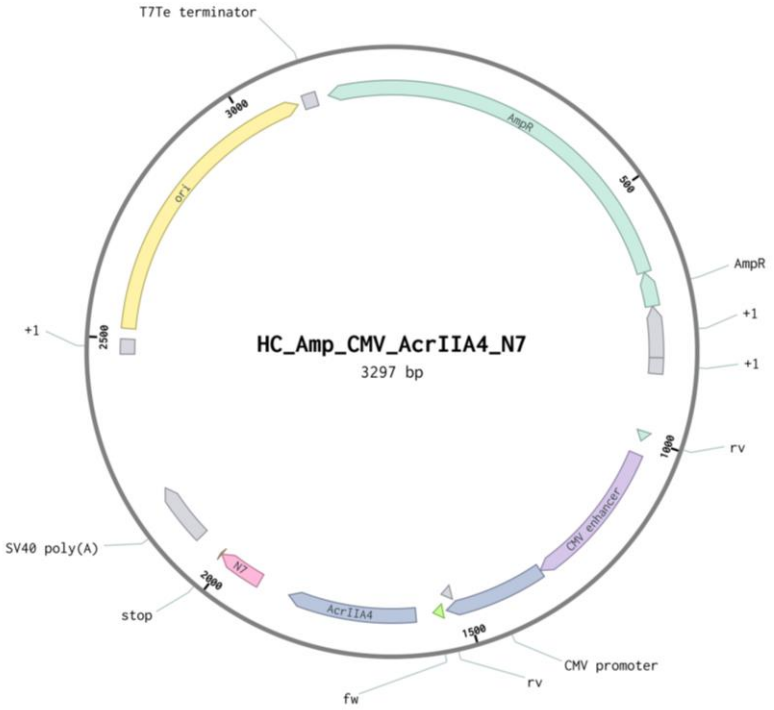

Figure A7: Plasmid expressing the anti-CRISPR protein AcrIIA4, fused with the Coiled Coil N7, under the control of the constitutive promoter CMV

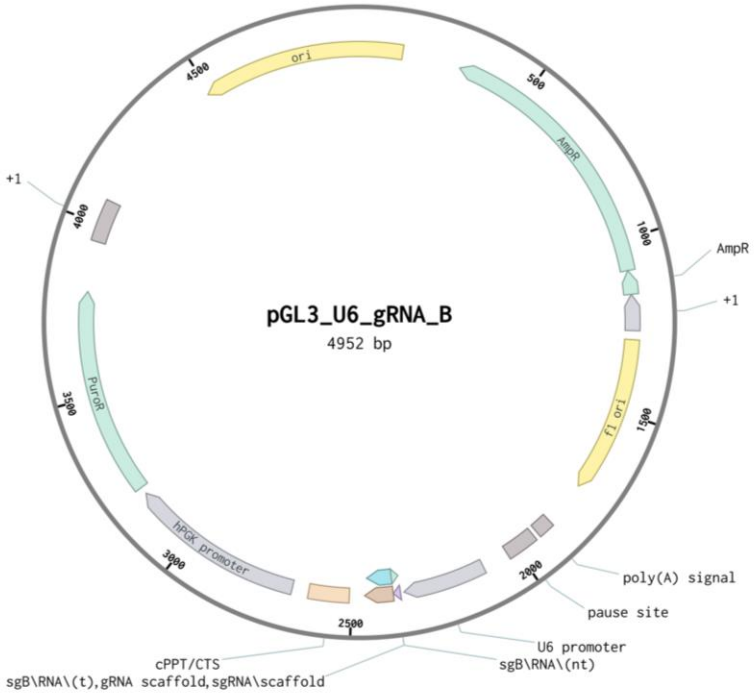

Figure A8: Plasmid expressing the guide RNA gRNA_B under the control of the constitutive promoter U6

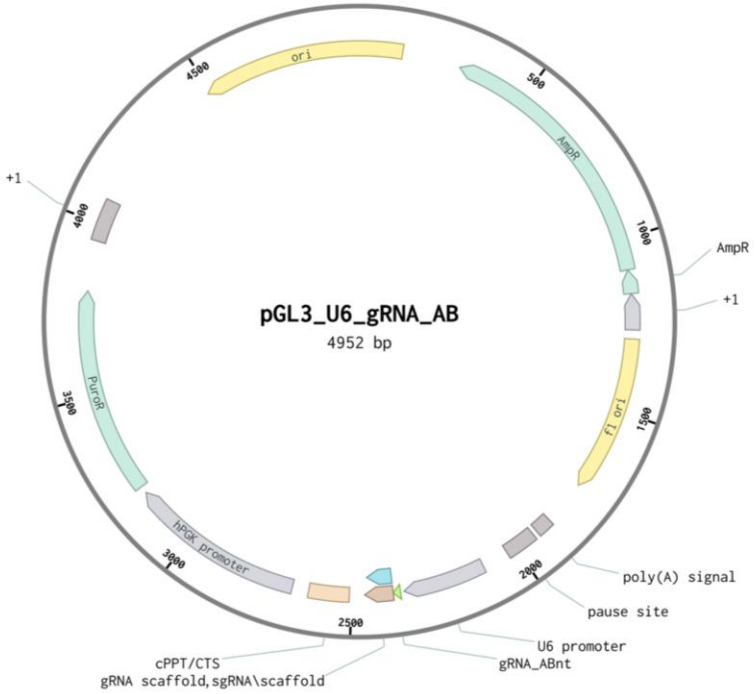

Figure A9: Plasmid expressing the guide RNA gRNA_AB under the control of the constitutive promoter U6

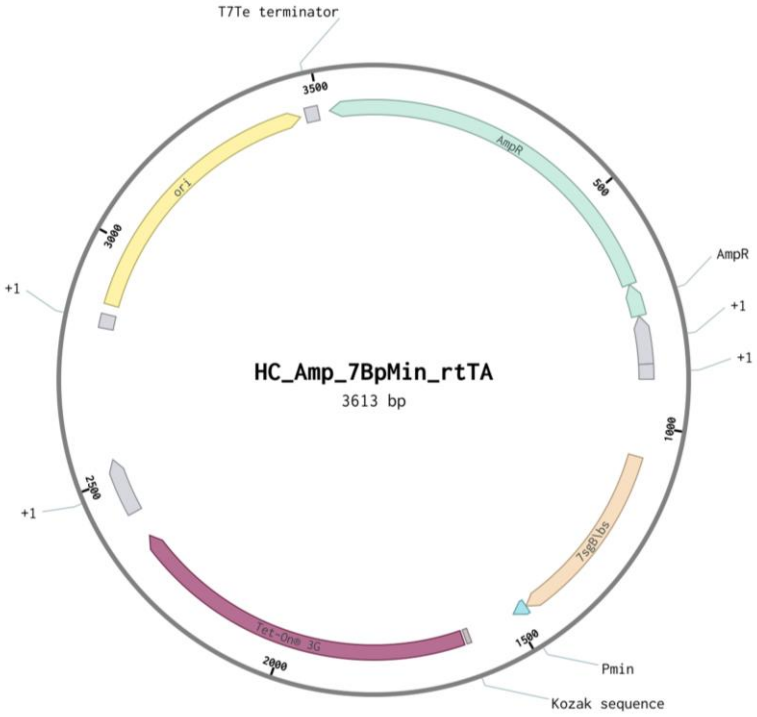

Figure A10: Plasmid expressing the transcription factor rtTA under the control of the gRNA-inducible 7B_pMin promoter

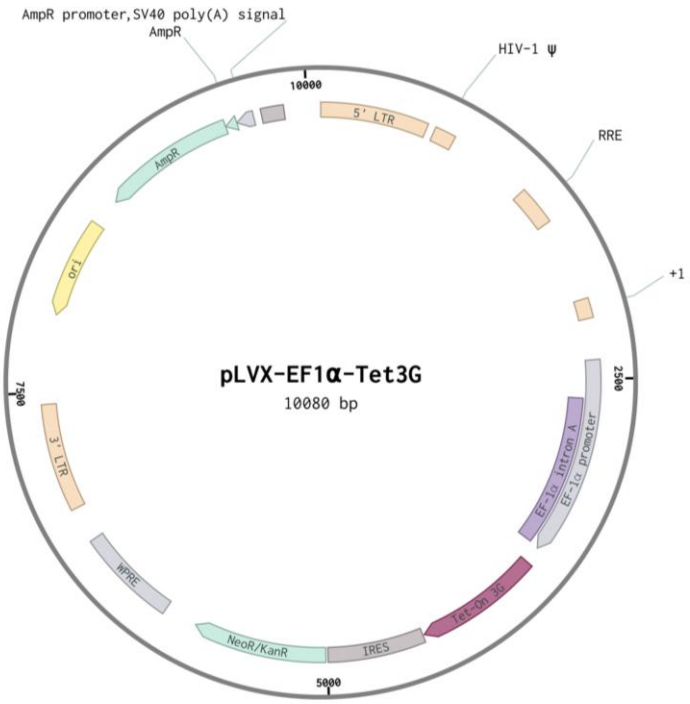

Figure A11: Plasmid expressing the transcription factor rtTA under the control of the constitutive promoter Ef1α

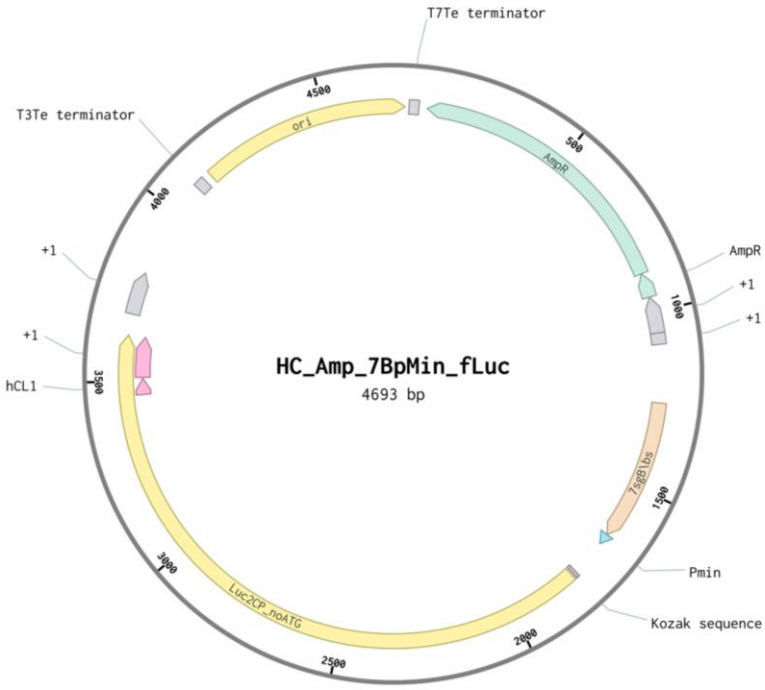

Figure A12: Plasmid expressing the luminescent reporter Firefly Luciferase under the control of the gRNA-inducible 7B_pMin promoter

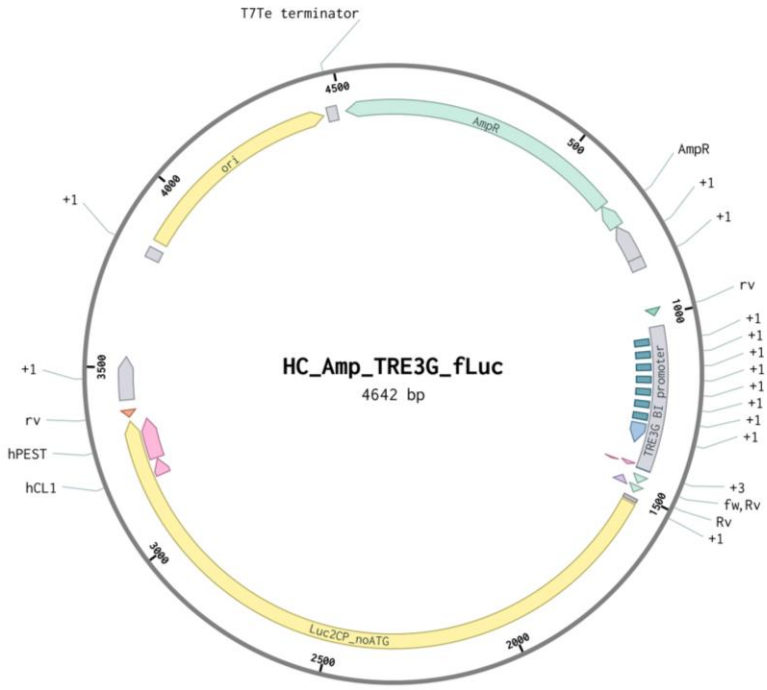

Figure A13: Plasmid expressing the luminescent reporter FireFly Luciferase under the control of the Doxycycline-inducible TRE3G promoter

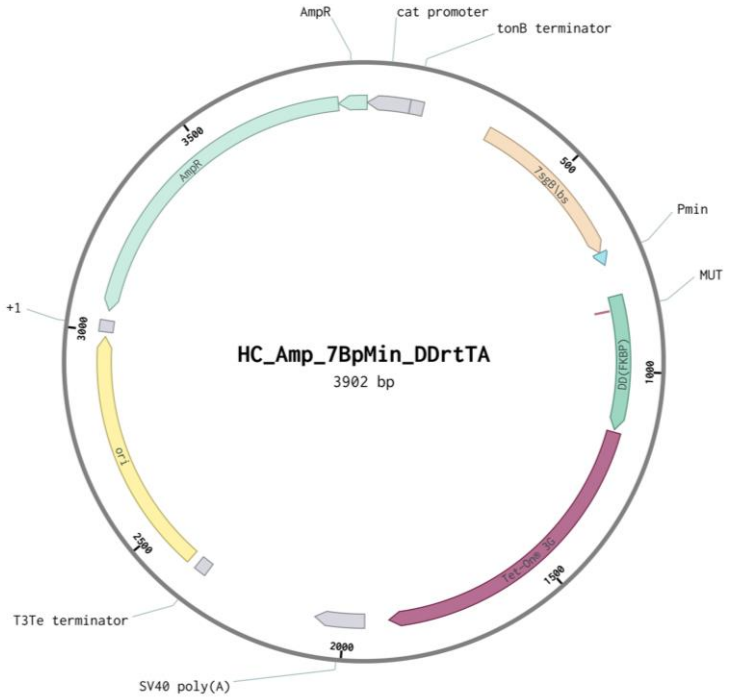

Figure A14: Plasmid expressing the transcription factor rtTA, fused with the FKBP-derived Destabilization Domain, under the control of the gRNA-inducible 7B_pMin promoter

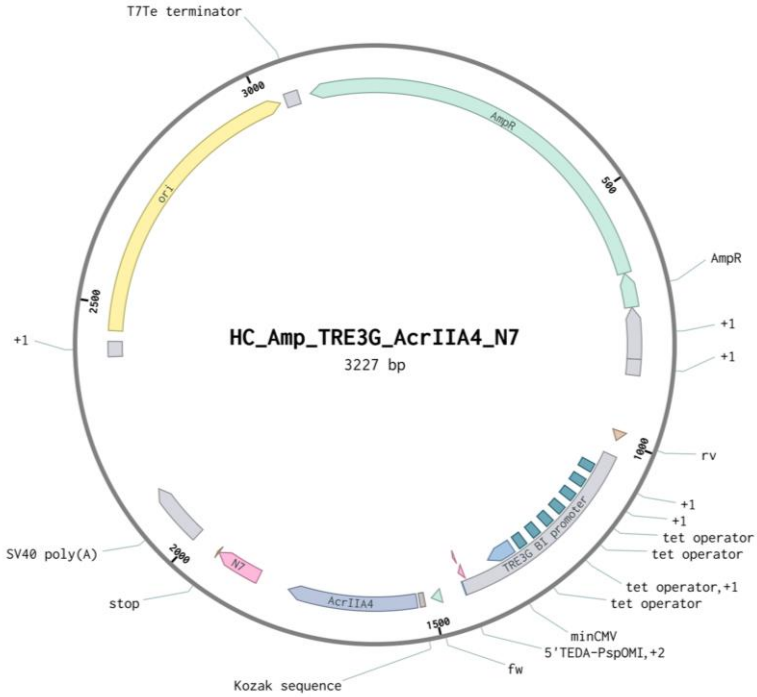

Figure A15: Plasmid expressing the anti-CRISPR protein AcrIIA4, fused with the Coiled Coil N7, under the control of the Doxycycline-inducible TRE3G promoter

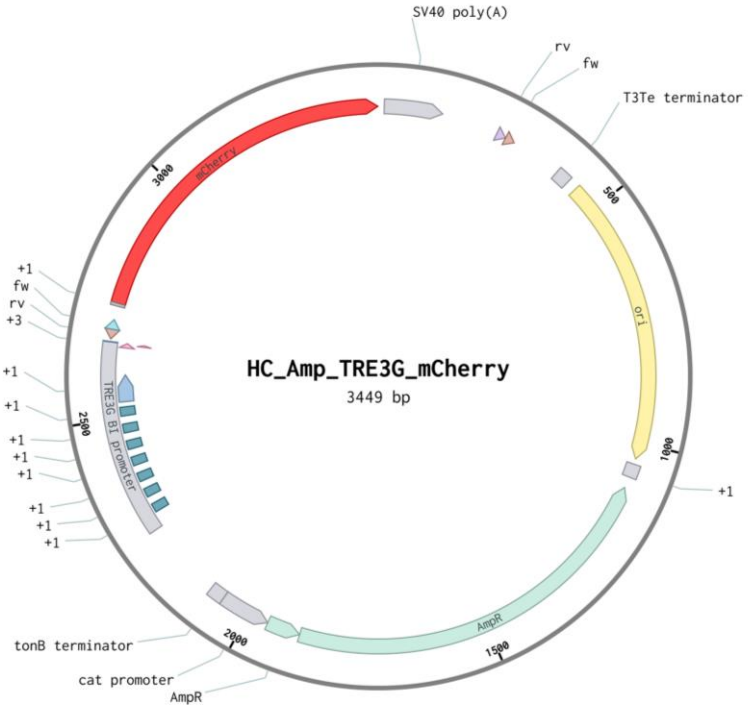

Figure A16: Plasmid expressing the fluorescent reporter mCherry under the control of the Doxycycline-inducible TRE3G promoter

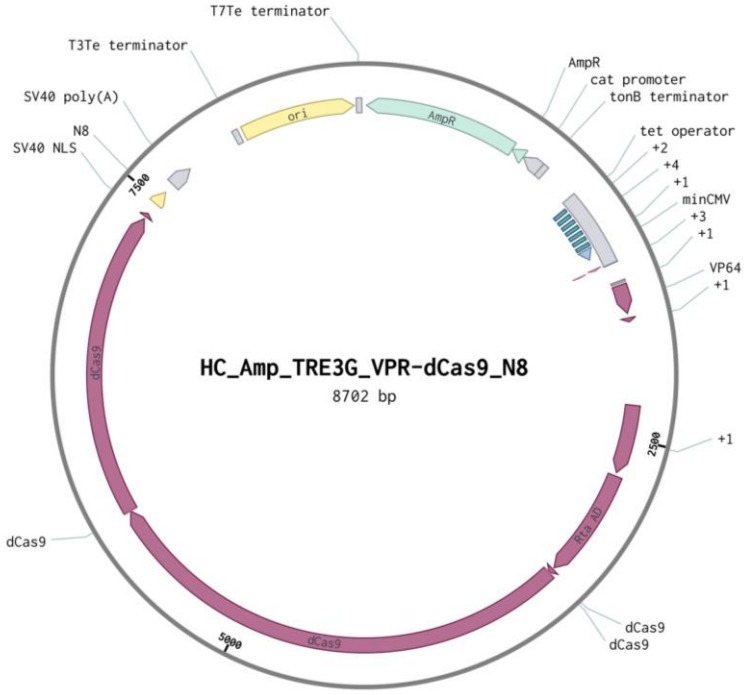

Figure A17: Plasmid expressing the transcription factor VPR-dCas9, fused with the Coiled Coil N8, under the control of the Doxycycline-inducible TRE3G promoter

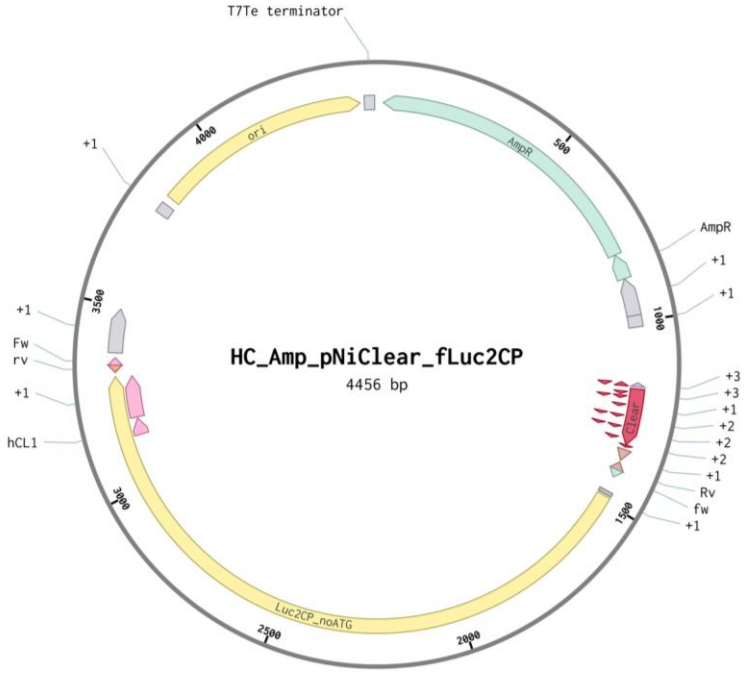

Figure A18: Plasmid expressing the luminescent reporter Firefly Luciferase under the control of the E-Box containing promoter NiClear

Figure A19: Plasmid expressing the anti-CRISPR protein AcrIIA4, fused with the Coiled Coil N7, under the control of the E-Box containing promoter NiClear

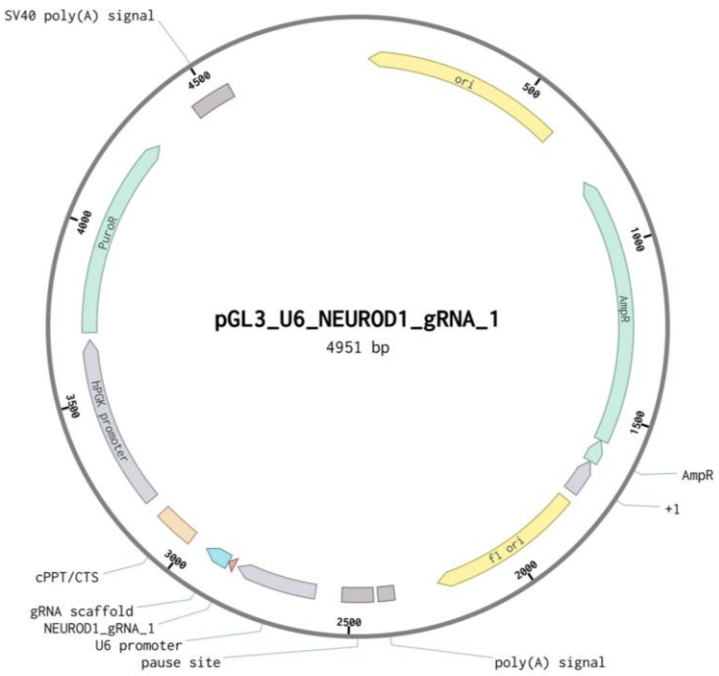

Figure A20: Plasmid expressing one of the guide RNAs for NEUROD1 (NEUROD1_gRNA_1) under the control of the constitutive promoter U6

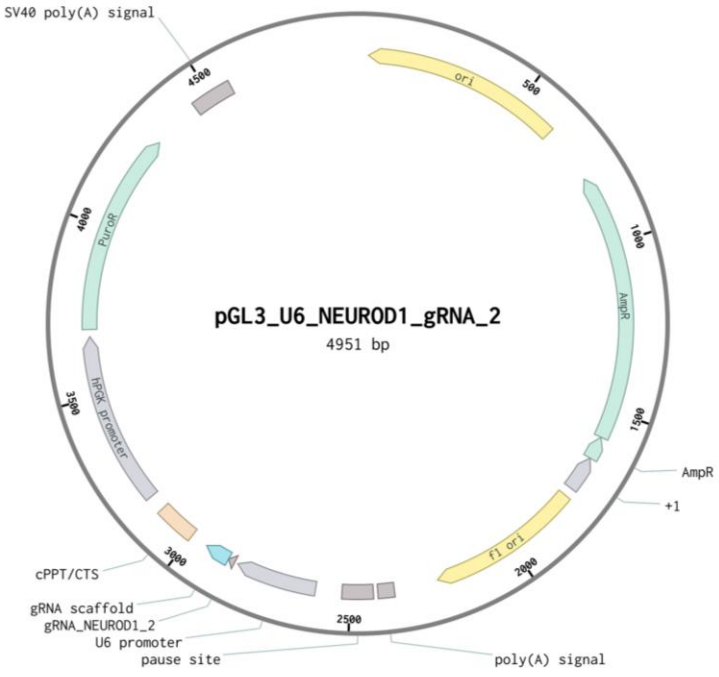

Figure A21: Plasmid expressing one of the guide RNAs for NEUROD1 (NEUROD1_gRNA_2) under the control of the constitutive promoter U6

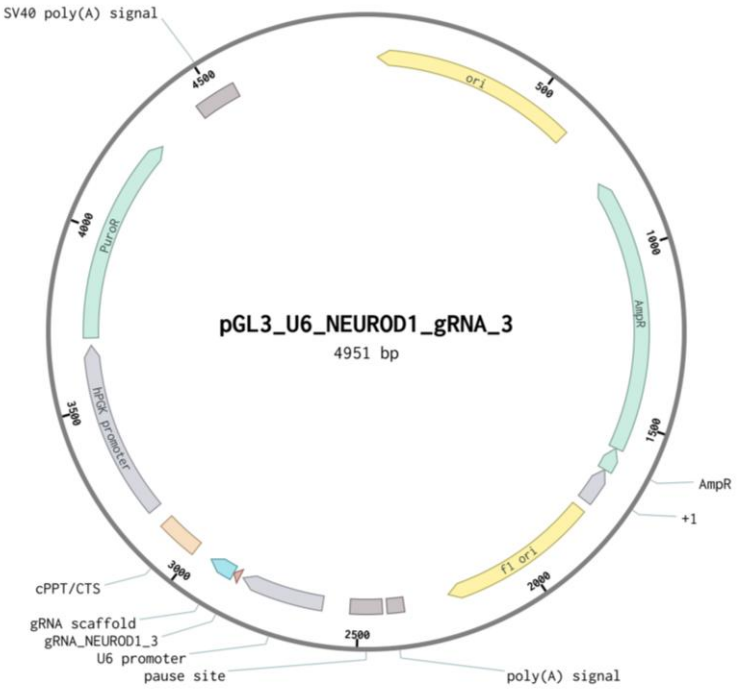

Figure A22: Plasmid expressing one of the guide RNAs for NEUROD1 (NEUROD1_gRNA_3) under the control of the constitutive promoter U6

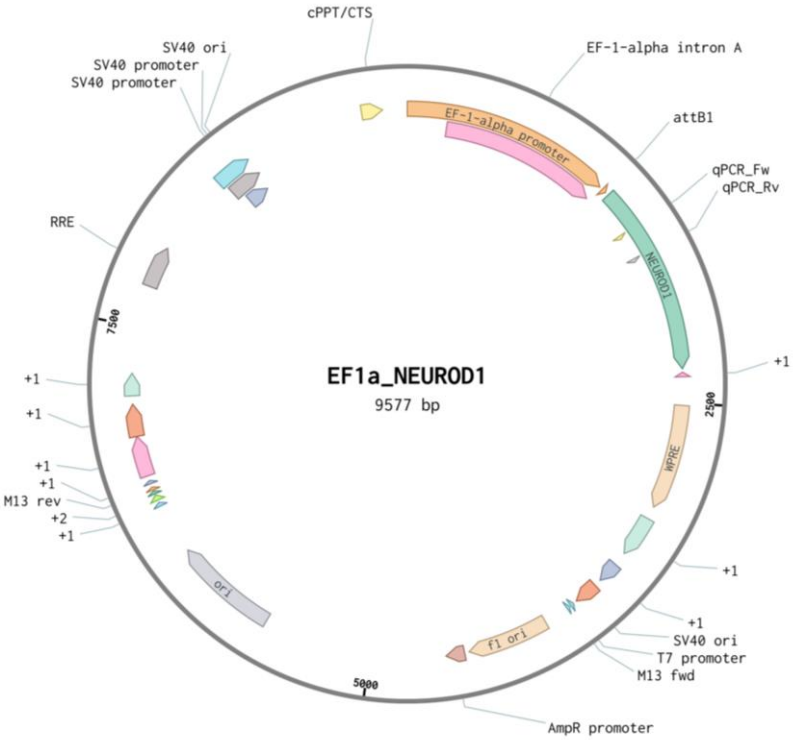

Figure A23: Plasmid expressing the transcription factor NEUROD1 under the control of the constitutive promoter EF1α

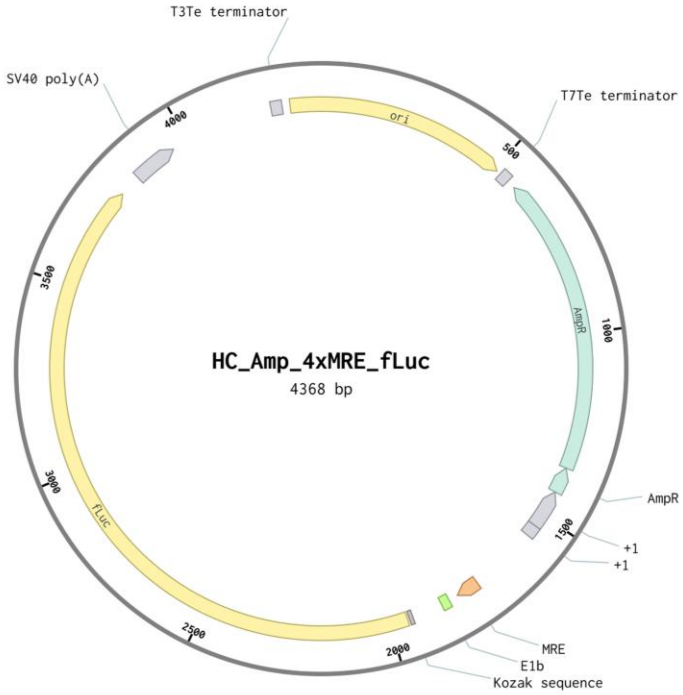

Figure A24: Plasmid expressing the luminescent reporter Firefly Luciferase under the control of the copper-inducible promoter 4xMRE_pMin

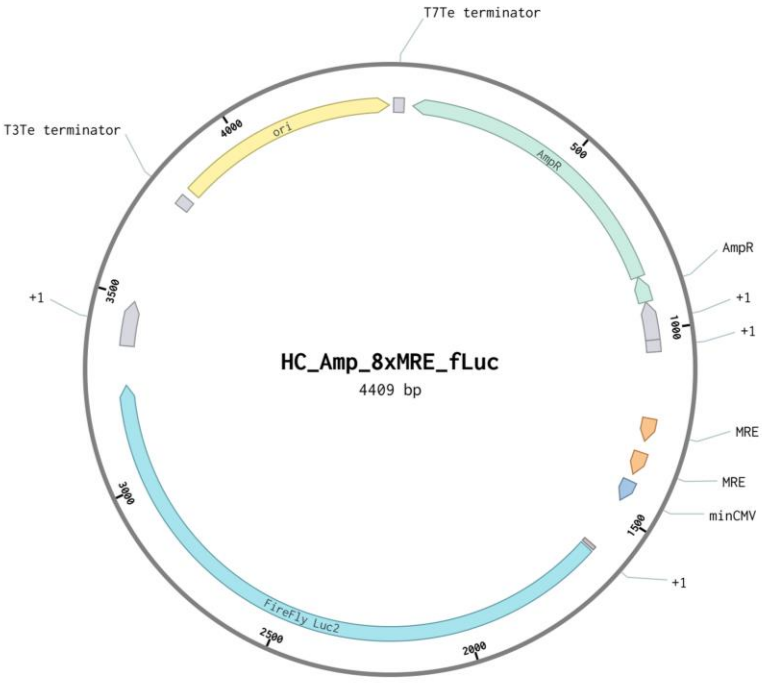

Figure A25: Plasmid expressing the luminescent reporter Firefly Luciferase under the control of the copper-inducible promoter 8xMRE_pMin

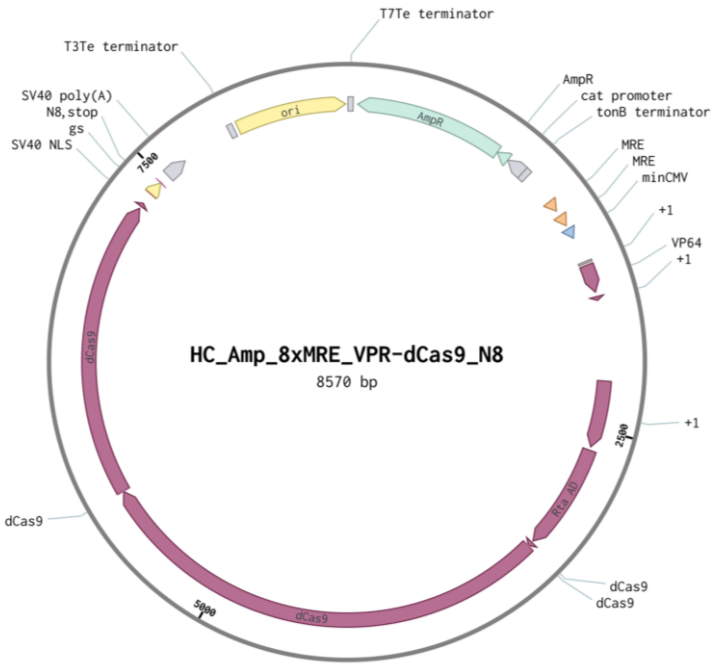

Figure A26: Plasmid expressing the transcription factor VPR-dCas9, fused with the Coiled Coil N8, under the control of the copper-inducible promoter 8xMRE_pMin

References

1. Watson, J. D. & Crick, F. H. C. Molecular structure of nucleic acids: A structure for deoxyribose nucleic acid. *Nature* (1953) doi:10.1038/171737a0.
2. KORNBERG, A. The biologic synthesis of deoxyribonucleic acid. *Stanford Med Bull* **18**, 66–75 (1960).
3. Raju, T. N. The Nobel Chronicles. *The Lancet* **352**, 244 (1998).
4. Jackson, D. A., Symons, R. H. & Berg, P. Biochemical method for inserting new genetic information into DNA of Simian Virus 40: circular SV40 DNA molecules containing lambda phage genes and the galactose operon of Escherichia coli. *Proc Natl Acad Sci U S A* **69**, 2904–2909 (1972).
5. Sanger, F., Nicklen, S. & Coulson, A. R. DNA sequencing with chain-terminating inhibitors. *Proc Natl Acad Sci U S A* **74**, 5463–5467 (1977).
6. Southern, E. M. Detection of specific sequences among DNA fragments separated by gel electrophoresis. *J Mol Biol* **98**, 503–517 (1975).
7. Balbás, P. *et al.* Plasmid vector pBR322 and its special-purpose derivatives--a review. *Gene* **50**, 3–40 (1986).
8. Itakura, K. *et al.* Expression in Escherichia coli of a chemically synthesized gene for the hormone somatostatin. *Science* **198**, 1056–1063 (1977).
9. Goeddel, D. V *et al.* Expression in Escherichia coli of chemically synthesized genes for human insulin. *Proc Natl Acad Sci U S A* **76**, 106–110 (1979).
10. Mullis, K. *et al.* Specific enzymatic amplification of DNA in vitro: the polymerase chain reaction. *Cold Spring Harb Symp Quant Biol* **51 Pt 1**, 263–273 (1986).
11. Shetty, R. P., Endy, D. & Knight, T. F. Engineering BioBrick vectors from BioBrick parts. *J Biol Eng* **2**, 1–12 (2008).
12. Engler, C., Kandzia, R. & Marillonnet, S. A One Pot, One Step, Precision Cloning Method with High Throughput Capability. *PLoS One* **3**, e3647 (2008).
13. Gibson, D. G. *et al.* Enzymatic assembly of DNA molecules up to several hundred kilobases. *Nat Methods* **6**, 343–345 (2009).
14. Weber, E., Engler, C., Gruetzner, R., Werner, S. & Marillonnet, S. A Modular Cloning System for Standardized Assembly of Multigene Constructs. *PLoS One* **6**, 1–11 (2011).
15. Martella, A., Matjusaitis, M., Auxillos, J., Pollard, S. M. & Cai, Y. EMMA: An Extensible Mammalian Modular Assembly Toolkit for the Rapid Design and Production of Diverse Expression Vectors. *ACS Synth Biol* **6**, 1380–1392 (2017).
16. Hughes, R. A. & Ellington, A. D. Synthetic DNA synthesis and assembly: Putting the synthetic in synthetic biology. *Cold Spring Harb Perspect Biol* **9**, (2017).
17. Khorana, H. G. Synthesis in the study of nucleic acids. The Fourth Jubilee Lecture. *Biochem J* **109**, 709–725 (1968).
18. Jacob, F. & Monod, J. Genetic regulatory mechanisms in the synthesis of proteins. *J Mol Biol* **3**, 318–356 (1961).
19. Banerji, J., Rusconi, S. & Schaffner, W. Expression of a β-globin gene is enhanced by remote SV40 DNA sequences. *Cell* **27**, 299–308 (1981).
20. Levine, M. & Tjian, R. Transcription regulation and animal diversity. *Nature* **424**, 147–151 (2003).
21. Shine, J. & Dalgarno, L. The 3' terminal sequence of Escherichia coli 16S ribosomal RNA: complementarity to nonsense triplets and ribosome binding sites. *Proc Natl Acad Sci U S A* **71**, 1342–1346 (1974).
22. Kozak, M. How do eucaryotic ribosomes select initiation regions in messenger RNA? *Cell* **15**, 1109–1123 (1978).
23. Salis, H. M., Mirsky, E. A. & Voigt, C. A. Automated design of synthetic ribosome binding sites to control protein expression. *Nat Biotechnol* **27**, 946–950 (2009).
24. Studier, F. W. & Moffatt, B. A. Use of bacteriophage T7 RNA polymerase to direct selective high-level expression of cloned genes. *J Mol Biol* **189**, 113–130 (1986).
25. Stinski, M. F. History of the molecular biology of cytomegaloviruses. *Methods Mol Biol* **1119**, 1–14 (2014).
26. Qin, J. Y. *et al.* Systematic comparison of constitutive promoters and the doxycycline-inducible promoter. *PLoS One* **5**, 3–6 (2010).
27. Wyborski, D. L. & Short, J. M. Analysis of inducers of the E.coli lac repressor system in mammalian cells and whole animals. *Nucleic Acids Res* **19**, 4647–4653 (1991).
28. Gossen, M. & Bujard, H. Tight control of gene expression in mammalian cells by tetracycline-responsive promoters. *Proc Natl Acad Sci U S A* **89**, 5547–5551 (1992).

29. Gossen, M. *et al.* Transcriptional activation by tetracyclines in mammalian cells. *Science (1979)* (1995) doi:10.1126/science.7792603.
30. Urlinger, S. *et al.* Exploring the sequence space for tetracycline-dependent transcriptional activators: Novel mutations yield expanded range and sensitivity. *Proc Natl Acad Sci U S A* **97**, 7963–7968 (2000).
31. Mullick, A. *et al.* The cumate gene-switch: A system for regulated expression in mammalian cells. *BMC Biotechnol* **6**, 1–18 (2006).
32. Klock, G., Strähle, U. & Schütz, G. Oestrogen and glucocorticoid responsive elements are closely related but distinct. *Nature* **329**, 734–736 (1987).
33. Searle, P. F., Stuart, G. W. & Palmiter, R. D. Building a metal-responsive promoter with synthetic regulatory elements. *Mol Cell Biol* **5**, 1480–1489 (1985).
34. de Mena, L., Rizk, P. & Rincon-Limas, D. E. Bringing Light to Transcription: The Optogenetics Repertoire. *Front Genet* **9**, 1–12 (2018).
35. Ishino, Y., Shinagawa, H., Makino, K., Amemura, M. & Nakata, A. Nucleotide sequence of the iap gene, responsible for alkaline phosphatase isozyme conversion in Escherichia coli, and identification of the gene product. *J Bacteriol* **169**, 5429–5433 (1987).
36. Mojica, F. J., Juez, G. & Rodríguez-Valera, F. Transcription at different salinities of Haloferax mediterranei sequences adjacent to partially modified PstI sites. *Mol Microbiol* **9**, 613–621 (1993).
37. Mojica, F. J. M., Díez-Villaseñor, C., García-Martínez, J. & Soria, E. Intervening sequences of regularly spaced prokaryotic repeats derive from foreign genetic elements. *J Mol Evol* **60**, 174–182 (2005).
38. Makarova, K. S., Aravind, L., Grishin, N. V, Rogozin, I. B. & Koonin, E. V. A DNA repair system specific for thermophilic Archaea and bacteria predicted by genomic context analysis. *Nucleic Acids Res* **30**, 482–496 (2002).
39. Jansen, R., Embden, J. D. A. van, Gaastra, W. & Schouls, L. M. Identification of genes that are associated with DNA repeats in prokaryotes. *Mol Microbiol* **43**, 1565–1575 (2002).
40. Makarova, K. S., Grishin, N. V, Shabalina, S. A., Wolf, Y. I. & Koonin, E. V. A putative RNA-interference-based immune system in prokaryotes: computational analysis of the predicted enzymatic machinery, functional analogies with eukaryotic RNAi, and hypothetical mechanisms of action. *Biol Direct* **1**, 7 (2006).
41. Jinek, M. *et al.* A programmable dual-RNA-guided DNA endonuclease in adaptive bacterial immunity. *Science* **337**, 816–821 (2012).
42. Christian, M. *et al.* Targeting DNA double-strand breaks with TAL effector nucleases. *Genetics* **186**, 757–761 (2010).
43. Urnov, F. D., Rebar, E. J., Holmes, M. C., Zhang, H. S. & Gregory, P. D. Genome editing with engineered zinc finger nucleases. *Nat Rev Genet* **11**, 636–646 (2010).
44. Miller, J. C. *et al.* A TALE nuclease architecture for efficient genome editing. *Nat Biotechnol* **29**, 143–150 (2011).
45. Mali, P. *et al.* RNA-Guided Human Genome Engineering via Cas9. *Science (1979)* **339**, 823–826 (2013).
46. Ran, F. A. *et al.* In vivo genome editing using Staphylococcus aureus Cas9. *Nature* **520**, 186–191 (2015).
47. Hsu, P. D., Lander, E. S. & Zhang, F. Development and applications of CRISPR-Cas9 for genome engineering. *Cell* **157**, 1262–1278 (2014).
48. Cong, L. *et al.* Multiplex genome engineering using CRISPR/Cas systems. *Science* **339**, 819–823 (2013).
49. Ran, F. A. *et al.* Double nicking by RNA-guided CRISPR Cas9 for enhanced genome editing specificity. *Cell* **154**, 1380–1389 (2013).
50. Larson, M. H. *et al.* CRISPR interference (CRISPRi) for sequence-specific control of gene expression. *Nat Protoc* **8**, 2180–2196 (2013).
51. Gilbert, L. A. *et al.* CRISPR-mediated modular RNA-guided regulation of transcription in eukaryotes. *Cell* **154**, 442–451 (2013).
52. Yeo, N. C. *et al.* An enhanced CRISPR repressor for targeted mammalian gene regulation. *Nat Methods* **15**, 611–616 (2018).
53. Perez-Pinera, P. *et al.* RNA-guided gene activation by CRISPR-Cas9-based transcription factors. *Nat Methods* **10**, 973–976 (2013).
54. Konermann, S. *et al.* Genome-scale transcriptional activation by an engineered CRISPR-Cas9 complex. *Nature* **517**, 583–588 (2015).

55. Gilbert, L. A. *et al.* Genome-Scale CRISPR-Mediated Control of Gene Repression and Activation. *Cell* **159**, 647–661 (2014).
56. Chavez, A. *et al.* Highly efficient Cas9-mediated transcriptional programming. *Nat Methods* **12**, 326–328 (2015).
57. Tanenbaum, M. E., Gilbert, L. A., Qi, L. S., Weissman, J. S. & Vale, R. D. A protein-tagging system for signal amplification in gene expression and fluorescence imaging. *Cell* **159**, 635–646 (2014).
58. Chavez, A. *et al.* Comparison of Cas9 activators in multiple species. *Nat Methods* **13**, 563–567 (2016).
59. Liu, Y. *et al.* CRISPR Activation Screens Systematically Identify Factors that Drive Neuronal Fate and Reprogramming. *Cell Stem Cell* **23**, 758-771.e8 (2018).
60. Ahmed, M. *et al.* CRISPRi screens reveal a DNA methylation-mediated 3D genome dependent causal mechanism in prostate cancer. *Nat Commun* **12**, 1–15 (2021).
61. Kampmann, M. CRISPRi and CRISPRa Screens in Mammalian Cells for Precision Biology and Medicine. *ACS Chem Biol* (2018) doi:10.1021/acschembio.7b00657.
62. Drobna-Śledzińska, M. *et al.* CRISPRi for specific inhibition of miRNA clusters and miRNAs with high sequence homology. *Sci Rep* **12**, 6297 (2022).
63. Heman-Ackah, S. M., Bassett, A. R. & Wood, M. J. A. Precision Modulation of Neurodegenerative Disease-Related Gene Expression in Human iPSC-Derived Neurons. *Sci Rep* **6**, 28420 (2016).
64. Yoshida, M. *et al.* Development of an integrated CRISPRi targeting ΔNp63 for treatment of squamous cell carcinoma. *Oncotarget* **9**, 29220–29232 (2018).
65. Moreno, A. M. *et al.* In Situ Gene Therapy via AAV-CRISPR-Cas9-Mediated Targeted Gene Regulation. *Mol Ther* **26**, 1818–1827 (2018).
66. Sokka, J. *et al.* CRISPR activation enables high-fidelity reprogramming into human pluripotent stem cells. *Stem Cell Reports* **17**, 413–426 (2022).
67. Liu, Y. *et al.* CRISPR Activation Screens Systematically Identify Factors that Drive Neuronal Fate and Reprogramming. *Cell Stem Cell* **23**, 758-771.e8 (2018).
68. Liu, P., Chen, M., Liu, Y., Qi, L. S. & Ding, S. CRISPR-Based Chromatin Remodeling of the Endogenous Oct4 or Sox2 Locus Enables Reprogramming to Pluripotency. *Cell Stem Cell* **22**, 252-261.e4 (2018).
69. Urrutia-Cabrera, D. *et al.* Combinatorial Approach of Binary Colloidal Crystals and CRISPR Activation to Improve Induced Pluripotent Stem Cell Differentiation into Neurons. *ACS Appl Mater Interfaces* **14**, 8669–8679 (2022).
70. Zhou, M. *et al.* Reprogramming astrocytes to motor neurons by activation of endogenous Ngn2 and Isl1. *Stem Cell Reports* **16**, 1777–1791 (2021).
71. Matharu, N. *et al.* CRISPR-mediated activation of a promoter or enhancer rescues obesity caused by haploinsufficiency. *Science* **363**, (2019).
72. Becirovic, E. Maybe you can turn me on: CRISPRa-based strategies for therapeutic applications. *Cellular and Molecular Life Sciences* Preprint at https://doi.org/10.1007/s00018-022-04175-8 (2022).
73. Bendixen, L., Jensen, T. I. & Bak, R. O. CRISPR-Cas-mediated transcriptional modulation: The therapeutic promises of CRISPRa and CRISPRi. *Molecular Therapy* **31**, 1920–1937 (2023).
74. Salvador, A. Uri Alon, An Introduction to Systems Biology: Design Principles of Biological Circuits, Chapman & Hall/CRC, London, ISBN 1584886420, GBP 30.99, 2007 (320 pp.). *Mathematical Biosciences - MATH BIOSCI* **215**, 193–195 (2008).
75. Elowitz, M. B. & Leibler, S. A synthetic oscillatory network of transcriptional regulators. *Nature* **403**, 335–338 (2000).
76. Tigges, M., Marquez-Lago, T. T., Stelling, J. & Fussenegger, M. A tunable synthetic mammalian oscillator. *Nature* **457**, 309–312 (2009).
77. Potvin-Trottier, L., Lord, N. D., Vinnicombe, G. & Paulsson, J. Synchronous long-term oscillations in a synthetic gene circuit. *Nature* **538**, 514–517 (2016).
78. Riglar, D. T. *et al.* Bacterial variability in the mammalian gut captured by a single-cell synthetic oscillator. *Nat Commun* **10**, 1–12 (2019).
79. Gardner, T. S., Cantor, C. R. & Collins, J. J. Construction of a genetic toggle switch in Escherichia coli. *Nature* **403**, 339–342 (2000).
80. Kramer, B. P. *et al.* An engineered epigenetic transgene switch in mammalian cells. *Nat Biotechnol* **22**, 867–870 (2004).
81. Riglar, D. T. *et al.* Engineered bacteria can function in the mammalian gut long-term as live diagnostics of inflammation. *Nat Biotechnol* **35**, 653–658 (2017).

82. Singh, V. Recent advances and opportunities in synthetic logic gates engineering in living cells. *Syst Synth Biol* **8**, 271–282 (2014).
83. Kramer, B. P., Fischer, C. & Fussenegger, M. BioLogic gates enable logical transcription control in mammalian cells. *Biotechnol Bioeng* **87**, 478–484 (2004).
84. Choe, J. H. *et al.* SynNotch-CAR T cells overcome challenges of specificity, heterogeneity, and persistence in treating glioblastoma. *Sci Transl Med* **13**, (2021).
85. Dannenfelser, R. *et al.* Discriminatory Power of Combinatorial Antigen Recognition in Cancer T Cell Therapies. *Cell Syst* **11**, 215-228.e5 (2020).
86. Esensten, J. H., Bluestone, J. A. & Lim, W. A. Engineering Therapeutic T Cells: From Synthetic Biology to Clinical Trials. *Annu Rev Pathol* **12**, 305–330 (2017).
87. Mangan, S. & Alon, U. Structure and function of the feed-forward loop network motif. *Proc Natl Acad Sci U S A* **100**, 11980–11985 (2003).
88. Becskei, A. & Serrano, L. Engineering stability in gene networks by autoregulation. *Nature* (2000) doi:10.1038/35014651.
89. Rosenfeld, N., Elowitz, M. B. & Alon, U. Negative autoregulation speeds the response times of transcription networks. *J Mol Biol* (2002) doi:10.1016/S0022-2836(02)00994-4.
90. Guinn, M. T. & Balázsi, G. Noise-reducing optogenetic negative-feedback gene circuits in human cells. *Nucleic Acids Res* **47**, 7703–7714 (2019).
91. Ma, W., Trusina, A., El-Samad, H., Lim, W. A. & Tang, C. Defining Network Topologies that Can Achieve Biochemical Adaptation. *Cell* **138**, 760–773 (2009).
92. Ciliberti, S., Martin, O. C. & Wagner, A. Robustness Can Evolve Gradually in Complex Regulatory Gene Networks with Varying Topology. *PLoS Comput Biol* **3**, e15 (2007).
93. Kitano, H. Biological robustness. *Nat Rev Genet* **5**, 826–837 (2004).
94. Shakiba, N., Jones, R. D., Weiss, R. & Del Vecchio, D. Context-aware synthetic biology by controller design: Engineering the mammalian cell. *Cell Syst* **12**, 561–592 (2021).
95. Soumpasis, D. A genetic switch: gene control and phage λ Mark Ptashne, Blackwell Scientific Publications and Cell Press, Palo Alto, CA, 1986, 138 pp., $16.95. *Mathematical Biosciences - MATH BIOSCI* **86**, 239–240 (1987).
96. Zhu, X.-M., Yin, L., Hood, L. & Ao, P. Calculating biological behaviors of epigenetic states in the phage lambda life cycle. *Funct Integr Genomics* **4**, 188–195 (2004).
97. Santillán, M. & Mackey, M. C. Why the lysogenic state of phage lambda is so stable: a mathematical modeling approach. *Biophys J* **86**, 75–84 (2004).
98. Alon, U., Surette, M. G., Barkai, N. & Leibler, S. Robustness in bacterial chemotaxis. *Nature* **397**, 168–171 (1999).
99. von Dassow, G., Meir, E., Munro, E. M. & Odell, G. M. The segment polarity network is a robust developmental module. *Nature* **406**, 188–192 (2000).
100. Ingolia, N. T. Topology and Robustness in the Drosophila Segment Polarity Network. *PLoS Biol* **2**, e123 (2004).
101. Kitano, H. Cancer robustness: Tumour tactics. *Nature* **426**, 125 (2003).
102. Kitano, H. *et al.* Metabolic syndrome and robustness tradeoffs. *Diabetes* **53 Suppl 3**, S6–S15 (2004).
103. Kumar, S. & Hasty, J. Stability, robustness, and containment: preparing synthetic biology for real-world deployment. *Curr Opin Biotechnol* **79**, 102880 (2023).
104. Tang, C. *et al.* On-demand biomanufacturing through synthetic biology approach. *Mater Today Bio* **18**, 100518 (2023).
105. Fusco, V., Fiore, D., di Bernardo, M. & di Bernardo, D. Next generation whole-cell biosensors. *IFAC-PapersOnLine* (2022) doi:10.1016/j.ifacol.2023.01.035.
106. McNerney, M. P., Doiron, K. E., Ng, T. L., Chang, T. Z. & Silver, P. A. Theranostic cells: emerging clinical applications of synthetic biology. *Nat Rev Genet* **22**, 730–746 (2021).
107. Siciliano, V. *et al.* MiRNAs confer phenotypic robustness to gene networks by suppressing biological noise. *Nat Commun* **4**, 1–17 (2013).
108. Lillacci, G., Benenson, Y. & Khammash, M. Synthetic control systems for high performance gene expression in mammalian cells. *Nucleic Acids Res* **46**, 9855–9863 (2018).
109. Kelly, C. L. *et al.* Synthetic negative feedback circuits using engineered small RNAs. *Nucleic Acids Res* **46**, 9875–9889 (2018).
110. Jones, R. D. *et al.* Robust and tunable signal processing in mammalian cells via engineered covalent modification cycles. *Nat Commun* **13**, 1720 (2022).
111. Jones, R. D. *et al.* An endoribonuclease-based feedforward controller for decoupling resource-limited genetic modules in mammalian cells. *Nat Commun* **11**, 5690 (2020).

112. Cella, F., Wroblewska, L., Weiss, R. & Siciliano, V. Engineering protein-protein devices for multilayered regulation of mRNA translation using orthogonal proteases in mammalian cells. *Nat Commun* **9**, 4392 (2018).
113. Araujo, R. P. & Liotta, L. A. The topological requirements for robust perfect adaptation in networks of any size. *Nat Commun* **9**, 1757 (2018).
114. Khammash, M. H. Perfect adaptation in biology. *Cell Syst* **12**, 509–521 (2021).
115. El-Samad, H., Goff, J. P. & Khammash, M. Calcium homeostasis and parturient hypocalcemia: An integral feedback perspective. *J Theor Biol* **214**, 17–29 (2002).
116. Barkai, N. & Leibler, S. Robustness in simple biochemical networks. *Nature* **387**, 913–917 (1997).
117. Hansen, C. H., Endres, R. G. & Wingreen, N. S. Chemotaxis in Escherichia coli: A Molecular Model for Robust Precise Adaptation. *PLoS Comput Biol* **4**, e1 (2008).
118. Yi, T.-M., Huang, Y., Simon, M. I. & Doyle, J. Robust perfect adaptation in bacterial chemotaxis through integral feedback control. *Proceedings of the National Academy of Sciences* **97**, 4649–4653 (2000).
119. Muzzey, D., Gómez-Uribe, C. A., Mettetal, J. T. & van Oudenaarden, A. A systems-level analysis of perfect adaptation in yeast osmoregulation. *Cell* **138**, 160–171 (2009).
120. Doyle, J. C. Even Noisy Responses Can Be Perfect If Integrated Properly. *Cell Syst* **2**, 73–75 (2016).
121. Briat, C., Gupta, A. & Khammash, M. Antithetic Integral Feedback Ensures Robust Perfect Adaptation in Noisy Bimolecular Networks. *Cell Syst* **2**, 15–26 (2016).
122. Aoki, S. K. *et al.* A universal biomolecular integral feedback controller for robust perfect adaptation. *Nature* vol. 570 533–537 Preprint at https://doi.org/10.1038/s41586-019-1321-1 (2019).
123. Frei, T., Chang, C. H., Filo, M., Arampatzis, A. & Khammash, M. A genetic mammalian proportional-integral feedback control circuit for robust and precise gene regulation. *Proc Natl Acad Sci U S A* **119**, 1–12 (2022).
124. Anastassov, S., Filo, M., Chang, C. H. & Khammash, M. A cybergenetic framework for engineering intein-mediated integral feedback control systems. *Nat Commun* (2023) doi:10.1038/s41467-023-36863-9.
125. Briat, C., Gupta, A. & Khammash, M. Antithetic Integral Feedback Ensures Robust Perfect Adaptation in Noisy Bimolecular Networks. *Cell Syst* **2**, 15–26 (2016).
126. Aoki, S. K. *et al.* A universal biomolecular integral feedback controller for robust perfect adaptation. *Nature* **570**, 533–537 (2019).
127. Olsman, N. *et al.* Hard Limits and Performance Tradeoffs in a Class of Antithetic Integral Feedback Networks. *Cell Syst* **9**, 49-63.e16 (2019).
128. Nakamura, M. *et al.* Anti-CRISPR-mediated control of gene editing and synthetic circuits in eukaryotic cells. *Nat Commun* **10**, 1–11 (2019).
129. Lebar, T., Lainšček, D., Merljak, E., Aupič, J. & Jerala, R. A tunable orthogonal coiled-coil interaction toolbox for engineering mammalian cells. *Nat Chem Biol* **16**, 513–519 (2020).
130. Praznik, A. *et al.* Regulation of protein secretion through chemical regulation of endoplasmic reticulum retention signal cleavage. *Nat Commun* **13**, 1–14 (2022).
131. Rauch, B. J. *et al.* Inhibition of CRISPR-Cas9 with Bacteriophage Proteins. *Cell* **168**, 150-158.e10 (2017).
132. Dong, D. *et al.* Structural basis of CRISPR-SpyCas9 inhibition by an anti-CRISPR protein. *Nature* **546**, 436–439 (2017).
133. Plaper, T. *et al.* Coiled-coil heterodimers with increased stability for cellular regulation and sensing SARS-CoV-2 spike protein-mediated cell fusion. *Sci Rep* **11**, 1–16 (2021).
134. Haugwitz, M., Garachtchenko, T., Nourzaie, O., Gandlur, S. & Sagawa, H. Rapid, on-demand protein stabilization and destabilization using the ProteoTuner™ systems. *Nat Methods* **5**, iii–iv (2008).
135. Ku, S. C. Y. *et al.* Regulation of XBP-1 signaling during transient and stable recombinant protein production in CHO cells. *Biotechnol Prog* (2010) doi:10.1002/btpr.322.
136. Ma, Y. & Hendershot, L. M. Delineation of a negative feedback regulatory loop that controls protein translation during endoplasmic reticulum stress. *Journal of Biological Chemistry* **278**, 34864–34873 (2003).
137. Zhang, W., Li, X., Wang, S., Chen, Y. & Liu, H. Regulation of TFEB activity and its potential as a therapeutic target against kidney diseases. *Cell Death Discov* **6**, (2020).

138. Pataskar, A. *et al.* NeuroD1 reprograms chromatin and transcription factor landscapes to induce the neuronal program. *EMBO J* **35**, 24–45 (2016).
139. Breslin, M. B., Zhu, M. & Lan, M. S. NeuroD1/E47 regulates the E-box element of a novel zinc finger transcription factor, IA-1, in developing nervous system. *Journal of Biological Chemistry* (2003) doi:10.1074/jbc.M306795200.
140. Matsuda-Ito, K., Matsuda, T. & Nakashima, K. Expression level of the reprogramming factor NeuroD1 is critical for neuronal conversion efficiency from different cell types. *Sci Rep* **12**, 1–11 (2022).
141. Moretti, M. Elucidating the gene regulatory network regulated by the TFEB transcription factor: an integrated experimental and computational approach. *Dibernardo.Tigem.It* (2013).
142. Bhalla, N., Jolly, P., Formisano, N. & Estrela, P. Introduction to biosensors. *Essays Biochem* (2016) doi:10.1042/EBC20150001.
143. Gheorghiu, M. A short review on cell-based biosensing: challenges and breakthroughs in biomedical analysis. *J Biomed Res* (2021) doi:10.7555/JBR.34.20200128.
144. Tellechea-Luzardo, J., Stiebritz, M. T. & Carbonell, P. Transcription factor-based biosensors for screening and dynamic regulation. *Frontiers in Bioengineering and Biotechnology* Preprint at https://doi.org/10.3389/fbioe.2023.1118702 (2023).
145. Singh, A. & Kumar, V. Recent advances in synthetic biology–enabled and natural whole-cell optical biosensing of heavy metals. *Analytical and Bioanalytical Chemistry* Preprint at https://doi.org/10.1007/s00216-020-02953-6 (2021).
146. Hernández-Candia, C. N., Wysoczynski, C. L. & Tucker, C. L. Advances in optogenetic regulation of gene expression in mammalian cells using cryptochrome 2 (CRY2). *Methods* (2019) doi:10.1016/j.ymeth.2019.03.011.
147. Belkin, S. & Roda, A. *Handbook of Cell Biosensors*. *Handbook of Cell Biosensors* (2020). doi:10.1007/978-3-319-47405-2.
148. Prabowo, B. A., Cabral, P. D., Freitas, P. & Fernandes, E. The challenges of developing biosensors for clinical assessment: A review. *Chemosensors* Preprint at https://doi.org/10.3390/chemosensors9110299 (2021).
149. Hicks, M., Bachmann, T. T. & Wang, B. Synthetic Biology Enables Programmable Cell-Based Biosensors. *ChemPhysChem* Preprint at https://doi.org/10.1002/cphc.201900739 (2020).
150. Daniel, R., Rubens, J. R., Sarpeshkar, R. & Lu, T. K. Synthetic analog computation in living cells. *Nature* (2013) doi:10.1038/nature12148.
151. Salman, H. M. *et al.* Biochemical testing for the diagnosis of Wilson's disease: A systematic review. *J Clin Lab Anal* (2022) doi:10.1002/jcla.24191.
152. Członkowska, A. *et al.* Wilson disease. *Nature Reviews Disease Primers* Preprint at https://doi.org/10.1038/s41572-018-0018-3 (2018).
153. Van Den Berghe, P. V. E. *et al.* Human copper transporter 2 is localized in late endosomes and lysosomes and facilitates cellular copper uptake. *Biochemical Journal* (2007) doi:10.1042/BJ20070705.
154. Du, Z. *et al.* Non-invasive UPR monitoring system and its applications in CHO production cultures. *Biotechnol Bioeng* (2013) doi:10.1002/bit.24877.
155. Prashad, K. & Mehra, S. Dynamics of unfolded protein response in recombinant CHO cells. *Cytotechnology* (2015) doi:10.1007/s10616-013-9678-8.
156. Baaske, J. *et al.* Dual-controlled optogenetic system for the rapid down-regulation of protein levels in mammalian cells. *Sci Rep* **8**, 1–10 (2018).
157. Benisch, M., Benzinger, D., Kumar, S., Hu, H. & Khammash, M. Optogenetic closed-loop feedback control of the unfolded protein response optimizes protein production. *Metab Eng* **77**, 32–40 (2023).
158. Jl, B., Deretic, V., Jp, W. & Bhaskar, K. Optical induction of autophagy via Transcription factor EB (TFEB) reduces pathological tau in neurons. (2019) doi:10.1101/600908.
159. DelRosso, N. *et al.* Large-scale mapping and mutagenesis of human transcriptional effector domains. *Nature* **616**, 365–372 (2023).
160. Mahata, B. *et al.* Compact engineered human transactivation modules enable potent and versatile synthetic transcriptional control. *bioRxiv* 2022.03.21.485228 (2022).
161. Ledford, H. Mini enzyme moves gene editing closer to the clinic. *Nature* **520**, 18 (2015).
162. Saito, M. *et al.* Fanzor is a eukaryotic programmable RNA-guided endonuclease. *Nature* **620**, 660–668 (2023).

163. Cao, Y. *et al.* Microfluidic Based Whole-Cell Biosensors for Simultaneously On-Site Monitoring of Multiple Environmental Contaminants. *Front Bioeng Biotechnol* **9**, 1–6 (2021).
164. Jones, S., Martella, A. & Cai, Y. *EMMA assembly explained: A step-by-step guide to assemble synthetic mammalian vectors*. *Methods in Enzymology* vol. 617 (Elsevier Inc., 2019).
165. Karottki, K. J. la C. *et al.* Awakening dormant glycosyltransferases in CHO cells with CRISPRa. *Biotechnol Bioeng* (2020) doi:10.1002/bit.27199.